Heretaunga Plains Aquifers: Groundwater Dynamics, Source and Hydrochemical Processes as Inferred from Age, Chemistry, and Stable Isotope Tracer Data

U Morgenstern
H Martindale
MJ Knowling
D Gordon
JG Begg
C Daughney
M Toews
RW van der Raaij
R Franzblau
V Trompetter
M Moreau
M Stewart
J Kaiser

GNS Science Consultancy Report 2017/33
April 2018

DISCLAIMER

The Institute of Geological and Nuclear Sciences Limited (GNS Science) and its funders give no warranties of any kind concerning the accuracy, completeness, timeliness or fitness for purpose of the contents of this report. GNS Science accepts no responsibility for any actions taken based on, or reliance placed on the contents of this report and GNS Science and its funders exclude to the full extent permitted by law liability for any loss, damage or expense, direct or indirect, and however caused, whether through negligence or otherwise, resulting from any person's or organisation's use of, or reliance on, the contents of this report.

BIBLIOGRAPHIC REFERENCE

Morgenstern U, Begg JG, van der Raaij RW, Moreau M, Martindale H, Daughney C, Franzblau R, Stewart M, Knowling MJ, Toews M, Trompetter V, Kaiser J, Gordon D, 2017. Heretaunga Plains Aquifers: Groundwater Dynamics, Source and Hydrochemical Processes as Inferred from Age and Chemistry Tracer Data. Lower Hutt (NZ): GNS Science. 82 p. (GNS Science report 2017/33). doi:10.21420/G2Q92G.

U Morgenstern, GNS Science, PO Box 30368, Lower Hutt 5040, New Zealand
JG Begg, GNS Science, PO Box 30368, Lower Hutt 5040, New Zealand
RW van der Raaij, GNS Science, PO Box 30368, Lower Hutt 5040, New Zealand
M Moreau, GNS Science, PO Box 30368, Lower Hutt 5040, New Zealand
H Martindale, GNS Science, PO Box 30368, Lower Hutt 5040, New Zealand
C Daughney, GNS Science, PO Box 30368, Lower Hutt 5040, New Zealand
R Franzblau, GNS Science, PO Box 30368, Lower Hutt 5040, New Zealand
M Stewart, GNS Science, PO Box 30368, Lower Hutt 5040, New Zealand
MJ Knowling, GNS Science, PO Box 30368, Lower Hutt 5040, New Zealand
M Toews, GNS Science, PO Box 30368, Lower Hutt 5040, New Zealand
V Trompetter, GNS Science, PO Box 30368, Lower Hutt 5040, New Zealand
J Kaiser, GNS Science, PO Box 30368, Lower Hutt 5040, New Zealand
D Gordon, Hawke's Bay Regional Council, Private Bag 6006, Napier 4142, New Zealand

www.gns.cri.nz

ISSN 2350-3424 (Online)
ISBN 978-1-98-853013-0 (Online)
http://dx.doi.org/10.21420/G2Q92G

CONTENTS

FIGURES

TABLES

APPENDICES

APPENDIX FIGURES

APPENDIX TABLES

ABSTRACT

Hawke's Bay Regional Council (HBRC) is presently undertaking a range of groundwater science investigations as part of its on-going focus on sustainable management of the hydrologic system of the Heretaunga Plains to inform policy development and a new Regional Resource Management Plan framework. This report provides enhanced conceptualisation of the regional groundwater-surface water system for the development of groundwater flow and transport models for the Heretaunga Plains aquifers.

This collaborative study between Hawke's Bay Regional Council, Hastings District Council, Napier City Council, and GNS Science aims to improve our understanding of the Heretaunga Plains aquifers in regard to groundwater recharge sources, flow dynamics, and interaction between groundwater and surface water.

Three main rivers discharge to the sea across the Heretaunga Plains. These rivers have large catchments that extend significantly beyond the Heretaunga Plains. Spring-fed streams and drains form sizeable perennial streams.

The Heretaunga Plains is underlain by Quaternary fluvial, estuarine-lagoonal, and marine deposits in-filling a subsiding syncline. Borehole data indicate that the deposition during the low sea level stands of the Last Glaciation was dominated by alluvial gravels accumulated from the bed load of the braided river systems of the Ngaruroro, Tutaekuri and Tukituki rivers. These materials make up the primary aquifer of the Heretaunga Plains. Overlying fine-grained materials deposited subsequently across much of the eastern Heretaunga Plains comprise an aquitard that confines the aquifer. Within the depositional sequence, river-channel gravels form an interconnected unconfined-confined aquifer system containing groundwater recharged from land surface recharge and the Ngaruroro River bed at the inland margin of the plain, 20 km from the coast. At the coast, gravel aquifers extend to a depth of 250 m. The multiple gravel layers are in general highly transmissive.

Tritium, CFCs, SF_6, ^2H, ^{18}O, Ar, N_2, CH_4, radon and major/minor ion hydrochemistry data are utilised with respect to understanding the dynamics of the groundwater from recharge to discharge and interaction with surface water, and understanding the processes that control the hydrochemical properties (quality) of the groundwater including denitrification. Age tracer and isotope data are available from c. 160 groundwater and surface water sites across the Heretaunga Plains.

Hierarchical Cluster Analysis (HCA) results provide context for the main drivers of hydrochemistry including oxic rivers and river-recharged groundwaters with little or no elevation of nutrient concentrations, association with limestone or carbonate geology, oxic rainfall-recharged groundwaters with moderate land-use impact and anoxic groundwater with chemistry typical of natural conditions. If suitable, the combination of these drivers can provide additional evidence for identification of recharge source. A combination of hydrochemistry, stable isotopes, and excess air was able to distinguish between recharge sources.

In the surface water discharges, tritium-derived mean ages show consistent patterns for the main rivers with mean transit times (MTT) of usually less than 2 years in the Tukituki, Waipawa, and Ngaruroro rivers, and somewhat older water with a MTT around 10 years discharging via the Tutaekuri River. Surface water discharging in proximity to limestone, sandstone and mudstone formations between the Ruataniwha and the Heretaunga Plains contain significantly older water, with a MTT of up to 140 years, including the Karamu tributaries which collectively drain this area, indicating drainage through considerable groundwater reservoirs.

Groundwater age tracers indicate that most of the wells within the Holocene unconfined gravel fans of the Ngaruroro River and the Tukituki River contain relatively young water with mean residence time (MRT) 0–10 years, and from the area of the main water loss from the Ngaruroro River towards the coast, the groundwater within the confined aquifer becomes progressively older. The drinking water wells southwest of Napier contain water with MRT between 20–40 years. Further toward the coast, the groundwater becomes significantly older with MRT 40–80 years, and close to the coast the water is even older, indicating sluggish flow at this part of the aquifer. Greater groundwater flow velocities in the confined aquifer toward the coast is indicated further south in the centre of the Plains. A tongue of very young groundwater with MRT < 5 years extends nearly half way towards the coast, and the groundwater near the coast is still relatively young with MRT 27–34 years. At the southern margin of the confined aquifer, older water of MRT >70 years prevails, again indicating more sluggish flow on the margin of the aquifer. Only around the Holocene gravel fan of the Tukituki River very young groundwaters of MRT <10 years occur.

Historic and recent tritium and SF_6 data show that groundwater abstracted from wells in the Heretaunga Plains often has a complex age distribution. A refined 3D geologic model developed by GNS' Urban Geology programme captures the complex structure of the aquifer system, where well screens intersect multiple layers of a heterogeneous aquifer. Highly conductive Holocene river gravel fans appear inter-fingered with the main aquifer. This refined geological model is in agreement with a new groundwater mixing model that we developed as a result of the new age tracer data.

We used binary mixing models (BMM) consisting of two parallel exponential piston flow models to represent complex age distributions. The BMMs produce excellent matches to the measured multi-age-tracer time-series data collected for most (>90%) of the drinking water wells. Due to the complex hydrogeologic setting, very young water from shallow flow pathways can be 'hidden' in overall old water from the deep main aquifer. Matching the BMM to the multi-age-tracer time-series data enabled identification of such young water.

Indicators for recharge temperature suggest that all investigated groundwaters were recharged under current climatic conditions. It is unlikely that any groundwater in the Heretaunga Plains is so old that it was recharged in a previous glacial period with colder climate.

All groundwater samples are to some degree depleted in oxygen, indicating the ubiquitous presence of organic matter in the Heretaunga Plains aquifers. With increasing age the groundwater becomes increasingly depleted in oxygen. Complete depletion of oxygen also has occurred in some young groundwater samples, suggesting high organic matter concentrations may occur locally.

Trends of groundwater quality parameters in relation to recharge time (groundwater age) can help to distinguish between anthropogenic and geologic impacts on groundwater quality. A number of key hydrochemical data, together with age data, indicate that the impact on groundwater quality by high-intensity land use is minor in the Heretaunga Plains groundwater system. Only a few groundwater samples display nitrate and sulphate concentrations slightly above the threshold concentration indicative of high-intensity land use. Dissolved reactive phosphate is elevated only in old groundwater recharged before land use intensification, indicating that these elevated concentrations are natural, likely with a geological origin.

The recharge source indicators (Ar, N_2, $\delta^{18}O$, nitrogen, calcium and CFCs) collectively show distinct recharge source patterns within the Heretaunga Plains aquifer. Two areas indicate recharge from the Ngaruroro River: around and southwest of Napier, and a band of river-

recharged groundwater located at the centre of the Plains. It is likely that this band represents a buried paleo river channel that is still hydraulically connected to the Ngaruroro River and thus enables fast seaward flow of water lost from the river. This is supported by the fact that the band of river-recharged groundwater coincides with young groundwaters. The Tutaekuri River appears not to be connected to the main Heretaunga Plains aquifer because its stable isotope and chemistry signatures are different to those of the groundwater in this part of the aquifer.

The shallow wells in the unconfined area of the Ngaruroro River gravel fan show a clear indication of local rain recharge. Previous $\delta^{18}O$ data indicate that the water lost from the Ngaruroro River flows at a depth of greater than about 100 m toward the coast, but is overlain by a thick layer with locally recharged rain water contributing to the groundwater resource. There also appears to be a band, between the two river-recharged areas, where land surface recharge is present and this may represent the drainage of the rain-recharged unconfined area of the Ngaruroro River gravel fan.

Groundwater age, isotope, gas, and chemistry data provide a conceptual flow model of the Heretaunga Plains aquifer system. Young groundwater ages of the water discharging from the Moteo Valley indicate high groundwater velocities of > 5 km/year through this system. Similarly, the groundwater in the Ngaruroro River gravel fan region, primarily containing water lost from the river, is also very young, indicating groundwater flow velocities of c. 5 km/year towards the north-east, and c. 2.8 km/year towards south-east. The flow velocity reduces considerably near the coast, by two orders of magnitude. Data near the coast are too scarce to derive information about continuation of flow off-shore.

The hydrochemistry and isotope signature of the groundwater in the confined aquifer that was identified as recharged from rivers indicates the Ngaruroro River as its source. The Tutaekuri River appears to have no or limited connection to the main Heretaunga Plains aquifer, either through the Moteo valley or the Tutaekuri River gravel fan. Water lost in the Tukituki River gravel fan could not be identified in groundwater wells in the area. It may re-surface via the springs and seeps along Karamu Stream. In the southern part of the Heretaunga Plains aquifer, covering about half of the area that is considered to be confined, the tracer signature indicates the presence of recharge from rain, locally and from the adjacent hills.

Radon data in surface water, despite being sparse, show a discharge pattern that is consistent with observed river and stream gain-loss distributions. Elevated radon concentrations in rivers and streams indicate groundwater discharge where resurfacing water from losing stretches further upstream is expected.

Despite the still-remaining limitations of the Heretaunga Plains age, gas, and isotope tracer data set (due primarily to absence of direct measurement of the input concentrations and seasonal variability into this hydrologic system), the current study has revealed insights into large-scale groundwater processes that are not obtainable by other hydrologic methods, e.g. the identification of recharge sources, elucidating surface water - groundwater interaction, and groundwater flow dynamics, to enable more realistic groundwater flow and transport models for improved management of these water resources.

KEYWORDS

Groundwater, surface water, Heretaunga Plains, groundwater age, groundwater quality, land-use impact, tritium, SF_6, CFCs, radon, stable isotopes, Ar, N_2

1.0 INTRODUCTION

Hawke's Bay Regional Council (HBRC) manages the land and water resources in the Greater Heretaunga Plains and associated river catchments that discharge into the Heretaunga Plains. HBRC is presently undertaking a range of groundwater science investigations as part of its on-going focus on sustainable management of the hydrologic system of the Heretaunga Plains. This information will be used to inform policy development and a new Regional Resource Management Plan framework for the Tutaekuri, Ahuriri, Ngaruroro and Karamu ('TANK') catchments, which includes the Heretaunga Plains aquifer system.

Due to the complexities of water flow paths underground, it is extremely difficult to predict the time scales of groundwater flow through aquifer systems (residence time). Age tracers provide new innovative approaches for understanding residence times, groundwater dynamics and hydrochemical evolution. For example, age tracers can be used to quantify the time lags between changes in land use and their impact on water quality, i.e., between initial recharge and the ultimate discharge of groundwater and any associated contaminants. This is essential for drinking water security, management of the groundwater resource, and preserving the integrity of surface waters that receive inflows from groundwater. Age tracer measurements can also be used to estimate groundwater recharge rates and sources, and to quantify the available groundwater storage that buffers river flows against drought.

This study is jointly undertaken by HBRC and GNS Science with a focus on the groundwater age and the isotopic and hydrochemical composition of the water in the Heretaunga aquifer system. This study fits within the context of broader investigations of the Heretaunga Plains hydrological system, where information is needed to understand the rates of groundwater flow through the aquifer and the interaction of groundwater with streams and rivers, i.e., how rivers recharge the aquifers, and how groundwater feeds rivers and streams. This information will contribute to an enhanced conceptualisation of the regional groundwater-surface water system and the development of groundwater flow and transport models for supporting future water management in the area.

This study makes use of the available age tracer data for the Heretaunga Plains, including: tritium, CFCs, SF_6, Ar, N_2, CH_4, radon, stable isotopic composition (^2H, ^{18}O), and major/minor ion hydrochemistry. We interpret the available tracer data for the Heretaunga Plains aquifer system in a consistent way in order to obtain groundwater age information which, together with complementary isotopic and hydrochemical water composition, is used to identify groundwater recharge sources, human and natural geologic impacts on groundwater quality, and lag time of land use on groundwater quality. The most robust age information in this study comes from time series of age tracer data collected over two decades for Napier City Council (NCC) and the Hastings District Council (HDC) with regards to compliance with the New Zealand Drinking Water Standard (NZDWS), and from monitoring data collected for the National Groundwater Monitoring Programme (NGMP) and the National Tracer Survey (NTS), operated by GNS Science. In addition to this data, HBRC also carried out a large age tracer sampling campaign between 2014 and 2016 for groundwater and surface water monitoring sites.

While this study was underway, an outbreak of gastroenteritis (Campylobacter) took place in Havelock North in August 2016. This led to a significant number of diagnostic age tracer tests on water supply bores located in the Heretaunga Plains aquifer system, aimed at understanding the age distribution of the extracted groundwater. Separately, the 3D geological model of the Heretaunga Plains was re-evaluated and refined to better reflect the complex

structure of the aquifer system. This work indicated that the groundwater age distributions at some sites are multi-modal and more complex than previously recognised. The additional age tracer work and 3D geological model refinement, while not originally a component of this study, have subsequently been utilised in this report.

This report collates and interprets the tritium and gas age tracer data, together with the isotope and hydrochemistry data. Key elements of this assessment include:

- Compilation of age tracer data available for the Heretaunga Plains, as analysed through the surveys outlined above;
- Compilation of hydrologic, hydrogeologic, and hydrochemistry data for these sites;
- Consistent age interpretation of all data using the newest information on tracer input functions, gas tracer alteration in groundwater systems, and mixing models, including where appropriate the use of refined mixing models to account for mixing of different groundwater sources and multi-modal age distributions;
- Interpretation with respect to groundwater sources of recharge; and
- Linking the age tracer and hydrochemistry data for improved understanding of hydrochemical evolution and the source and fate of contaminants (e.g., NO_3, PO_4).

This report is structured as follows. In the following section (Setting), we first provide a summary of the climate and hydrology of the greater Heretaunga Plains catchment. This has implications for the isotopic signature of the water from the various river catchments. We then provide a summary of information from a new geologic model of the Heretaunga Plains including tectonic deformation and deposition of materials. This provides context regarding the occurrence and distribution of aquifers, aquicludes, and swamp materials that impact on the redox conditions, with a particular focus on the HDC drinking water wells given that these wells, with their excellent multi-age-tracer and time series data, have been used to develop a complex groundwater mixing model. A summary of previously published hydrogeology investigation results is then provided, followed by an overview of water supply and monitoring well data used in this study. In the following section (Methods and Results), we first describe the various hydrochemical and isotopic tracer techniques employed, using data from the Heretaunga Plains groundwater system. These results then form the basis for further analyses presented in the following section (Discussion) in the context of enhancing our understanding of groundwater source and flow dynamics in the Heretaunga Plains aquifers. Last, a summary of the main findings of this work and some suggestions for future work is then provided in the Conclusions and Recommendations sections.

2.0 SETTING

2.1 CLIMATE AND HYDROLOGY OF THE WIDER HERETAUNGA PLAINS CATCHMENT

The Hawke's Bay region lies to the east of mountain ranges up to 1675 m high that provide somewhat of a shelter from the predominantly westerly winds. The eastward-facing aspect of Hawke's Bay means it is affected by weather systems accompanied by easterly winds. Anticyclones and intervening troughs of low pressure dominate the weather in Hawke's Bay, which has a sunny temperate climate with warm summers (average 17°C), mild winters (average 10°C), and a mean annual rainfall of about 800 mm near the coast (Dravid and Brown 1997). Heretaunga Plains surface flows exhibit strong seasonal variability, as a response to climate and abstraction.

Three main rivers discharge to the sea across the Heretaunga Plains (Figure 2.1). These rivers have large catchments that extend significantly beyond the Heretaunga Plains. Spring-fed streams and drains form sizeable perennial streams (Dravid and Brown 1997).

The *Ngaruroro River* drains from the northeast flanks of the Kaimanawa Range and the southwest flanks of the Kaweka Range, and has a catchment area of 2500 km^2. The estimated mean annual low flow (MALF) flow in the Ngaruroro River at Whanawhana is 8.3 (median 25) m^3/s (Waldron 2015). Downstream of Whanawhana, more than 4 m^3/s infiltrates into the aquifers of the Heretaunga Plains (Wilding 2017), providing a significant source of groundwater recharge.

The *Tutaekuri River* drains from the western and southern flanks of the Kaweka Range, and has a catchment area of 900 km^2. The Tutaekuri River previously discharged into the Ahuriri Lagoon, north of Napier. As a result of the 1931 Hawke's Bay earthquake, the river mouth was shifted from Ahuriri to Waitangi. The estimated MALF is 3.9 (median 8.6) m^3/s at Puketapu (Waldron 2015). Concurrent gaugings have not identified a net loss of flow from the Tutaekuri River downstream from Puketapu (Wilding 2017). Losses from the Tutaekuri River of the order of 0.8 m^3/s have been measured upstream of Puketapu (Wilding 2017) and are thought to feed the Moteo Valley groundwater system which subsequently contributes to the flow of the Tutaekuri-Waimate Stream along the western margin of the Heretaunga Plains. Identification of the potential contribution of the Tutaekuri River to the groundwater and surface water system of the Heretaunga Plains is part of this investigation.

The *Tukituki River* drains part of the eastern north and central Ruahine Range, with a catchment area of 2470 km^2. The estimated MALF for the Tukituki River is 6 (median 22) m^3/s (Waldron 2015). Limited concurrent gauging information suggested a typical flow loss of 0.9 m^3/s between Red Bridge and Black Bridge (Wilding 2017).

The main *spring-fed streams* are the Tutaekuri-Waimate Stream, Karamu Stream, Raupare Stream, Irongate Stream, and Mangateretere Stream. The Tutaekuri-Waimate Stream has a MALF of about 1.9 m^3/s, with most of this likely to be derived from the Ngaruroro River water lost upstream of Fernhill, and from the Tutaekuri River via the Moteo groundwater system. The Raupare Stream, with a MALF of about 0.4 (median 0.6) m^3/s is also likely to be fed by the Ngaruroro River-recharged groundwater system. The Mangateretere Stream, discharging at MALF of about 0.05 (median 0.18) m^3/s into Karamu Stream, originates from a series of spring seepage areas near the Tukituki River, which suggests the Tukituki River constitutes its potential primary source. However, the spring area is perched and hydraulically interconnected to the main aquifer, with the possibility of upward leakage of Ngaruroro River-sourced water. Irongate Stream, with a MALF of 0.17 (median 0.33) m^3/s, follows an old course of the

Ngaruroro River and was thought to be sourced by this river. The MALF for the Karamu Stream increases from 0.25 (median 0.73) m^3/s downstream of the Irongate confluence to 0.97 (median 1.8) m^3/s upstream of its Raupare confluence (Wilding 2017). After accounting for the tributary inflows, there is a shortfall of 0.57 (median 0.7) m^3/s that likely originates from springs downstream of the Mangateretere confluence (Wilding 2017). The current investigations set out to improve our understanding of the water sources of these spring-fed streams.

Submarine discharges from the confined aquifer are highly uncertain. Fresh-water springs on the Hawke Bay seafloor about 20 km from the coast are thought to have been identified in 1954, but were not confirmed in a later survey (Brown et al. 1999).

2.2 Geology of the Heretaunga Plains — Factors in Better Understanding Groundwater

This outline of the geology of the Heretaunga Plains provides a broad overview of the geological environment within which the Heretaunga Plains groundwater system resides. The Heretaunga Plains occupy a fault-bounded depression between about 900 m deep (Dravid and Brown 1997) and a maximum of 1600 m deep (Beanland et al. 1998). A series of active faults extend from the Waipukurau area northeast to the southwestern margin of the Heretaunga Plains, and are known to continue beneath the plains (Figure 2.1). Seismic acquisition data suggest that some inactive faults, such as the Ngaruroro River (Roys Hill) and Napier faults, also lie at depth beneath the Quaternary sediments (Beanland et al. 1998; Dravid and Brown 1997).

Eocene to Late Pliocene/early Quaternary sediments, largely of marine origin, underlie the hills that immediately surround the Heretaunga Plains, including the Roys Hill, Fernhill, the basal section of Bluff and Hospital hills, and the hills south of Pakipaki. Early to middle Quaternary (Black, 1992) conglomerate, pumiceous sandstone and carbonaceous mudstone are preserved at Cape Kidnappers, south of Havelock North and as isolated remnants on the hilltops west of Napier (Figure 2.1). Seismic reflection profiles and sparse borehole data indicate that these rocks underlie the Heretaunga Plains at depth. Younger middle to late Quaternary deposits present beneath the Heretaunga Plains are of alternating fluvial and marginal marine origin (Brown and Dravid 1997).

Interpretation of the stratigraphy of the Heretaunga Plains used here relies on a long-standing geological model based on continuing deposition within a deforming basin through the cyclical global climatic changes of the Quaternary Period (Dravid and Brown 1997). These principles are based on drillhole logs, seismic reflection data and the international sea level curve (e.g. Siddall et al. 2003; Lisiecki and Raymo 2005).

Borehole data indicate that across the Heretaunga Plains area, deposition during the low sea level stands of the Last Glaciation (71,000 to c. 12,000 years ago) was dominated by alluvial gravels accumulated from the bed load of the braided river systems of the Ngaruroro, Tutaekuri and Tukituki rivers. These materials make up the primary aquifer of the Heretaunga Plains. Overlying fine-grained materials deposited subsequently across much of the eastern Heretaunga Plains comprise an aquitard that confines the aquifer.

Sea level rose rapidly following the 18,000-year low stand (c. -115 m) to c. -60 m by c. 12,000 years (below current sea level; Bard et al. 1996, Siddall et al. 2003), c. -30 m at 10,000 years, c. -10 m by 8000 years and reaching present sea level at c. 6500 years ago (Gibb 1986). As sea-level rose, the shoreline moved landward, and the effect of this rising sea level was felt behind the contemporary coastline with a fringe of reduced energy river environments and fine-

grained deposition (sand, silt and peat). As the coastline moved further inland, marine sand and silt were deposited on top of these alluvial silt deposits, which in turn overlie the more energetic alluvial gravels deposited when sea level was lower.

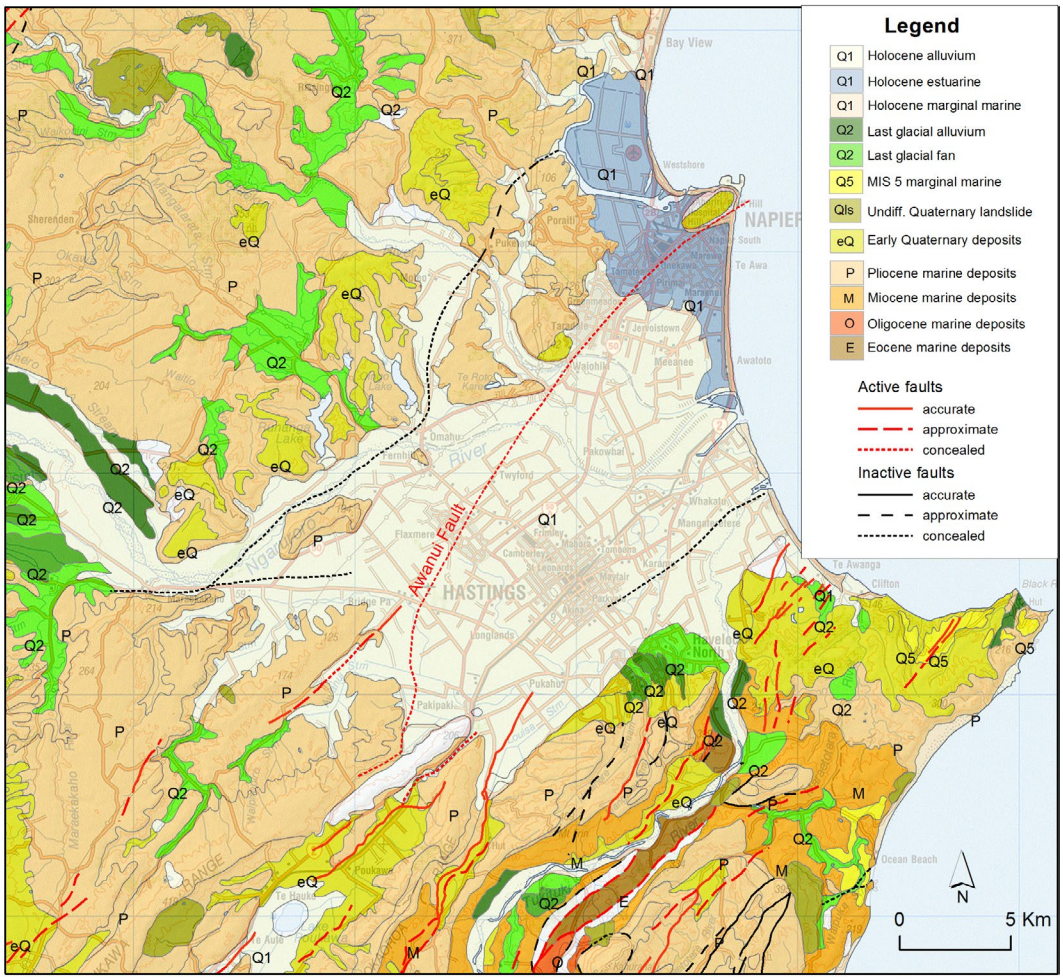

Figure 2.1 Surface geological map of the Heretaunga Plains area (after Heron (comp) 2014).

The landward-migrating paleo-shoreline probably crossed the position of the present-day shoreline well before 8000 years ago, possibly as much as 10,000 years ago, and was close to central Hastings by c. 7000 years ago, (see radiocarbon ages, Dravid and Brown 1997). At c. 6500 years ago, the shore line reached its farthest inland extent, the shoreline extended from Taradale through Camberley to Pakipaki. During this entire period, the Tukituki and Ngaruroro rivers continued to deliver their bedload gravels to the contemporary shorelines, including into this embayment. A barrier bar started to develop across the mouth of the bay south from Bluff Hill c. 8000 years ago, and north from Haumoana c. 6000 years ago, and the marine embayment evolved into an enclosed estuary (see Radiocarbon ages, Dravid and Brown 1997). With stability of sea level, infilling of the estuary by materials supplied by the Ngaruroro, Tutaekuri and Tukituki rivers commenced and continued until c. 2000 years ago, since when the plains had become the low-lying swampy, forested, scrubby, grassy alluvial plains that Maori and European settlers alike might have recognised. The oldest historical map of the Heretaunga Plains area (Rochford, 1876) shows the land subdivision of the day, but also illustrates the Ahuriri Harbour and its lagoons, the courses of the rivers and presence of swamps of the time.

2.2.1 Tectonic deformation

The destructive 1931 Mw 7.9 Napier Earthquake resulted in differential deformation across central Hawkes Bay and across the Heretaunga Plains themselves (Hull 1990; Figure 2.2). The Napier/Ahuriri Lagoon experienced uplift of 1.5 to 2 m, while the Karamu area subsided by c. 1 m. The earthquake was triggered by a failure on a largely sub-surface, NW-dipping reverse fault, probably the Awanui Fault, which extends beneath the Heretaunga Plains from about Bridge Pa through to the south-eastern side of Bluff Hill. There are some surface displacements of the fault near the south-western side of the plains near Bridge Pa (Langridge and Reis 2015). Deformation associated with the 1931 earthquake is characterised by an elongate zone of uplift extending NNE from Fernhill through the Ahuriri Lagoon to the mouth of the Aropaoanui River in northern Hawke's Bay, and a sub-parallel zone of subsidence between Poukawa and Haumoana.

The slip rate on this active fault is thought to be moderate (Active Faults database), suggesting that periodic rupture through the Holocene may have progressively deformed geological units.

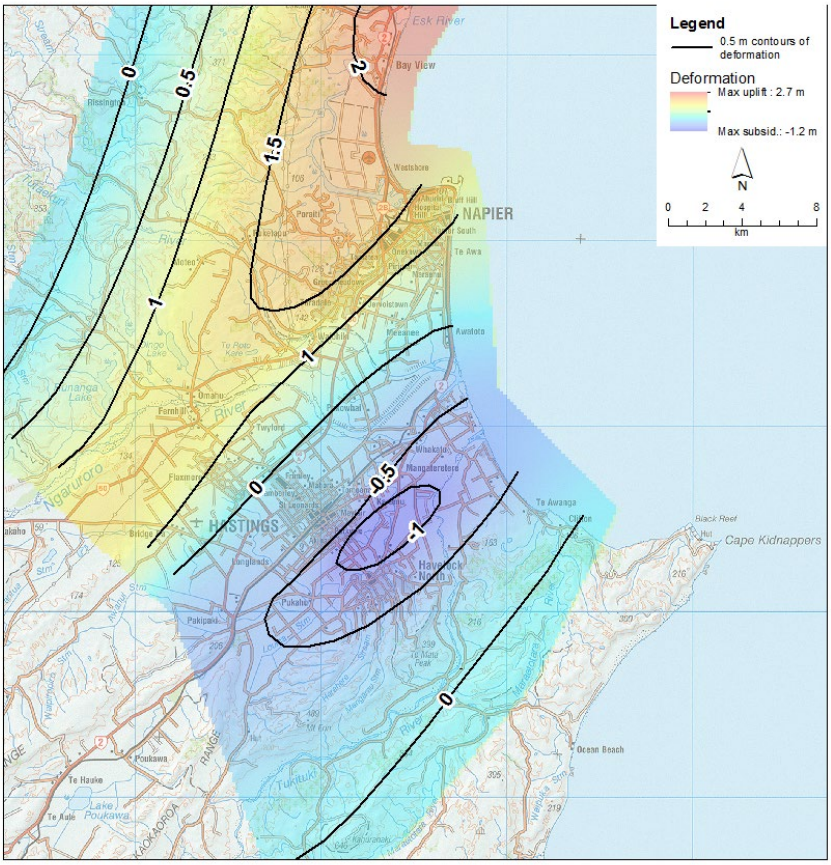

Figure 2.2 Deformation associated with the 1931 Napier Earthquake measured with respect to sea level; deformation contours are in half metre intervals and negative values represent subsidence while positive values represent uplift.

If the Awanui Fault has ruptured a number of times since the commencement of the Holocene marine inundation and deformation associated with each rupture approximates that of the 1931 rupture, it may be possible to recognise that signature from borehole logs. However, other possibilities include: a) relaxation following fault rupture may partly cancel out this pattern of deformation; and/or b) that a number of other potential sources of deformation present in and around the Heretaunga Plains may contribute towards a pattern of cumulative deformation.

Recently processed InSAR (interferometric synthetic aperture radar) data currently indicates rates of deformation during short time periods (little more than a decade). In the Hawke's Bay area interferometric studies reveal two subparallel belts aligned along a similar strike to the 1931 deformation, with a belt of uplift between Tikokino and Bay View and a belt of subsidence between Omakere and Clifton. The axis of the belt of subsidence lies c. 7 km to the southeast of the axis of the 1931 subsidence (I. Hamling pers. comm. August 2016).

The distribution/presence of peat and shells within borehole logs suggests that the Heretaunga Plains embayment developed preferentially south-westwards from the time that the shoreline crossed the location of the present shoreline. This preferential embayment development approximates the peak zone of subsidence recorded for the 1931 Napier Earthquake (Hull 1990), and it seems reasonable to assume that the two are related. This is even true when the deformation associated with the 1931 earthquake is taken out of the drillhole record, indicating that at least one deformation event akin to the 1931 earthquake was experienced in the area since c. 10,000 years ago.

Tectonic deformation, even during the relatively short geological time frames we deal with on the Heretaunga Plains, is likely to have influenced the spatial distribution of the lithological units that are important for understanding groundwater.

2.2.2 Three dimensional relationships and distribution of aquifers and aquicludes

Understanding the materials deposited during this period, and their spatial distribution, is important for understanding the Heretaunga Plains groundwater system (a significant economic element in modern society), its water usage and water quality.

During the cold climatic period (18,000 years ago) when the shoreline was far to the east of its present position, the axial ranges, stripped of their forest cover and subject to extreme freeze and thaw climatic conditions, shed vast quantities of rock material into the headwaters of the Ngaruroro, Tutaekuri and Tukituki catchments. This pulse of coarse rock materials propagated downstream to the shoreline of the times, far to the east of the present Heretaunga Plains. When these rivers reached the tectonic depression now represented by the Heretaunga Plains, their coalescing alluvial fans formed a semi-continuous alluvial plain, underlain by a largely continuous gravel geological unit. Given the sparsity of borehole logs that penetrate beneath these Last Glacial gravels, it is difficult to estimate their thickness, but in some places, it must exceed 20 metres.

Surface geological mapping shows that in the west, upstream from Maraekakaho, Last Glacial terraces are elevated 20 m above the level of the riverbed and are underlain by alluvial gravels on each side of the Ngaruroro River (Figure 2.3). Here, the terrace surface lies at c. 90 m above sea level but it slopes more steeply downstream than the present riverbed. The same surface lies close to present day sea level at Flaxmere, where the ground surface (the upper surface of Holocene alluvial gravels is c. 29 m elevation). The volume between the projected elevation of the Last Glacial surface and the riverbed is filled by younger (Holocene) alluvial gravels, here described as Holocene fan gravels.

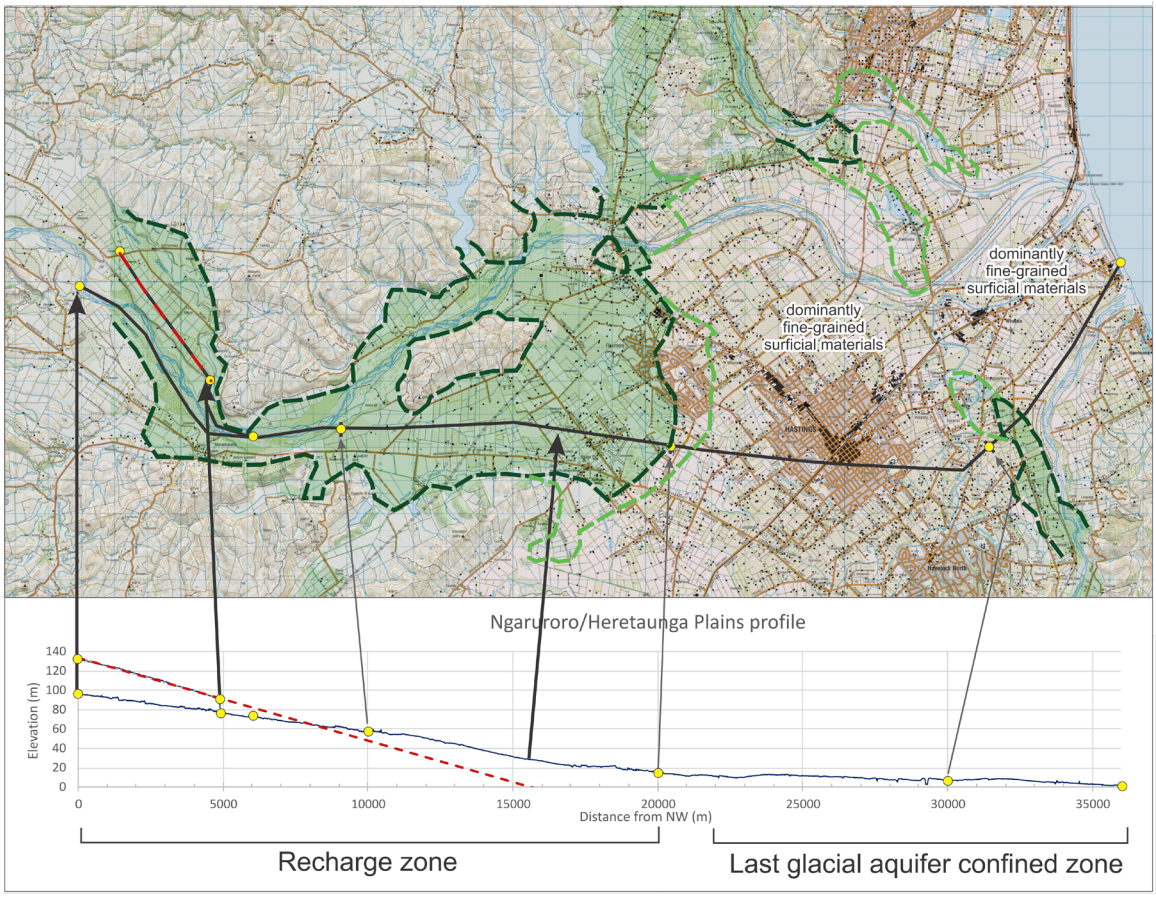

Figure 2.3 Profiles derived from a LiDAR-based DEM across the Heretaunga Plains showing the extent of the unconfined Last Glacial gravels (green shaded, with dashed green outline) The Last Glacial gravel surface lies above the current river elevation above the Maraekakaho Gorge (dashed red line in the profile located northeast of the river) and dips down-valley steeper than the present river elevation (extrapolated beneath the surface as a dashed red line). The volume between the surface (dark blue line in the profile) and the dashed red line, where it lies below the surface, is occupied by Holocene gravels of the Ngaruroro River. The light green dashed line represents the generalised eastern extent of Holocene river gravels close to the surface. East of this line, the Last Glacial aquifer is confined beneath dominantly fine-grained materials (uncoloured). Arrows between the map and profile, and yellow points relate the two elements of the figure. The base map is the LINZ TOPO50 map.

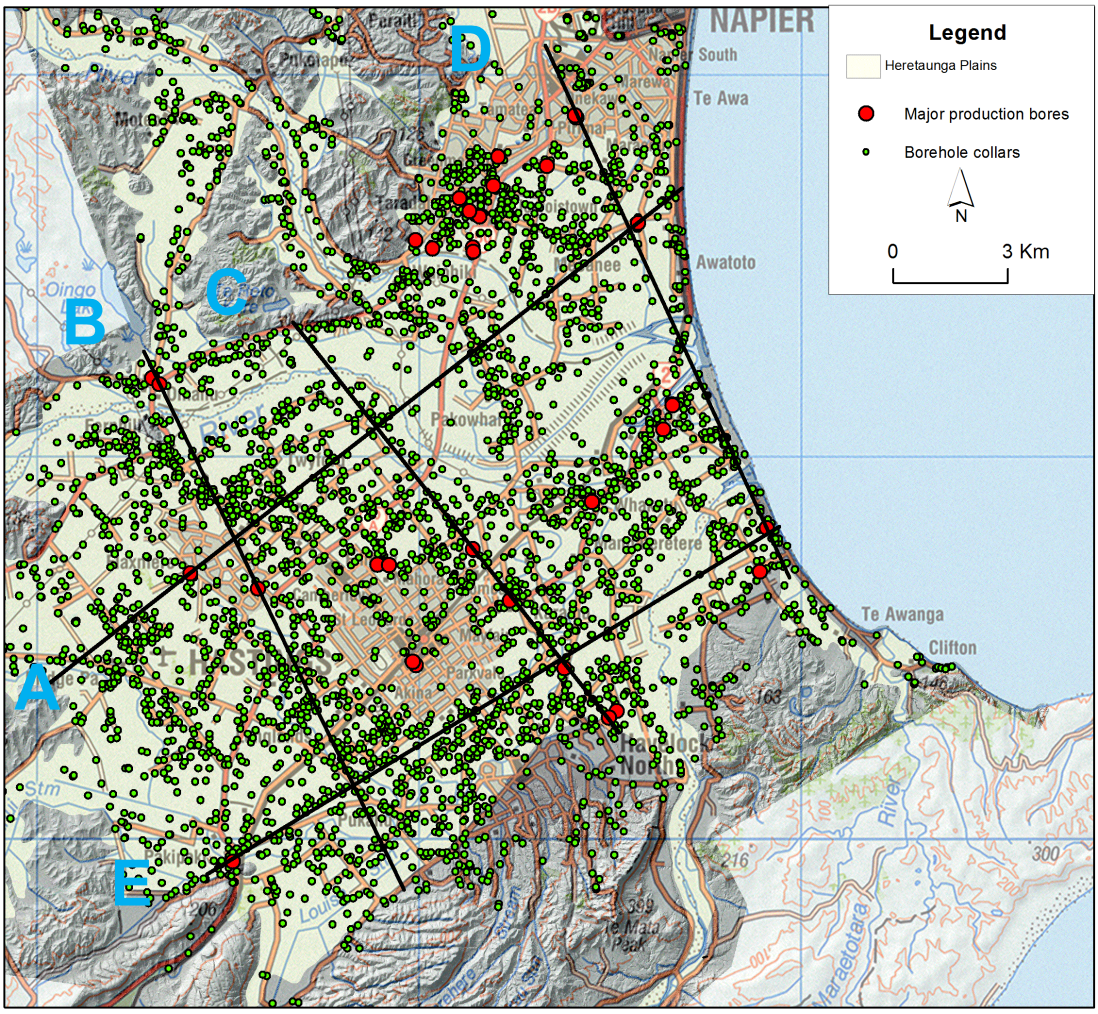

Figure 2.4 Location of borehole collars, production bores (drinking water supply) constraining the Heretaunga Plains geological model. The base map is the LINZ Topo250 map, underlain by the LiDAR-derived 1 m digital elevation model. The annotated lines represent the location of cross sections depicted in Figure 2.5.

As the sea level rose following its low Last Glacial elevations, it advanced landward across this alluvial plain. Borehole logs shows that beneath the Heretaunga Plains the first sign of this rising sea level is seen in deposition of swampy deposits (peat and mud, but also silt and sand) on top of the Last Glacial alluvial gravels. These low energy alluvial and swamp deposits are overlain by marginal marine materials that include marine shells. The transgression of the shoreline across the land as sea level rose (in the early and middle Holocene) can be tracked spatially using the distribution of shells recorded in borehole logs. Shells are found at greatest depth near Awatoto/Meanee and their distribution extends rapidly south-westwards at decreasing depths to the maximum transgression, at an elevation close to present day sea level, but far inland from the present shoreline. Bluff Hill was an island at the time, with the mainland shoreline stretching from the hills behind the Ahuriri Lagoon, through Taradale and Flaxmere to Pakipaki before turning north past the Havelock North hills to Haumoana. The alluvial fans of the Ngaruroro and Tukituki rivers fed into this embayment.

The Heretaunga embayment was cut off from the open ocean by rapidly developing sandy gravel barrier bars from both the Bluff Hill end and from Haumoana by at least this time, c.6500 years before present. The Tukituki, Ngaruroro and Tutaekuri rivers flowed into the embayment and subsequently into the estuary, depositing fans of gravel.

Where these fans were proximal to the rivers' entries to the plains during the early part of the Holocene, they rest directly on the underlying Last Glacial alluvial gravels. But later in the early

and middle Holocene, the gravel fans were deposited in isolation from the underlying gravels, separated by silt, peat and mud, which comprise an aquiclude. In the late Holocene, the gravel fans are in hydraulic contact with the Last Glacial gravels in some places, but distally, are separated by fine-grained estuarine and alluvial overbank deposits. The Last Glacial gravels beneath the surface are in direct contact with the Holocene fan gravels in the Ngaruroro riverbed between Maraekakaho and at least Bridge Pa and are re-charged by it in this area. Downstream from Flaxmere, where present, the youngest Holocene fan gravels are isolated from the underlying Last Glacial gravels by a silty aquitard (alluvial overbank and swamp deposits), and seawards from Pakowhai, by marine/estuarine materials.

A database of existing digital borehole logs has been used to build a three-dimensional lithological model in Leapfrog Geo (version 4). Details of methods used in building the model are not yet documented but will be within the coming year. This model has been used to generate cross sections through major production bores across the Heretaunga Plains as illustrated in Figure 2.4 and Figure 2.5. These cross sections illustrate the relationships between geological units that approximate the aquifer and aquiclude groundwater system units. Precision of boundary locations and detail within the model are limited by borehole coverage, and quality heterogeneity, and by other factors associated with model scale.

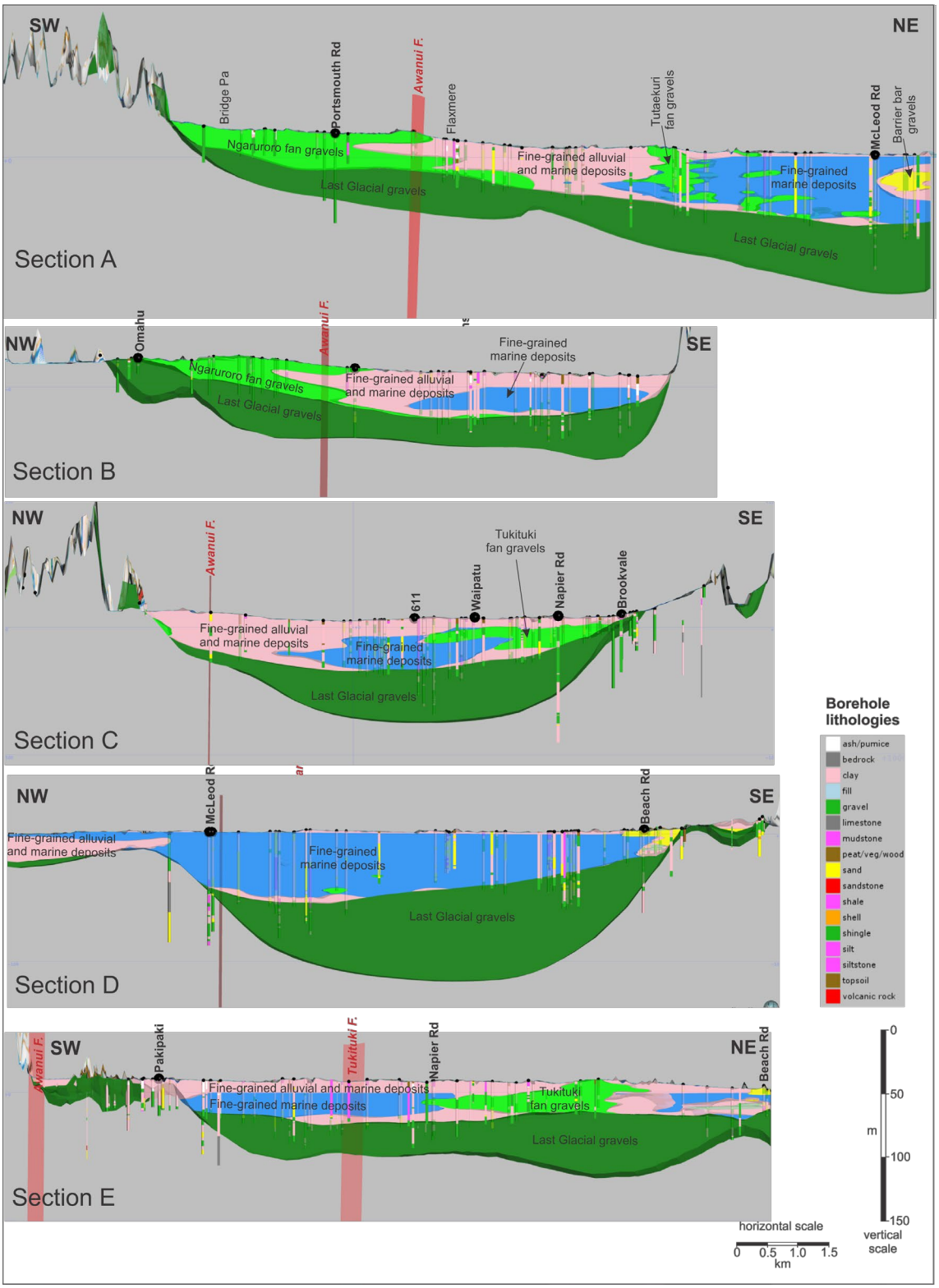

Figure 2.5 Geological cross sections: A: Bridge Pa (left) to Awatoto (right); B: Fernhill (left) to Pukahu (right); C: Te Roto Kare (left) to Annandale (right); D: Napier CBD (left) to Haumoana (right); and E: Pakipaki (left) to Haumoana (right). The sections show borehole data falling within 200 m of the section line and the geological units above the top of the Last Glacial alluvial gravels (dark green). Boreholes are coloured by primary lithologies (see legend). Limited confidence is placed on the location of the base of the Last Glacial gravels, the primary groundwater aquifer for the Heretaunga Plains, due to sparsity of borehole data at that depth. Light green units represent Holocene alluvial fan gravels (of the Ngaruroro, Tutaekuri and Tukituki rivers) and barrier bar gravels at Napier and Haumoana are shown in yellow; the blue unit represents the modelled fine-grained Holocene marine/estuarine materials and the pink unit represents dominantly fine-grained Holocene overbank alluvial and/or marine deposits. Large black balls at the surface mark production well-sites and small black balls represent other borehole collars. Sub-vertical red lines/rectangles represent the location of active faults, their thickness dictated by obliquity of the section line to the strike of the faults. Vertical exaggeration 35 x.

2.2.3 Stratigraphy, modelling and screening of drinking water production bores

The cross sections in Figure 2.4 and Figure 2.5 are set to cover particularly the drinking water supply wells. To assess the aquifer geology in relation to the drinking water sources, a total of 34 drinking water production boreholes were available for analysis. Of these, five have no information on screen depth. Limitations in certainty of the screened geological unit are imposed on 11 additional bores close to the margins of the Heretaunga Plains due to modelling uncertainties. These bores include Burness, Peddie, T3 riverside, Greenmeadows, King, Pakipaki, Omahu Pa, Omahu, Brookvale #1, Brookvale #3 and Parkhill. Of these, it is probably reasonable to conclude that Burness (T1), Peddie (T2), Greenmeadows (T4), Pakipaki and Parkhill are screened in Last Glacial gravels but some uncertainty of the screened unit remains for the other six.

Of the remaining 18 production bores, there is reasonable confidence that 16 are screened in Last Glacial gravels, but some uncertainty remains for Waipatu and Whakatu, which are screened above the modelled Last Glacial gravel surface (5.4 and 3.4 m respectively) and are in close proximity to modelled Holocene fan gravels. This may be due to inaccurate modelling.

Modelling of the Holocene fans of the Ngaruroro and Tukituki rivers suggest that Last Glacial gravels are overlain by Holocene fan gravels of the Ngaruroro and Tukituki rivers at twelve of the production bores sites (Omahu Pa, Omahu, Portsmouth Road, Wilson Road, Brookvale #1, Brookvale #3, Waipatu, Whakatu, and Napier Rd/Hastings, but possibly also Lyndhurst, Lyndhurst Rd #3 and Eastbourne #5). Where this is the case, there is some potential for hydraulic continuity between the Holocene fan gravels and underlying Last Glacial gravels.

Section 3.5.2 shows an excellent example in which complex age distribution of the groundwater discharge from a drinking water well could be established in detail, with the complex geology providing the context for the binary mixing. Most of the drinking water supply wells have such robust age tracer time series data to allow for correlations between the hydrogeological settings of wells and the obtained age distribution of the water discharged from them, enabling the geology to provide the context for the complex age distributions.

2.3 HYDROGEOLOGY OF THE HERETAUNGA PLAINS - SUMMARY

The hydrogeology of the Heretaunga Plains has been the subject of extensive previous investigations that involve stream gauging, geophysical surveys, test drilling and sampling, well logging, piezometric surveys, pump tests, and groundwater balance analyses. Detailed summaries of the Heretaunga Plains groundwater system conceptualisation developed from these data are provided by Brown et al. (1999) and Dravid and Brown (1997). While a short summary is given below, for details the reader is referred to the two references listed above.

The Heretaunga Plains is underlain by Quaternary fluvial, estuarine-lagoonal, and marine deposits in-filling a subsiding syncline. Within the depositional sequence, river-channel gravels form one of New Zealand's most important aquifer systems. An interconnected unconfined-confined aquifer system contains groundwater with significant recharge from the Ngaruroro River bed at the inland margin of the plain, 20 km from the coast. At the coast, gravel aquifers extend to a depth of 250 m. High-quality groundwater is abstracted for city and rural water supply, agriculture, industry, and horticulture.

The intention of this report was not to perform further hydrogeologic investigations but to use new information on isotopic, gas, and chemical tracers in the surface water and groundwater to provide insight into the interconnection between surface and groundwater, the recharge sources of the groundwater, and groundwater flow dynamics.

In addition to the detailed information given in Brown et al. (1999) and Dravid and Brown (1997), we show here only one additional figure that summarises the unique properties of the Heretaunga Plains groundwater system. Figure 2.6 shows tritium, measured in recent years after the decay of the bomb-tritium from nuclear atmospheric weapons testing in the 1950s and 1960s, versus well depth. For context, data for the Heretaunga Plains (red) are shown alongside a few other New Zealand groundwater data sets, including the National Groundwater Monitoring Programme (NGMP) of New Zealand (Morgenstern and Daughney 2012), the neighbouring Horizons region, and Southland. It is obvious that tritium, an indicator of young water, occurs at significantly greater depth (>100 m) in the Heretaunga Plains aquifers, compared to other aquifers (typically <50 m). This implies significantly higher hydraulic conductivities in the Heretaunga Plains aquifers, as indicated in Brown et al. (1999).

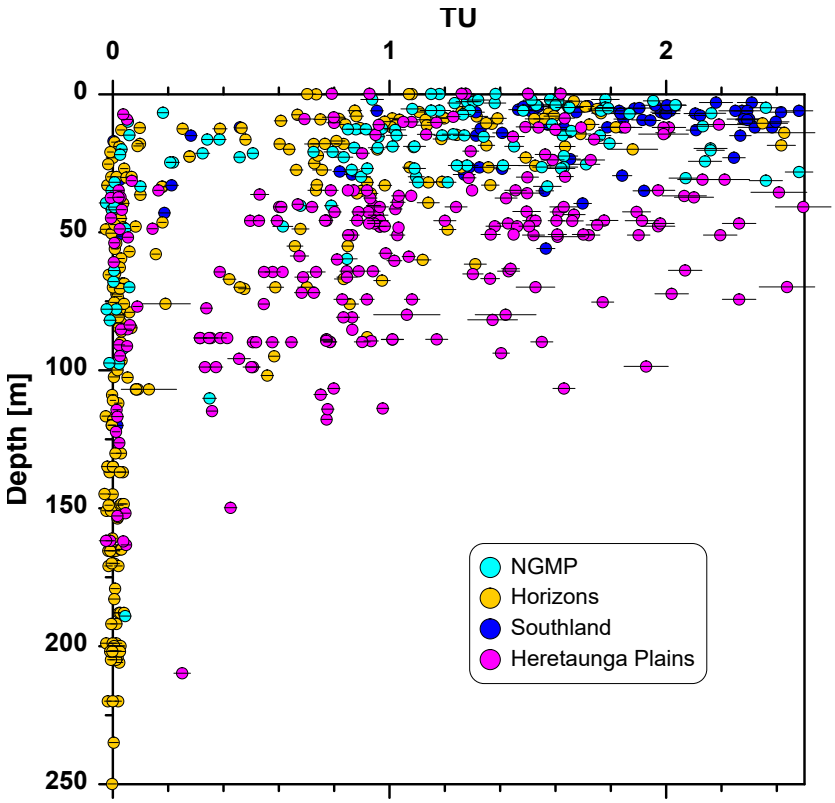

Figure 2.6 Tritium versus well-depth, for the Heretaunga Plains groundwater compared to other New Zealand groundwater data sets.

The Heretaunga Plains groundwater system is considered to be extremely complex in nature. Multiple highly transmissive gravel layers, interfingered by several gravel fans with extremely fast groundwater flow pathways, interconnection of various aquifer layers in the groundwater wells, and isotopic input signatures from various river catchments with different climatic conditions pose challenges to understanding this system, and the tracer signature in it.

2.4 Well Locations and Well Data

Wells used in this study which have available age, isotope and gas tracer data are located throughout the Heretaunga Plains (Figure 2.7). These include drinking water supply wells for Hastings District Council (HDC) and Napier City Council (NCC), wells sampled for the NGMP, HBRC State of the Environment (SoE) monitoring wells, and several wells investigated for other projects over time. In most cases, the HDC and NCC drinking water wells and the NGMP wells have available age tracer time series data and interpretations of these data into Mean Residence Time (MRT) are considered very robust. These wells are specifically labelled in consecutive figures.

Wells located in the western part of the Heretaunga Plains, particularly between the Ngaruroro and Tutaekuri rivers, are typically shallow, ranging from 7–40 m (yellow colours). Around Hastings, a number of wells are significantly deeper, between 100–200 m (dark brown colours). The wells located near the coast, particularly north of Awatoto where the depth to the confined aquifer increases, are deeper than 60 m.

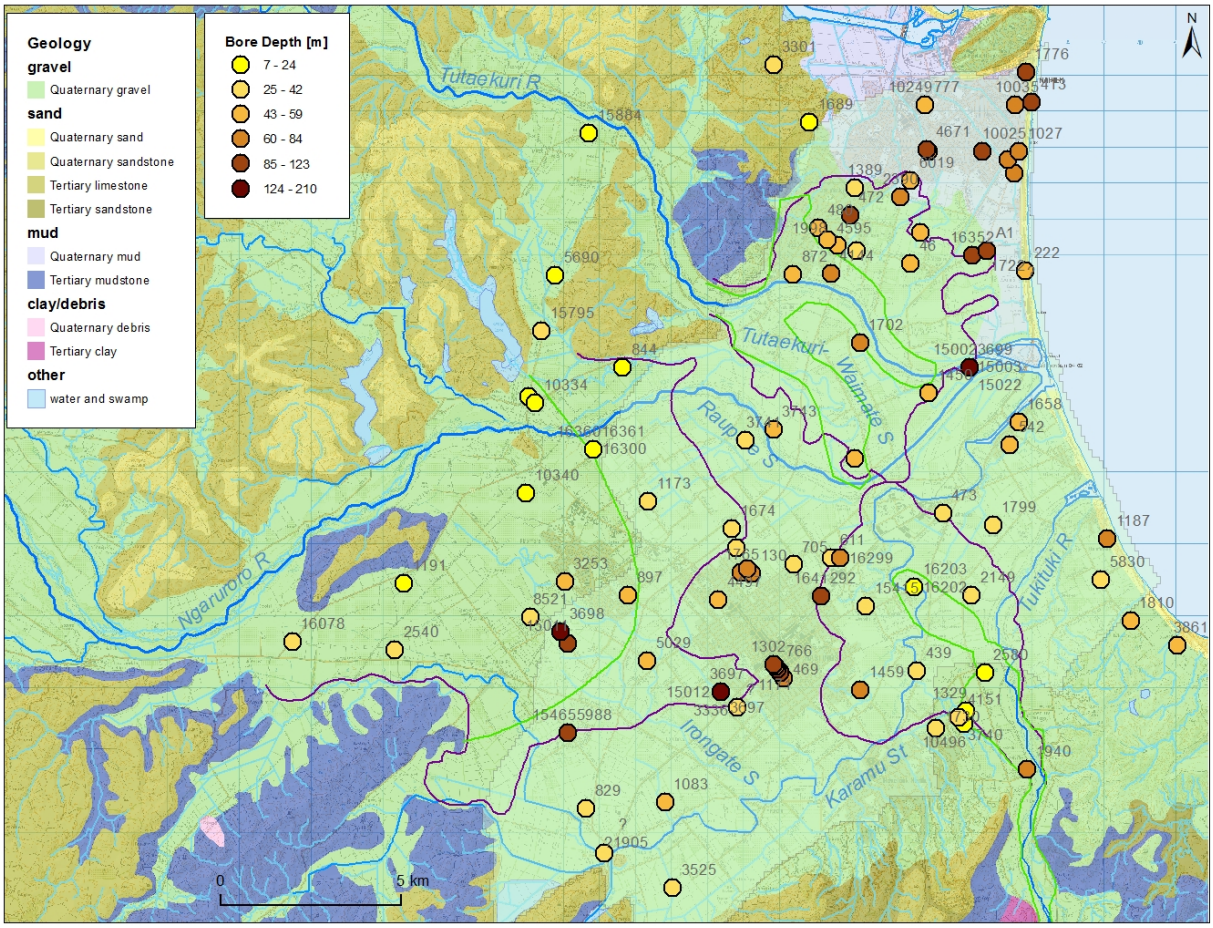

Figure 2.7 Map of sample locations with colour-coded well depth. Labels are HBRC well-IDs (Appendix 3). In the southern coastal region, the alluvium includes the Kidnappers group which is early Quaternary. The Quaternary gravel includes sand and mud. Green and purple lines indicate surface and subsurface extension of the Holocene river gravel fans, respectively. Confined aquifer is indicated in light green.

For this summary report, approximately 160 wells with available age-tracer or stable isotope data were identified. Data types included tritium, CFC (CFC-11, CFC-12 and CFC-113), SF_6, radon, and stable isotope ratios of $\delta^{18}O$ and $\delta^{2}H$.

CFCs and SF_6 have been analysed by gas chromatography using an electron capture detector (GC ECD) with detection limits of approximately 3 x 10^{-15} mol kg^{-1} for CFCs and 2 x 10^{-17} mol kg^{-1} for SF_6. The analytical procedure for CFCs is similar to that of Busenberg and Plummer (1992). The analytical procedure for SF_6 is described in van der Raaij (2003). CFC samples are analysed in duplicates. Dissolved argon, nitrogen and methane are measured simultaneously with CFCs by GC/thermal conductivity detector (TCD).

Tritium is measured by electrolytic enrichment and liquid scintillation counting using Quantulus low-level counters (Morgenstern and Taylor 2009). The detection limit is approximately 0.02 tritium units where 1 TU is a $^{3}H/^{1}H$ ratio of $1:1\times10^{18}$.

Stable isotope data were collected from two sources: The first includes measurements performed by the GNS Stable Isotope Laboratory using an isotope ratio mass spectrometry with reported precisions of 0.1 ‰ for $\delta^{18}O$ and 1.0 ‰ for $\delta^{2}H$. The second source of stable isotope data is those captured during the tritium enrichment process (Trompetter et al. 2016).

To give an overview of the history of tracer studies in the Heretaunga Plains, Figure 2.8 shows tritium, SF_6, and CFC tracer analyses over time. Apart from two tritium studies in the Heretaunga Plains on groundwaters in the mid-1960s and on surface water in 1970, the first

comprehensive survey was performed in the mid-1990s by HBRC (Dravid and Brown 1997). Thereafter, through to 2014, most of the age dating work was undertaken as part of drinking water security assessments by HDC and NCC. These systematic data, over the last decades, also including CFC, SF_6, Ar and N_2 data, form the basis of multi-tracer time series' that enabled identification of complex binary mixing models (Section 3.5.2). During this time, GNS Science also contributed to an improved understanding of the Heretaunga Plains groundwater flow dynamics via its National Groundwater Monitoring Programme and National Tracer Survey. During the period 2014–2016, HBRC performed an additional comprehensive multi-tracer study on groundwater and surface water samples with the aim of understanding the interconnection and groundwater flow dynamics within the Heretaunga Plains. Higher resolution quarterly age tracer surveys of the drinking water wells were performed through 2016/17 following the aforementioned contamination of Havelock North's drinking water.

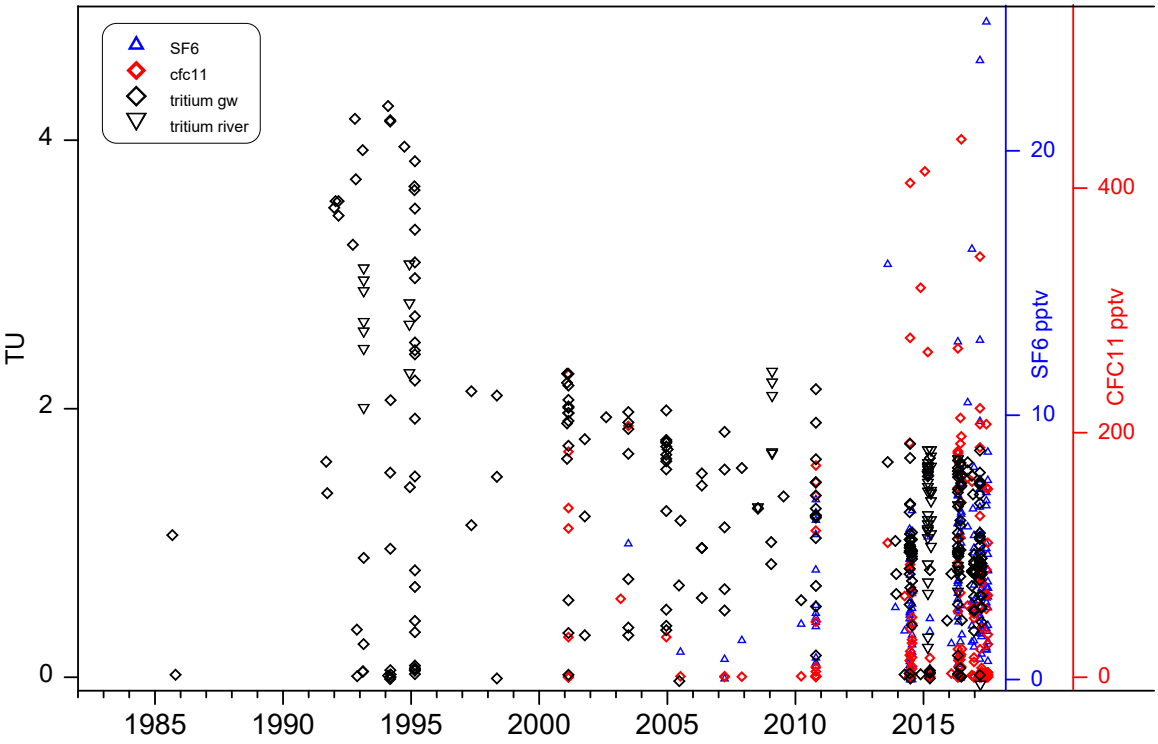

Figure 2.8 Available analyses of tritium, SF_6, and CFC tracer data over time.

The tracer age data for the groundwater well and surface water samples are provided in the supplementary Microsoft Excel file (Summary Age Data.xlsx), together with the coordinates of the sampling sites, well and lithology data, and hydrochemistry as provided by the various institutions. A summary of the surface water hydrologic data and age data is listed in Appendix 2, and of groundwater age interpretation data, mean residence time (MRT) and fraction of the exponential flow volume within the total volume of the exponential flow model (E%PM, see Appendix 1), is listed in Appendix 3, together with well ID, coordinates, well and screen depth, and results of the Hierarchical Custer Analysis.

3.0 METHODS AND RESULTS

3.1 HYDROCHEMISTRY

Hydrochemistry data were obtained from three sources: historical data provided by HBRC, including SoE monitoring data; historical data provided by GNS Science through the NGMP; and new analyses from samples collected during 2015–2017 in association with this investigation or other drinking water security assessments conducted in the study area. The "raw" hydrochemical data are provided as an electronic annex (folder: Raw Chemistry Data).

A statistical summary of the available hydrochemical data for each parameter at each site was produced using the Microsoft Excel spreadsheet calculator of Daughney (2007; 2010). The statistical summary included calculation of the median value for each parameter at each site, based on a log-probability regression method that is suitable for datasets containing many results that are reported as being below some detection limit. Note some of the sites had been sampled on only one occasion whereas other sites had been sampled multiple times. Sites that had been sampled only once were still included in the hydrochemical assessment to maximise the number of sites available. The input and output data files from the statistical assessment of hydrochemistry are also provided as electronic annexes (HCA_results_2017).

Hierarchical cluster analysis (HCA) is a multivariate statistical method that categorises the input data based on similarities in selected characteristics. HCA was undertaken in this study to identify common hydrochemical categories within the dataset and assign groundwater and surface water sites to these categories in an attempt to identify links between groundwater and surface water bodies. HCA was undertaken using the calculated site-specific median values of 13 different parameters: Ca^{2+}, Na^{+}, K^{+}, Mg^{2+}, HCO_3^{-}, Cl^{-}, NO_3-N, NH_3-N, Soluble Reactive Phosphorous (SRP), Mn, Fe, pH and Total Dissolved Solids (TDS). Any site that had not been analysed for all 13 of these parameters was excluded from HCA. In total, 115 groundwater sites and 28 surface water sites were included in the HCA for this study.

Approaches for HCA were based on best-practices from previous experience in New Zealand and overseas (e.g., Güler et al. 2002, Daughney and Reeves 2005). HCA was initially conducted using the nearest neighbour linkage rule. This approach identifies sites whose hydrochemistry is most different from other sites. On this basis, five sites were identified as potential outliers in the dataset (see Electronic Annex: HCA_results_2017). These sites were therefore excluded from subsequent HCA analysis to avoid biasing effects. Secondly, HCA was conducted with non-outlier sites using Ward's linkage rule (Ward 1963). Ward's method is based on an analysis of variance, and produces smaller distinct clusters than other linkage rules, such that each site in a cluster is more similar to other sites in the same cluster than to any site assigned to a different cluster. The square of the Euclidean distance was used in HCA as the measure of similarity for both linkage rules.

The HCA analyses were undertaken in *R* (R Core Team, 2016) using the pvclust package, which allows for assessment of the uncertainty in the HCA output. For each cluster in hierarchical clustering, quantities called p-values are calculated via multiscale bootstrap resampling. The AU (Approximately Unbiased) p-value is computed by multiscale bootstrap resampling, and is a better approximation to unbiased p-value than the Bootstrap Probability (BP) p-value that is computed by normal bootstrap resampling. The pvclust package reports p-values on a scale of 0 to 100%, where for example an AU p-value of >95% would indicate that the subdivision of one cluster into two subclusters is significant at the 95% confidence level.

HCA results using Ward's linkage are displayed as a dendrogram in Figure 3.1. On this type of diagram, the terminus of each vertical coloured line at the X-axis represents a single site (either a groundwater site or a surface water site). Horizontal coloured lines join sites and groups of sites. The degree of similarity (or otherwise) between sites and groups of sites is indicated by the height (Y-axis) of the respective connecting horizontal line. The lowermost horizontal lines join sites or groups of sites with the most similar chemistry.

Selection of appropriate threshold lines divides the sites into clusters with similar chemistry. In this investigation, a threshold is selected to divide the sites into five hydrochemical clusters, providing an appropriate degree of distinction. Figure 3.2 displays the AU and BP p-values for the subdivision of clusters on the dendrogram. The selected separation threshold divides the sites into five clusters, each having an AU p-value that is >95. Any lower selection threshold is not applied in this investigation because it would produce some subdivisions with non-significant hydrochemical differences (AU p-values <95).

Table 3.1 summarises the hydrochemical features and geographic distribution of the five clusters defined by the HCA. and provides interpretations for the main controls of hydrochemistry. The range of site-specific median values for each parameter are displayed as a box-whisker plot in Figure 3.3. The site cluster assignments are mapped in Figure 3.4.

Table 3.1 Hydrochemical characteristics of the five HCA-defined clusters.

Cluster	Description	Interpretation
1	64 groundwater sites and 16 surface water sites. Lower TDS than other clusters, usually with Ca and HCO_3 as the dominant cation and anion, respectively. Low NO_3-N and low or non-detectable NH_3-N, Fe and Mn. Wide-spread geographic occurrence. Median field DO concentrations at 30 groundwater sites range from <0.1 mg/L to 8.3 mg/L.	Oxic rivers and river-recharged groundwaters with little or no elevation of nutrient concentrations.
2	23 groundwater sites and 12 surface water sites. Similar hydrochemistry to cluster 1 except for having higher TDS and higher concentrations of Ca and HCO_3. Low NO_3-N and low or non-detectable NH_3-N, Fe and Mn. Geographically most prevalent in-land and along the margins of the Heretaunga Plains. Median field DO available at 10 groundwater sites range from <0.1 mg/L to 3 mg/L.	Oxic rivers and river-recharged groundwaters associated with limestone or carbonate geology, with little or no elevation of nutrient concentrations.
3	10 groundwater sites and no surface water sites. Moderate TDS with Na or Ca as the dominant cation and HCO_3 as the dominant anion. NO_3-N indicative of moderate land-use impact, suggesting rainfall recharge. Low or no detectable NH_3-N, Fe or Mn. May be associated with shallower wells but otherwise no clear geographic pattern to occurrence.	Oxic rainfall-recharged groundwaters with moderate land-use impact.
4	11 groundwater sites and no surface water sites. Moderate TDS with Na or Ca as the dominant cation and HCO_3 as the dominant anion. Strongly elevated Fe, Mn and/or NH_3-N with low or no detectable NO_3-N. Higher SRP than other clusters. May be associated with deeper wells near the coast.	Anoxic groundwater with chemistry typical of natural conditions.
5	2 groundwater sites and no surface water sites. Higher TDS than any other cluster with Na and Cl as the dominant cation and anion. Strongly elevated NH_3-N and low but detectable NO_3-N. Detectable Fe and Mn. No clear geographic pattern to occurrence.	Anoxic groundwater potentially influenced by wastewater.

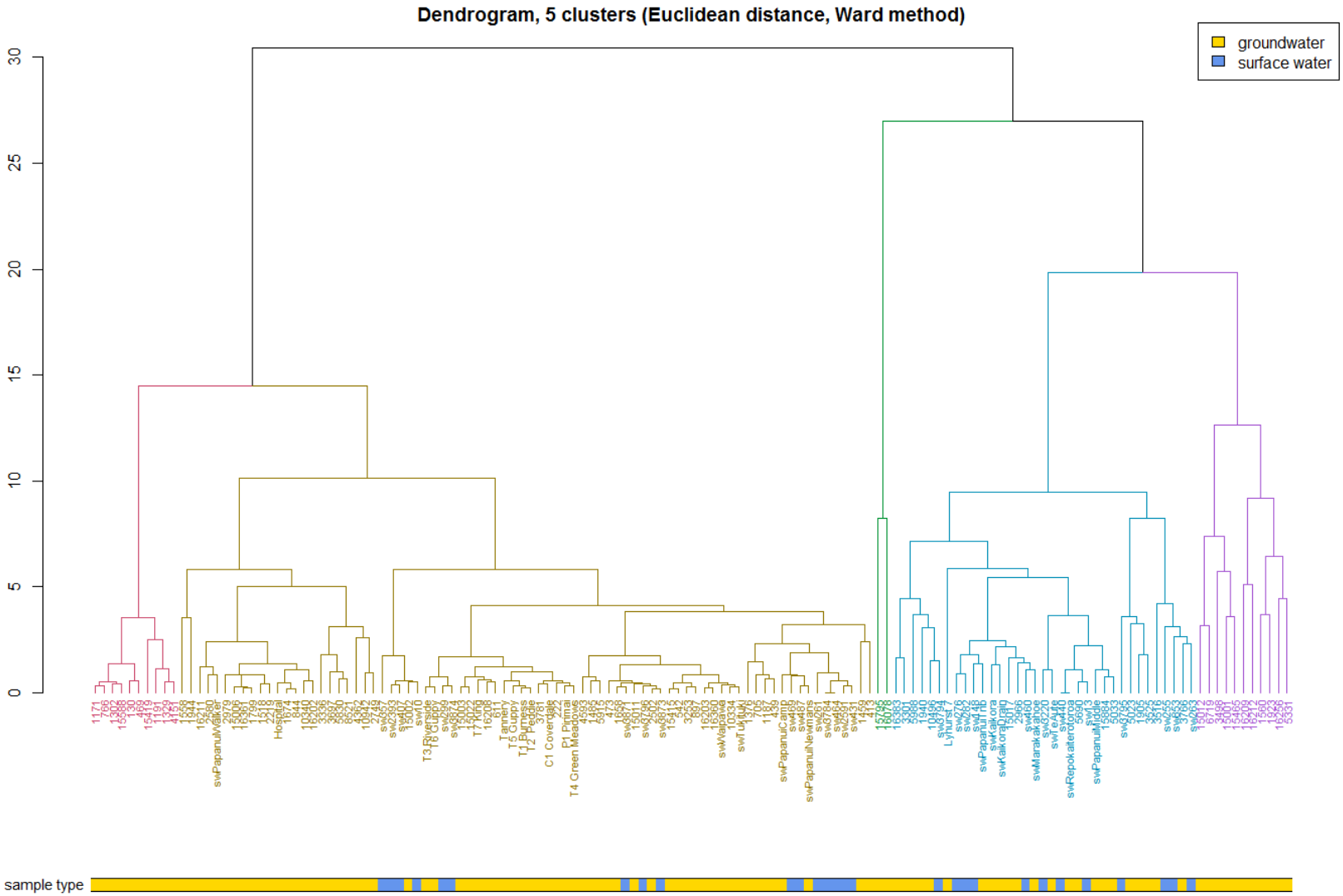

Figure 3.1 Dendrogram produced by hierarchical cluster analysis of 115 groundwater sites and 28 surface water sites in the Heretaunga Plains, based on site-specific median values of Ca, Na, K, Mg, HCO3, Cl, NO3-N, NH3-N, SRP, Mn, Fe, pH and TDS. Colours are used to group the samples into five hydrochemical categories.

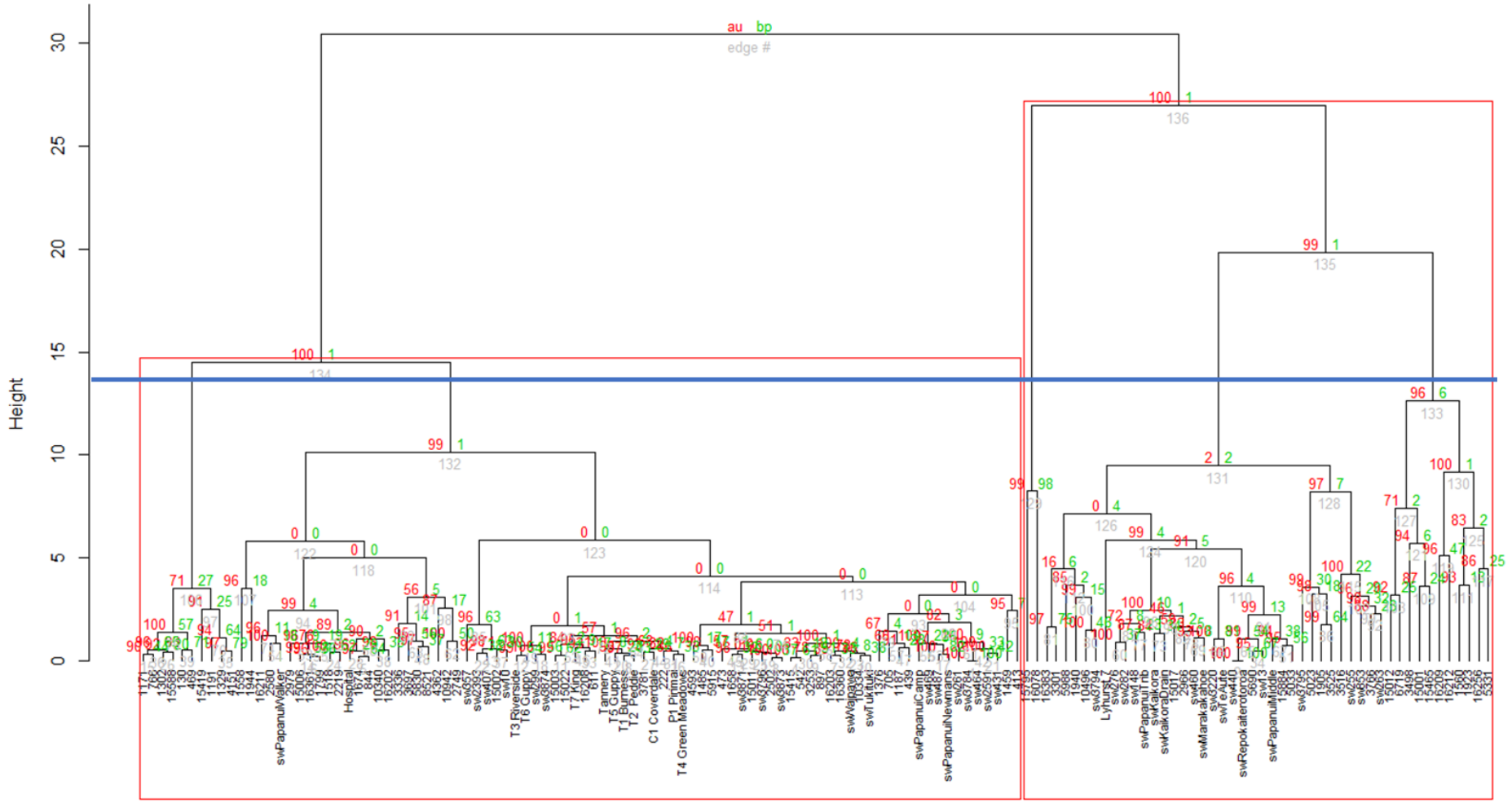

Figure 3.2 P-values produced by pvclust and selected separation threshold (blue line), corresponding to the dataset and colour coding used in the dendrogram in Figure 4.1.The Approximately Unbiased (AU) p-values and the Bootstrap Probability (BP) p-values are shown in red and green text, respectively. The selected separation threshold divides the sites into five clusters with all subdivisions significant at a confidence level of >95%.

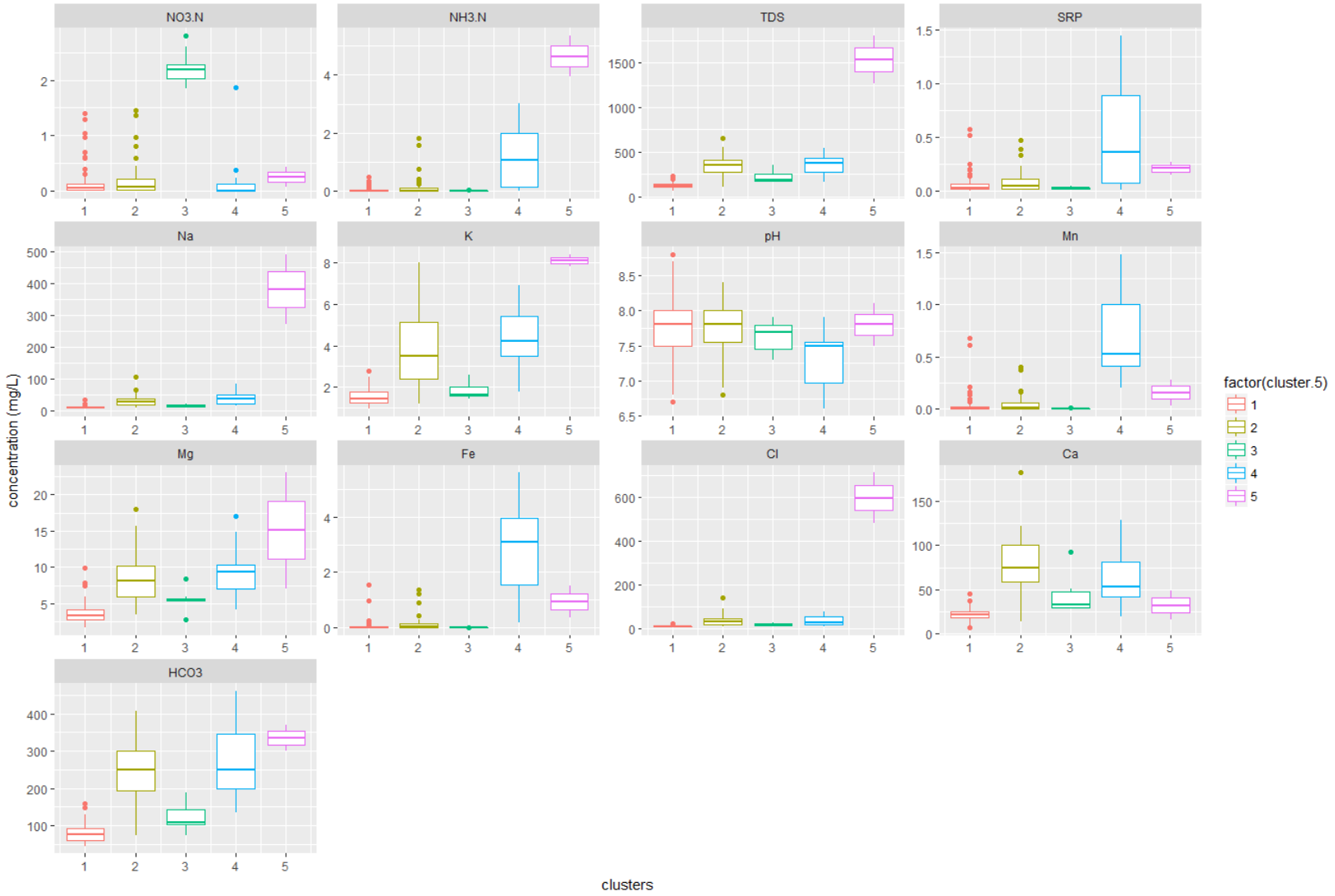

Figure 3.3 Box-whisker plots showing range of site-specific median values in each of the five clusters defined by hierarchical cluster analysis. Note that colours do not correspond to those used on Figure 4.1.

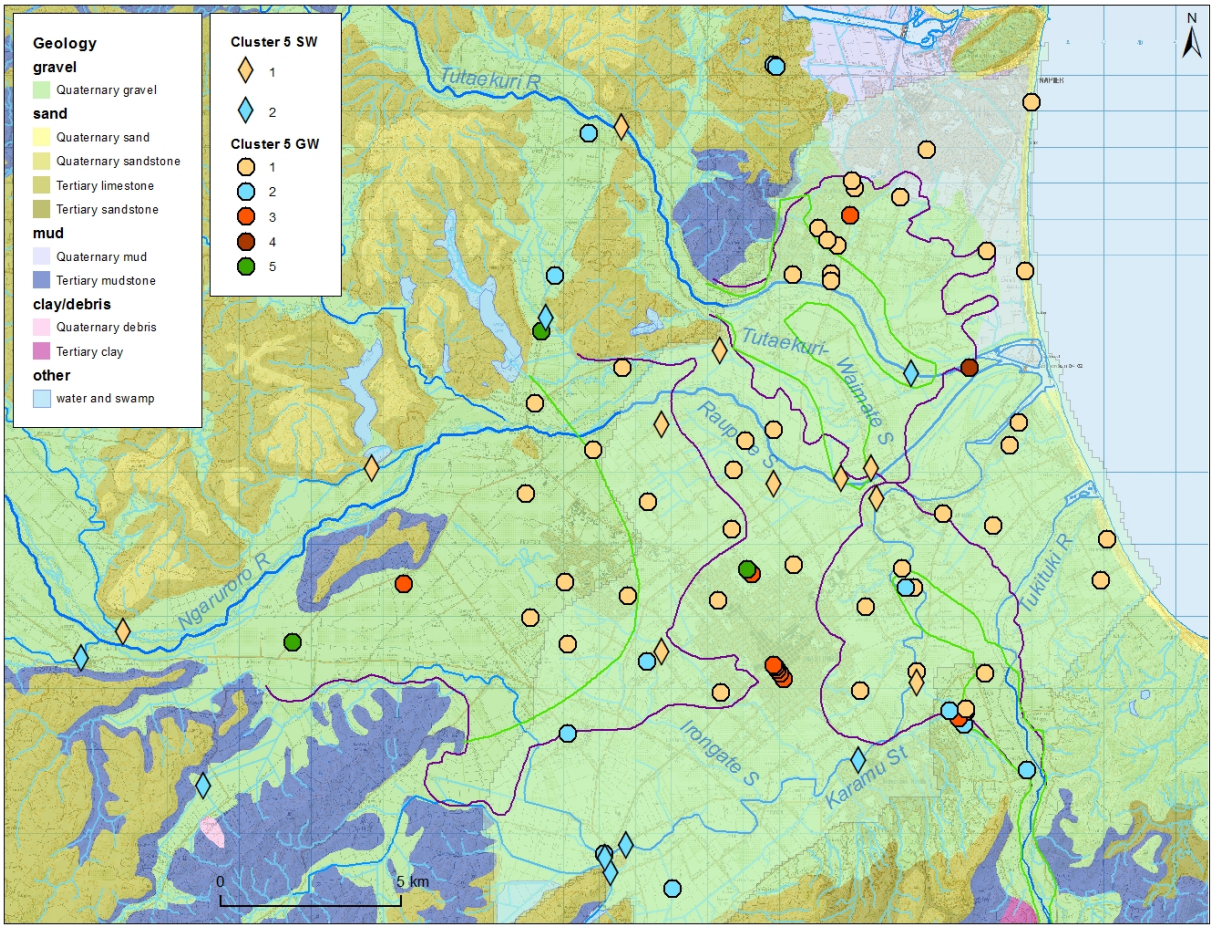

Figure 3.4 Map of hydrochemical cluster assignments for groundwater (circles) and surface water (diamonds) sites considered in this study, with clusters described in Table 3.1. Green and purple lines indicate surface and subsurface extension of the Holocene river gravel fans, respectively.

3.2 STABLE ISOTOPES OF WATER

Stable isotope ratios $^{2/1}H$ and $^{18/16}O$ in groundwater and surface water have been assessed to identify any patterns in these ratios that may be used to distinguish between recharge derived from rivers with higher altitude catchments and recharge derived from local rainfall. The ratios are expressed as δ values where:

$$\delta\ ^{18}O_{VSMOW}\ (‰) = [(^{18}O/^{16}O)_{sample}/(^{18}O/^{16}O)_{VSMOW}\ - 1] \times 1000$$

δ^2H is calculated in a similar manner. The δ values represent the difference in parts per thousand between isotope ratios in water relative to those in Vienna Standard Mean Ocean Water (V-SMOW).

Results show that $\delta^{18}O$ values for groundwater range from -9.6 ‰ to -5.3 ‰ (with a median value of -7.8‰) and δ^2H values between -64 ‰ and -30 ‰ (median -49 ‰). Isotopic values reflect the prevailing weather patterns of the region and plot between the Local Meteoric Water Line (LMWL) for ^2H and ^{18}O ($\delta^2H=8x\delta^{18}O$ +13) that has been previously observed in westerly rainfall and river water in New Zealand and the Global Meteoric Water Line (GMWL) ($\delta^2H=8x\delta^{18}O$ +10) (Stewart and Morgenstern 2001). In comparison, $\delta^{18}O$ values from streams and rivers in the region measured in 2015–16 range between -7.7 ‰ and -5.8 ‰, and for δ^2H between -49 ‰ and -41 ‰ (Figure 3.5). The surface waters sampled in 2015–16 exhibit a positive bias due to evaporation, as they were sampled at the end of summer. Rivers generally

show a strong seasonal fluctuation, primarily due to temperature effects (Figure 3.6). Average values for the Tukituki and Ngaruroro Rivers, from monthly data collected between June 2009 to September 2010 at Red Bridge on the Tukituki River and at Chesterhope on the Ngaruroro River are -7.0 ‰ and -8.0‰ for $\delta^{18}O$ respectively; and -45 ‰ and -53 ‰ for $\delta^{2}H$ respectively (Figure 3.5).

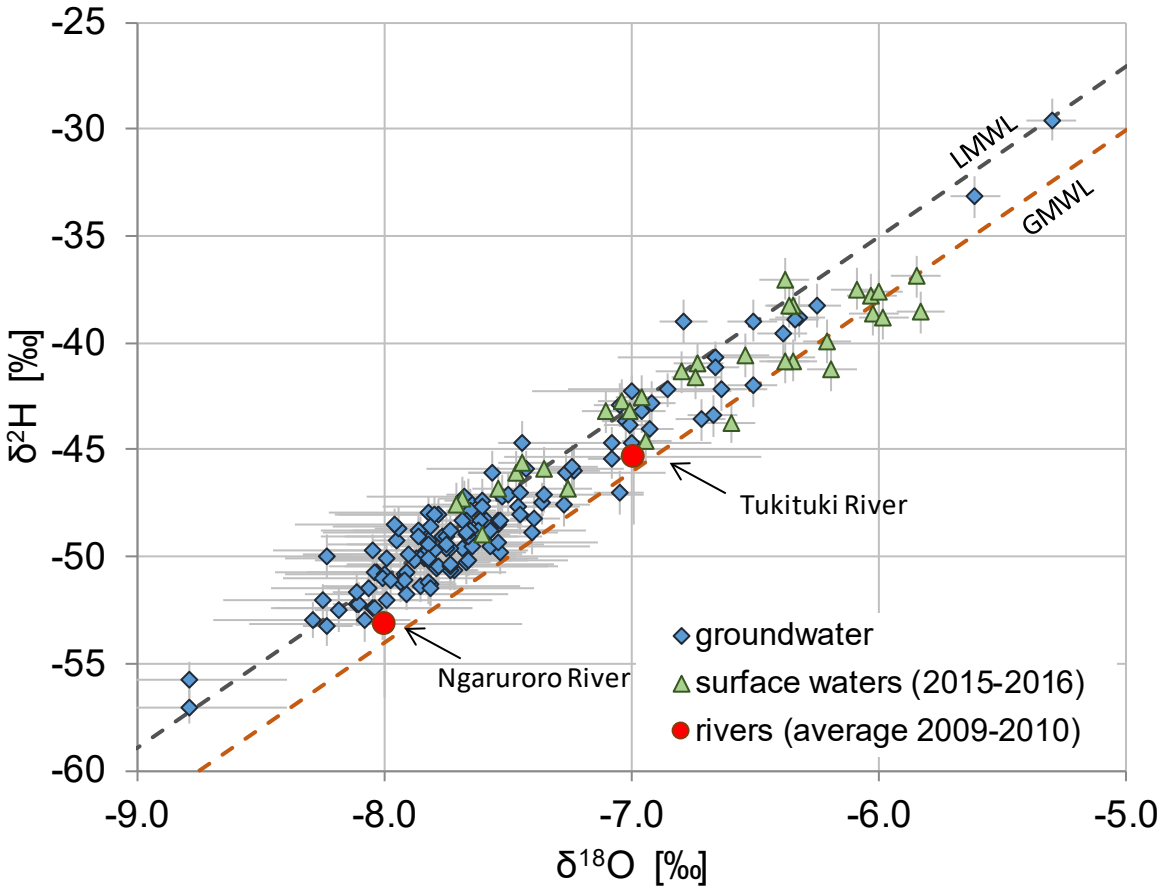

Figure 3.5 Plot of $\delta^{18}O$ against $\delta^{2}H$ for groundwater and surface water in the Heretaunga Plains. Groundwater and surface water data are shown in blue and green, respectively. Average values of selected rivers (obtained from monthly data between June 2009 to September 2010) are shown in red. The grey dashed line is the Local Meteoric Water Line ($\delta^{2}H=8x\delta^{18}O+13$) observed for river water and rainfall in the west of New Zealand, while the orange dashed line is the Global Meteoric Water Line ($\delta^{2}H=8x\delta^{18}O+10$) (Stewart and Taylor 1981).

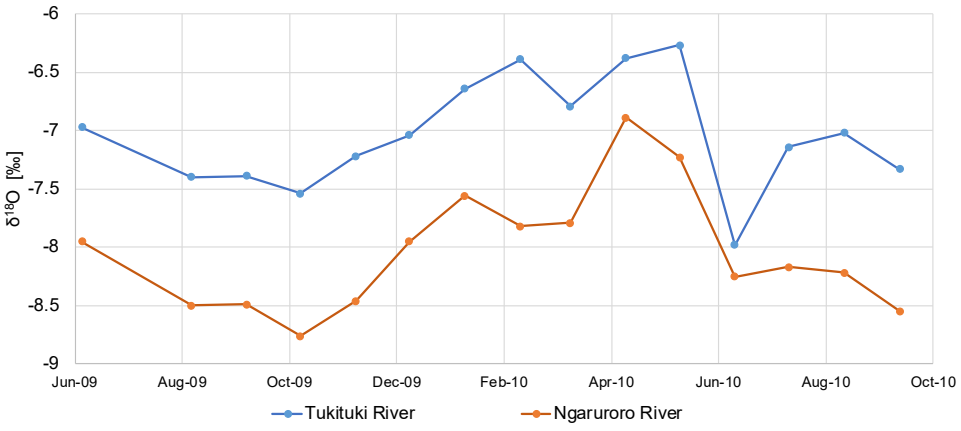

Figure 3.6 Seasonal δ18O variation for the Tukituki and Ngaruroro Rivers.

In general terms, stable isotope ratios become more negative (depleted) as rain moves inland from the coast, due to rain-out effects (Rayleigh distillation) as well as the effects of temperature and altitude. This is apparent in the isotopic signatures of the Tukituki and Ngaruroro rivers, with headwaters of the Ngaruroro River being at higher altitude than Tukituki headwaters (Figure 3.5 and Figure 3.6). There is a contrast between the isotopic ratios observed in the Ngaruroro River and those of local rainfall in the Napier area, which on average are expected to be less negative than -7 ‰ for $\delta^{18}O$ and -45 ‰ for $\delta^{2}H$ (Brown et al. 1999, Baisden et al. 2016). Rainfall has considerable seasonal variability in isotopic signature, but this variability is considerably smoothed during infiltration to the groundwater zone (Stewart and McDonnell 1991). This allows for differentiation between recharge derived from the Ngaruroro River and recharge from local precipitation. Figure 3.7 shows the geographic distribution of $\delta^{18}O$. Much of the groundwater in the central part of the plains and also that close to Napier City appears to have a substantial river derived component. On the south-eastern side of the plains, the possible influence of recharge from the Tukituki River, which also has a less negative isotopic signature, confounds the distinction between local rainfall and river recharge (Figure 3.5 and Figure 3.7).

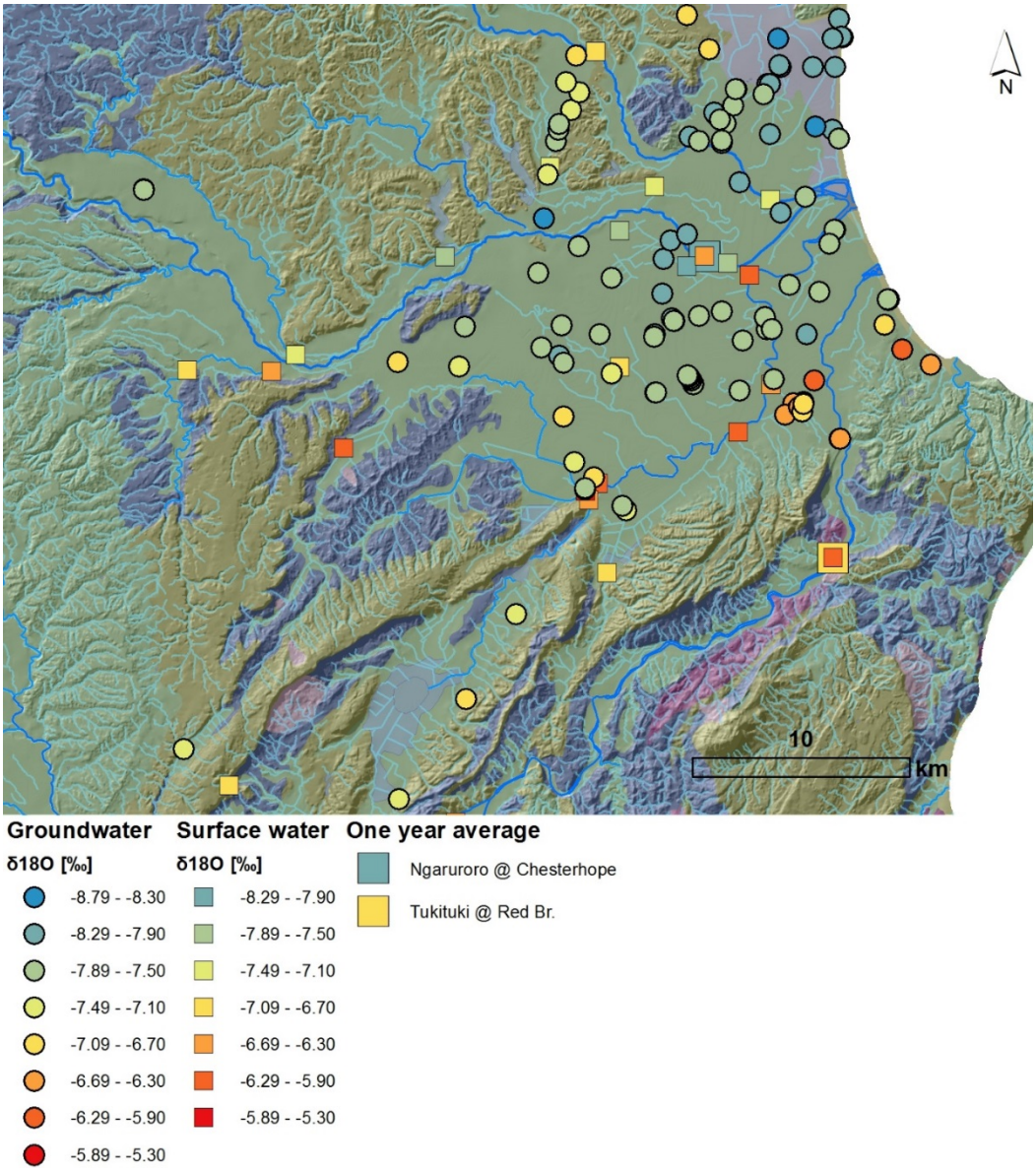

Figure 3.7 Geographic distribution of $\delta^{18}O$ in river water and groundwater in and around the Heretaunga Plains. For the geology colour code refer to Figure 2.7.

Comparison of stable isotope ratios to analytes such as nitrate and chloride often help to elucidate the recharge sources of groundwater. River water generally has low concentrations of these analytes, which do not increase significantly in gravel river beds, and is reflected in groundwater recharged from river sources. Rainfall-recharged groundwater has higher concentrations of these analytes as they are leached by water from the soils and finer sediments.

A plot of $\delta^{18}O$ against chloride concentrations shows that high chloride (>20 mg/L) concentrations generally occur in groundwater with less negative (enriched) isotopic ratios above -7.7 ‰ (Figure 3.8). Groundwater with less negative (enriched) isotopic ratios above -7.7 ‰ accompanied by high chloride are likely to have significant recharge contribution from local rainfall. Groundwater with more negative (depleted) isotopic values (around -8 ‰) have lower chloride concentrations, likely reflecting recharge from the Ngaruroro River, which has longer term average $\delta^{18}O$ of -8.0 ‰. A similar relationship is observed for $\delta^{18}O$ and nitrate concentrations (Figure 3.8).

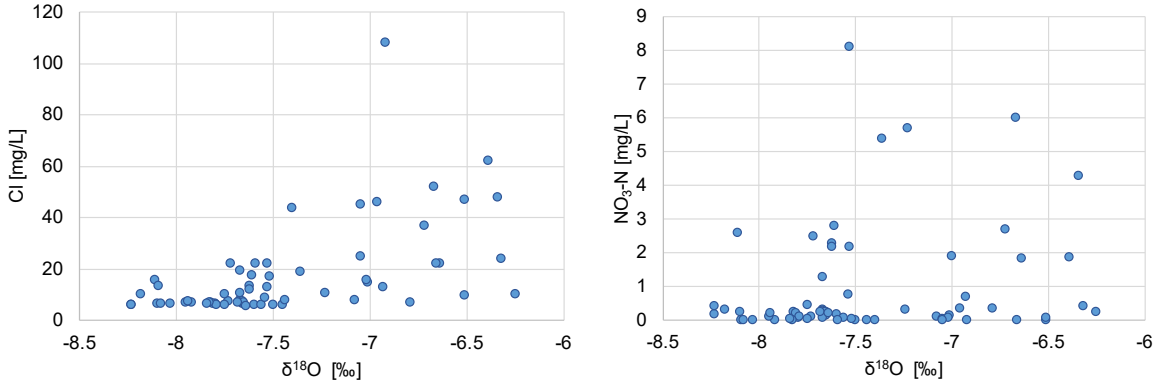

Figure 3.8 Plot of $\delta^{18}O$ versus chloride concentrations (left) and versus nitrate-N concentrations (right).

3.3 RADON IN GROUNDWATER

Radon-222 (Rn) is a soluble colourless, gaseous, unstable isotope (Cecil and Green 2000). It is generated as part of the uranium decay series. Uranium is ubiquitous in almost all rocks and soils, resulting in the release of radium, and subsequently radon, from uranium-bearing minerals in groundwater (Stellato et al. 2013). Radon is abundant in groundwater but has almost negligible concentrations in surface waters due to a short half-life of 3.8 days (Cecil and Green 2000) and because radon rapidly degasses when exposed to air (Garcia-Vindas and Monnin 2005, Kies et al. 2005). Thus, surface waters with elevated concentrations of radon indicate a location where groundwater is freshly discharging into the surface water. Conversely, groundwater which has lower than expected radon concentrations can indicate surface water recharge, as surface water with negligible concentrations of radon entering the groundwater system take approximately 3 weeks (5–6 half-lives) to equilibrate to the ambient concentration of the groundwater (Close et al. 2014, Stellato et al. 2013).

Radon concentrations can vary considerably within groundwater systems and are affected by the uranium content and radon emanation potential of the aquifer material. Generally, geological units that are higher in uranium will produce groundwater higher in radon. For example, quartzite can have radon concentrations of over 900 Bq/L, whereas sands or ignimbrites can have radon concentrations of less than 3 Bq/L (Cecil and Green 2000).

Radon can also be removed from the water by adsorption onto organic material such as peat. Due to the short half-life of radon, all of the isotope decays before the reverse process of

desorption occurs, resulting in groundwater having a zero or very low radon concentration (Morgenstern et al. 2012).

Within the Heretaunga Plains, 35 groundwater samples have been collected and analysed for radon. The measured radon concentrations range from 7.6 Bq/L to 44.7 Bq/L. The distribution of radon concentrations is shown in Figure 3.9 and their geographical locations are identified in Figure 3.10. Almost all of the measured radon concentrations fall within the range of concentrations previously observed in other New Zealand studies in quaternary gravels (Martindale et al. 2016). However, one site (well 3699), was below this expected range, with a radon concentration of 7.6 Bq/L. This lower concentration of radon can be an indicator for a number of phenomena, including: recharge of surface water to the groundwater system; contamination with air during sampling; an indication of low amounts of material containing the uranium-parent; adsorption of radon on organic material; or highly evolved conditions to the stage of methane fermentation causing degassing. The latter two reasons for the observed low concentration are more likely given the groundwater chemistry, well depth and the groundwater age data for well 3699 indicating an MRT of 140 years (below).

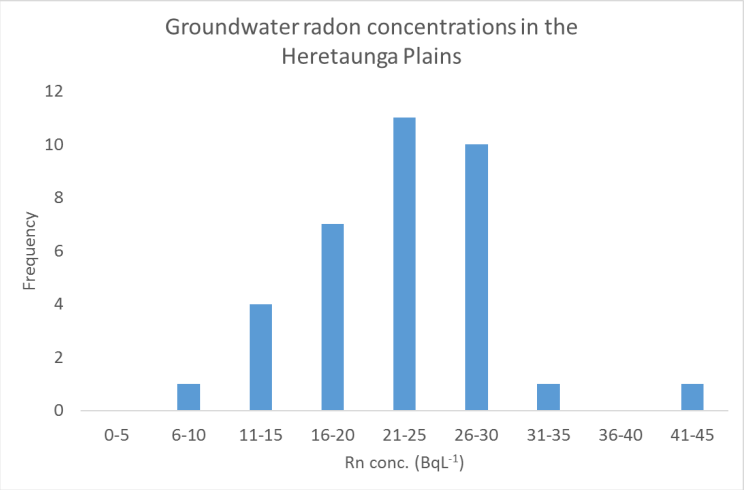

Figure 3.9 Distribution of measured radon concentrations within the Heretaunga Plains.

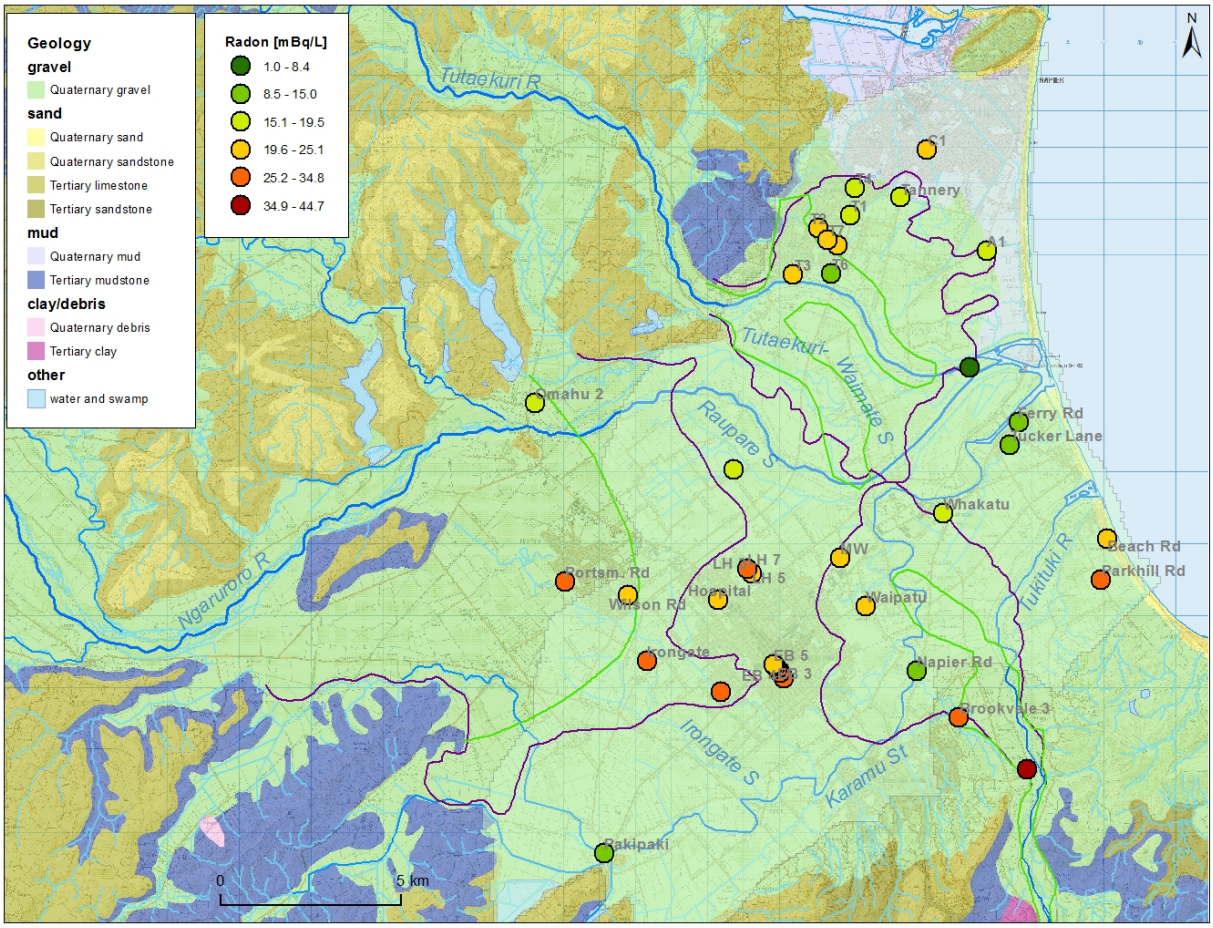

Figure 3.10 Radon concentrations measured in the Heretaunga Plains groundwater. Green and purple lines indicate surface and subsurface extension of the Holocene river gravel fans, respectively.

Groundwater associated with limestone (elevated calcium, Figure 4.17) in the southern part of the Heretaunga Plains has the highest radon concentrations. The higher radon concentrations are also associated with low phosphorous and iron concentrations, indicating that the low radon concentrations are partially a result of radon removal in highly anoxic conditions, e.g. adsorption onto organic matter (Section 4.5.6).

3.4 Recharge Temperature and Excess Air

Recharge temperature and excess air, calculated from Ar and N_2 concentrations, can provide insight into the mechanisms controlling recharge. Ingram et al. (2007) found that excess air concentrations are linked to the magnitude of fluctuations in groundwater level and used this relationship to delineate recharge sources and rates. River-recharged groundwaters, where groundwater levels might be expected to show small fluctuations, can have lower excess air concentrations than rainfall-recharged groundwater in areas with large groundwater level fluctuations. Apparent high excess air concentrations caused by denitrification, and/or the presence of excess N_2, are also indicative of recharge source, as high nitrate concentrations are associated with land surface (rainfall) recharge.

Recharge temperatures and a component of dissolved excess air have been derived from dissolved argon and nitrogen concentrations using the total dissolution model of Heaton and Vogel (1981). In this model, small bubbles of air entrapped in soil pores are completely dissolved into the groundwater under favourable recharge conditions, thus forming an excess air component. Plotting the measured concentrations of argon and nitrogen against each other

indicates the recharge temperature, as well as the amount of excess air in the samples (Figure 3.11).

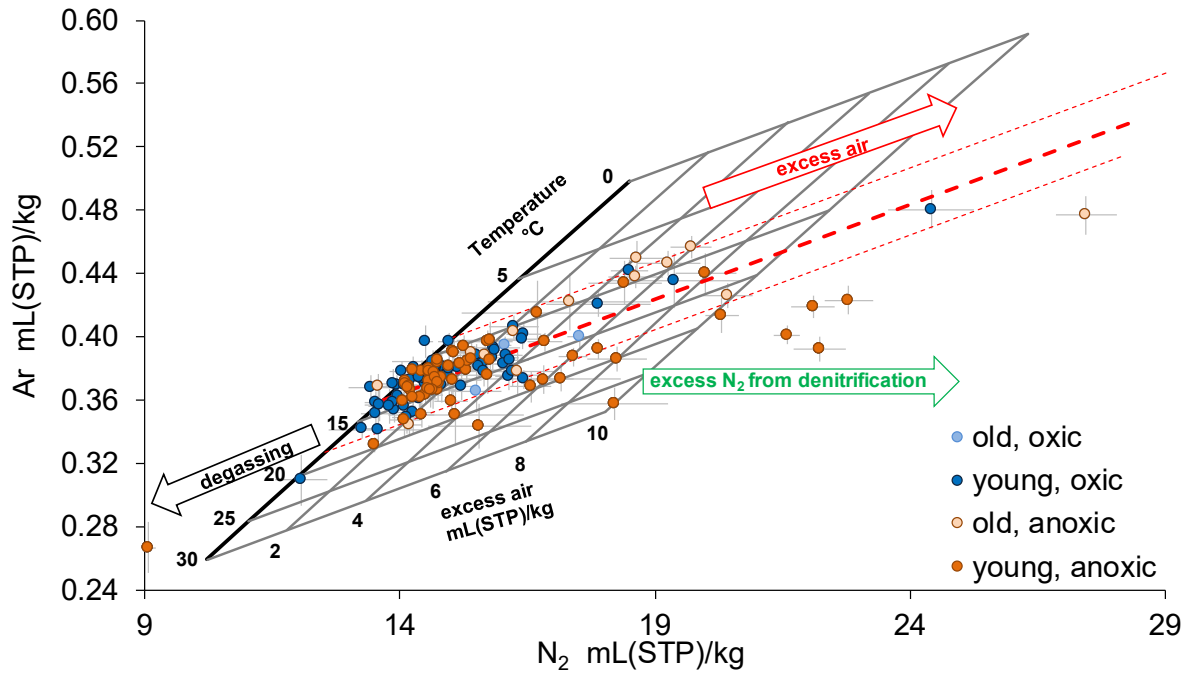

Figure 3.11 Plot of dissolved nitrogen versus dissolved argon concentrations, normalised to sea level, from all available data (historic and that collected for this study) in the study area.

The positions of the samples within the grid indicate their recharge temperatures and excess air concentrations (Heaton and Vogel 1981). The bold line on the left of the grid is for gas concentrations in water which are in equilibrium with the atmosphere. Dissolved Ar, N_2 and excess air concentrations are expressed in mL of the respective gas at standard temperature and pressure (STP=273.15 °K, 101.325 kPa) per kg of water. The dashed bold red line is the mean recharge temperature (13.1°C) of oxic groundwaters (with ±2sd limits indicated). The arrows indicate competing processes that can alter gas concentrations. Young groundwaters are those with MRT < 100 years. Anoxic groundwaters are those classed as anoxic or mixed (oxic/anoxic) under the scheme of McMahon and Chapelle (2008) and are shown in orange.

Comparison of dissolved argon and nitrogen concentrations can also allow the identification of "excess" dissolved nitrogen caused by denitrification (Figure 3.11, green arrow). Denitrification is a natural process that is mediated by the metabolism of aquifer microorganisms and by which dissolved nitrate is reduced eventually to nitrogen gas (Chapelle 1993) (Equation 1). This process increases the nitrogen concentration but leaves the argon concentration unaltered, and thus the source can be identified, as distinct from excess air (Figure 3.11, red arrow).

$$NO_3 \rightarrow NO_2 \rightarrow NO_{(g)} \rightarrow N_2O_{(g)} \rightarrow N_{2\,(g)} \qquad \text{Equation 1}$$

Groundwater recharge temperatures are often observed to be similar to the mean annual air temperature of the recharge area (Busenberg and Plummer 1992, Heaton and Vogel 1981). This is dependent on the depth of the unsaturated zone, as dissolved gases are continuously equilibrating with unsaturated zone air until isolated from air in the saturated zone. Mean annual air temperatures for the region over the period 1981–2010 range from 13.1°C in Whakatu to 14.6 °C in Nelson Park, Napier (NIWA National Climate Database 2017). Derived

recharge temperatures from the entire dataset range from 7.4°C to 34.0°C, with a median of 13.1°C. Unusually high and somewhat unrealistic recharge temperatures derived from the dissolved Ar and N_2 concentrations are likely to be related to elevated N_2 concentrations resulting from denitrification (Figure 3.11). Denitrification occurs under anoxic conditions - if we exclude groundwater classed as anoxic or mixed (oxic/anoxic) under the classification scheme of McMahon and Chapelle (2008), recharge temperatures for the remaining oxic groundwaters range from 8.0°C to 20.9°C (median of 13.0°C).

Excess air concentrations range from -3.1 mL(STP)/kg to 21.2 mL(STP)/kg. Negative excess air concentrations indicate that the gas tracers at these wells have been influenced by degassing (Figure 3.11, black arrow). Most of the highest excess air concentrations appear to have been altered by denitrification, and the highest excess air concentration from oxic groundwater is 14.4 mL(STP)/kg. The spatial distribution of excess air is shown in Figure 3.12.

Excess N_2 from denitrification has been estimated for selected sites which have Ar/N_2 derived recharge temperatures that fall above 2 standard deviations of the mean recharge temperature for oxic sites (which are expected to be unaffected by denitrification). A correction to the excess air concentrations at these sites has also been made (Figure 3.12). Other sites with anoxic groundwater may also be affected by excess N_2, but this is not as quantifiable as the recharge temperatures because these sites fall within the same range as for the oxic sites. Excess N_2 concentrations range between 0.2 mL(STP)/kg and 4.2 mL(STP)/kg for 16 sites (median 1.5 mL[STP]/kg). Equivalent nitrate concentrations, assuming all of the excess nitrogen is derived from denitrification, range from 0.3 mg/L to 5.3 mg/L. These nitrate concentrations are likely to be an underestimation of the original nitrate concentrations in the groundwater preceding denitrification for several reasons: firstly, the estimation of excess N_2 is conservative and the actual recharge temperatures for these sites is probably lower than 2 standard deviations above the mean recharge temperature for oxic sites; and secondly, losses of nitrate to other gaseous forms (e.g. N_2O) may also be occurring.

Comparison of excess air concentrations to other parameters linked with recharge source, such as chloride and nitrate concentrations do not show a clear relationship of this type for the current dataset. However, comparison of excess air concentrations to $\delta^{18}O$ show a possible relationship whereby the majority of high excess air concentrations are associated with less negative $\delta^{18}O$ values > -7.75 ‰ (Figure 3.12) such as might be expected for land surface (rainfall) recharge (Section 3.2).

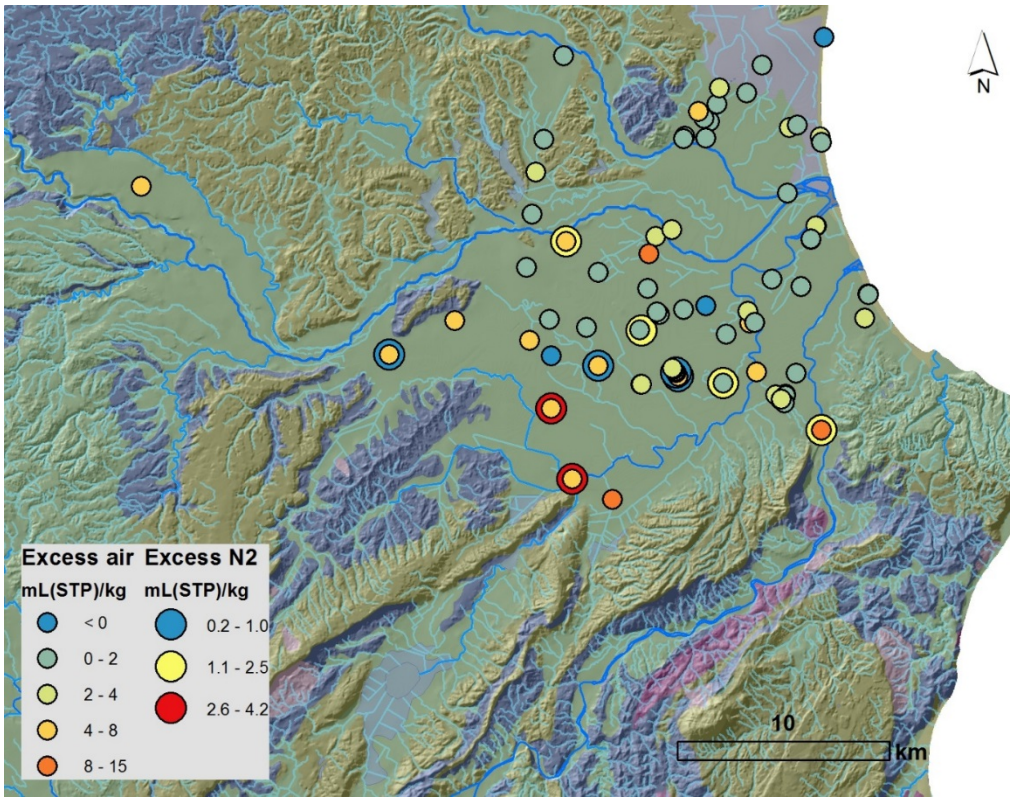

Figure 3.12 Geographic distribution of excess air (mL[STP]/kg) in groundwater samples on the Heretaunga Plains. For the geology colour code refer to Figure 2.6. Excess N_2 from denitrification as described in the main text is indicated by the larger circles. Excess air concentrations for these sites have been corrected.

3.5 GROUNDWATER DATING

3.5.1 Age tracers

The methods for groundwater dating in the Southern Hemisphere are described in Morgenstern and Daughney (2012) and in Appendix 1. Groundwater dating utilises convolution of a known tracer input via the rain into the groundwater, with a suitable system response function, and matching to the tracer concentration measured in the groundwater. A range of groundwater source and age tracers are available (Beyer et al. 2014), which should be applied in a complementary way, as application of a single tracer can result in ambiguous interpretations. Multi-tracer approaches can improve the robustness of the age interpretation and help us to understand groundwater recharge processes. In New Zealand, we routinely use the most robust and cost-effective tracers, i.e., tritium, SF_6, CFCs, Ar, and N_2.

Tritium has now become the most robust groundwater dating tool in New Zealand. Due to the lower impact in the Southern Hemisphere from bomb tritium produced during atmospheric nuclear weapons testing in the early 1960s in the Northern Hemisphere, this relatively small amount of bomb-tritium has now decayed and no longer produces ambiguous age interpretations for New Zealand hydrologic systems. Tritium now also allows the dating of river and stream water. In other parts of the world, the application of accurate and robust groundwater dating for the understanding of hydrological systems on large scales with respect to groundwater lag times, storage, and recharge, hydrochemical evolution, and land use versus geologic impact on groundwater quality, is not yet possible. Therefore, this method currently leads to a significant improvement in the understanding of hydrologic systems in both national and international contexts.

For the interpretation of age tracers, it is important to understand that gas tracers in groundwater samples can be contaminated due to air contact during sampling or in the well head, and in the aquifer due to anthropogenic sources in the recharge area (Appendix 1, and Morgenstern et al. 2017). In contrast to many other regions of New Zealand, where contamination is commonly found near industrial and horticulture areas (Morgenstern and Daughney 2012), there are no extremely high CFC contaminations detected in the Heretaunga Plains aquifer area. Only very few groundwater sites in the Heretaunga Plains aquifers show significant CFC contamination. Therefore, CFC contamination through anthropogenic point sources probably only has a minor impact on dating young groundwater. On the other hand, these elevated point-source CFC concentrations can be used to identify recharge from local rain as elevated CFC concentrations do not occur in river water.

Tritium in rain of the Heretaunga Plains and in the higher altitude rivers is expected to show a slight spatial variability. Near the coast, where there is a direct input of air masses from the ocean, tritium is expected to be lower in concentration compared to rainfall further inland, due to dilution of tritium-rich high altitude meteoric water by low-tritium oceanic moisture. For this study, the rain tritium record for Kaitoke Regional Park (40 km north of Wellington) was used but scaled by a factor between 0.93 and 1.00, with 0.93 used for rain close to the coast, and 1.00 used for the large rivers with significant high-altitude catchments.

Groundwater usually comprises a mixture of water of different ages due to mixing processes underground. We used the Exponential Piston Flow Model (EPM) to account for mixing of groundwater with different flow-path lengths, and therefore different age (Appendix 1). For wells with a long well screen interval in unconfined conditions, a high fraction of exponential (mixed) flow of 80–95% was applied. For wells with a narrow screen interval in confined conditions, a low fraction of exponential flow of 50–60% was used, according to Morgenstern and Daughney (2012).

For most of the drinking water wells — those with a long and multi-age tracer time series available — the gas tracer data and the most recent tritium data were inconsistent with the outputs of a simple EPM model. This indicates that more complex mixing models are required for such a complex hydrogeological setting, where wells intersect several discrete vertical layers of a heterogeneous aquifer due to the inter-fingering of the Holocene river gravel fans with the main aquifer and the extent to which waters from distinct sources are mixed (Section 2.2). We used binary mixing models (BMM) consisting of two parallel EPMs. A BMM consisting of just two parallel EPMs was sufficient to resolve misfit with tracer data. This new mixing model approach is explained in the following section 3.5.2.

The age distribution parameters, MRT and fraction of exponential flow within the total flow volume (E%PM), are listed in Appendix 2 and 3, and in the supplementary electronic file (Summary Age Data.xlsx). Except for the drinking water wells that have time series data, in most cases the mixing fraction had to be estimated. For most of the drinking water wells there were sufficient time series data available to establish the mixing fraction, or the parameters for a BMM. Tritium data were usually used as the most robust age tracer data.

3.5.2 Binary mixing models

Tritium data-sets collected from the drinking water wells in 2016 — the first time when the tritium data was no longer affected by the bomb spike — showed that for some wells a simple EPM could not fit both the historic and the 2016 tritium data. The SF_6 data from the 2016 data set was now robust enough to indicate that a simple EPM could also not fit both the SF_6 and the tritium data. It became obvious that a more complex mixing model was required for these

wells. The need for a more complex mixing model in parts of the aquifer is also supported by the refined geological model (Section 2.2).

The need for a more complex mixing model is demonstrated by the data of a bore that has excellent time series data (Figure 3.13). The tritium time series (1–5) can be matched with the EPM mixing model, commonly applied to such hydrogeological settings, with an MRT of 42 years (blue curve). However, the 2016 tritium data point (6) indicates that this model is not sufficient. Tritium no longer matches the proposed EPM model as indicated by the mismatch of the model output (blue line) with the measured data (red points). The measured tritium in 2016 is too high for this model. Using a simple EPM model, the 2016 tritium concentration (6) indicates that the water is younger (pink curve).

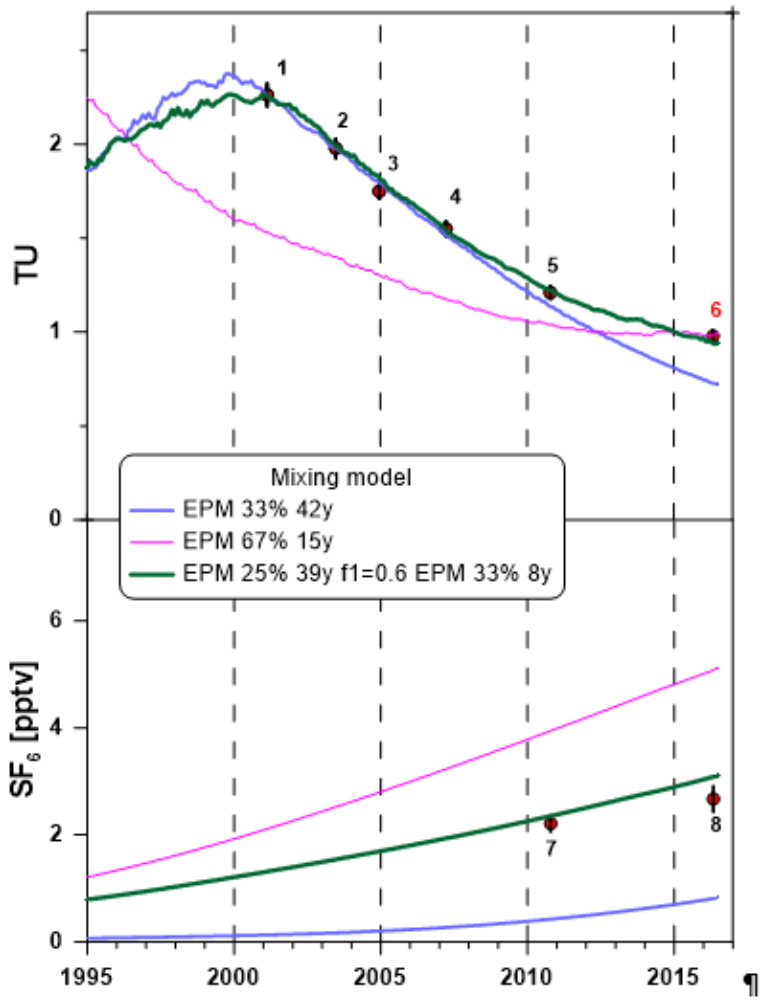

Figure 3.13 Age interpretation of HDC drinking water bore at Tucker Lane, Clive.

Furthermore, the SF_6 data (7+8) do not match the blue model curve in this example. SF_6 concentrations are too high to be consistent with such old water. The measured SF_6 concentrations (7+8) would also not match a younger EPM age model (pink curve). However, the consistent trend of the SF_6 data indicated that the SF_6 data can be considered robust.

We applied various BMM and obtained good fits between the model output and the measured data with a binary model of parallel connection of two EPMs. Such a model is able to match all the data 1–8 (green curve), tritium time series and SF_6. The hydrogeological explanation for such BMM is that in some wells young water from shallow aquifers is mixed with older water from deeper aquifers.

4.0 DISCUSSION — GROUNDWATER DYNAMICS AND PROCESSES

In this section, the surface water and groundwater tracer results of the techniques listed above are interpreted with respect to catchment storage and retention processes, and groundwater dynamics from recharge to discharge, interaction with surface water, recharge source, and understanding of the processes that control groundwater hydrochemistry (quality), including denitrification. The techniques are complementary and the results improve significantly by integrating all techniques.

4.1 SURFACE WATER LAG TIME — AN INDICATOR OF HYDROGEOLOGICAL PROCESSES ON CATCHMENT SCALE

The hydrogeologic properties of geologic formations, such as the ability of the rainwater to enter a groundwater system and the amount of groundwater storage, can be characterised by the mean transit time (MTT) of the water through these formations, the time between rainfall and discharge of the water, for example via springs and seeps into rivers and streams. With increasing contribution of deeper groundwater, associated with larger dynamic groundwater volume, the transit time of the water through these large groundwater stores increases.

Usually water drains from an area through a combination of shallow quick-flow run-off and slow-flow deeper groundwater systems with larger water storage that maintain water flow in the rivers during dry periods. The dynamics of the water movement through catchments, as a result of the interaction between these processes, depend on the hydraulic properties of the geologic formations such as permeability and porosity, and are generally still poorly understood in New Zealand and internationally.

In general, younger clastic sediments, including sand and gravel, have the highest permeability and porosity. However, in many places these young permeable rocks may be thin (e.g., alluvial gravels may be up to a few metres thick). Tertiary sandstone and limestone have moderate to high permeability, whereas finer grained or poorly sorted sediments such as silt, clay and mud have lower permeability. Lithified or indurated rocks may have high or low permeability, depending on jointing and fracture density; more joints allow more connected pore space, thus higher permeability.

To characterise the transit time of the water through the various geologic formations in the Heretaunga Plains and hydraulically connected river catchments, the age tracer tritium was measured in samples collected from rivers and streams that represent the discharge from these geologic formations. Samples were collected from the wider catchments of the main rivers that flow through and potentially interact with the Heretaunga Plains aquifers, and from spring-fed streams within the Heretaunga Plains. Low base flow conditions were chosen for sampling because this allows identification of the oldest water in the flow system, which typically dominates river flow during the summer months when demand for the water resource is greatest including recreation, and when water quality is of greatest concern. Understanding the transit times of water in catchments and groundwater storage is vital for protecting riverine ecosystems, and assessing the impact of contamination and the potential consequences of groundwater pumping on these rivers.

Tritium ages show consistent patterns in the main rivers (Appendix 2, Figure 4.1): MTTs of usually less than 2 years in the Tukituki, Waipawa, and Ngaruroro rivers (green symbols), and somewhat older water with a MTT around 10 years discharging via the Tutaekuri River (yellow orange symbols). Surface water discharging in proximity to limestone, sandstone and mudstone formations (Raukawa and Kaokaoroa Ranges) between the Ruataniwha and the

Heretaunga Plains contain significantly older water, with a MTT of up to 140 years (red symbols), including the Karamu tributaries, which collectively drain this area.

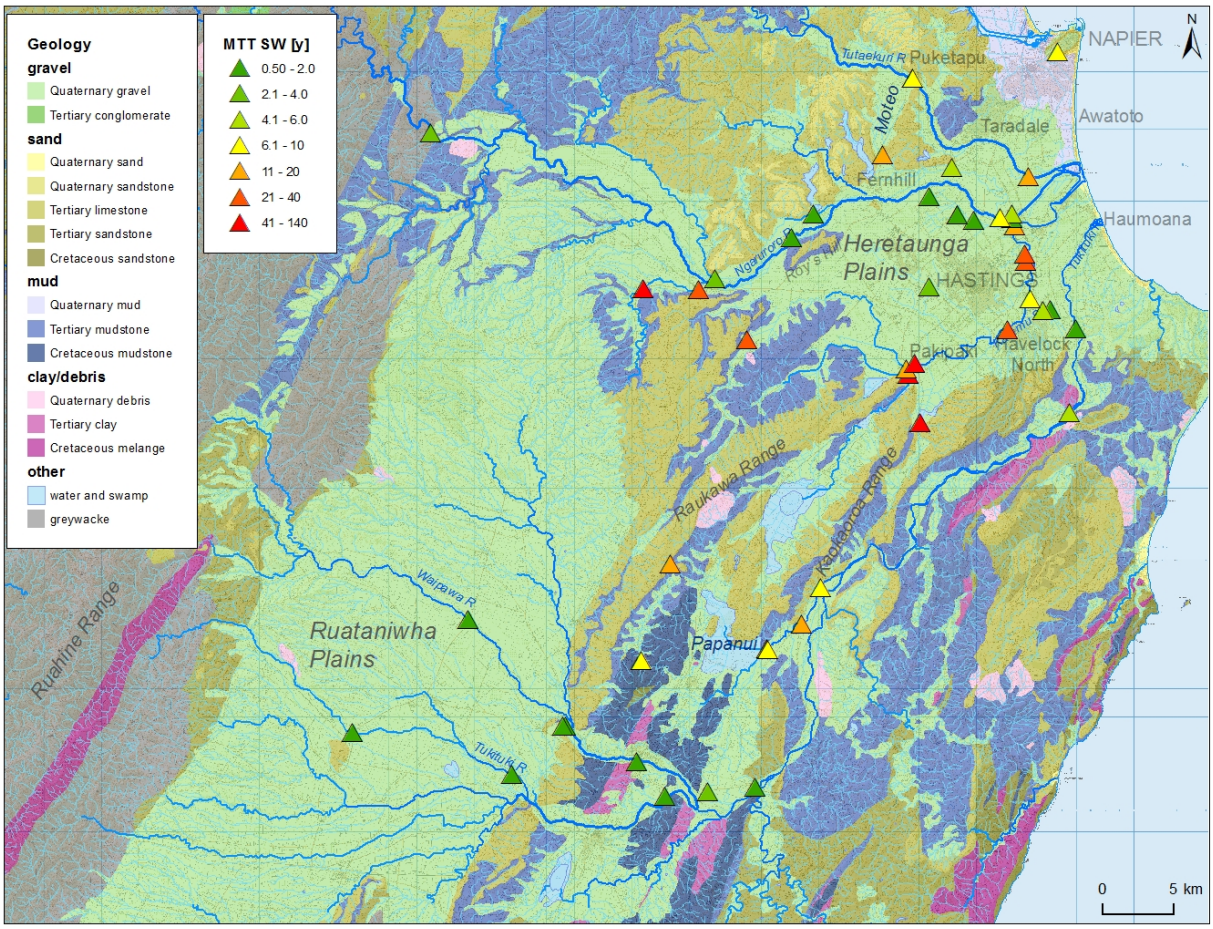

Figure 4.1 Map of mean transit times (MTT) of surface water.

The very young water with a MTT of <2 years in the Tukituki, Waipawa, and Ngaruroro Rivers, draining the eastern Ruahine and Kaimanawa Ranges (north-west of area shown in figure), reflects the nature of their upstream catchments, which have impermeable basement rock such as greywacke near the surface or are covered with only a thin layer of high-permeability gravels, which have short water-retention times. All of these rivers drain consistently young water throughout most of their course, except in the lower reaches where the water is slightly older, with a MTT of c. 3 years, indicating some older water contribution, such as from the limestone formation (Tukituki) or backflow from the Heretaunga Plains groundwater system (Ngaruroro). The drains that contribute to the Raupare Stream also contain very young water, indicating their source is likely the young Ngaruroro River water lost downstream of Roy's Hill.

The Tutaekuri River drains water with a MTT 8–12 years, reflecting its origin from mainly sandstone/mudstone formations. The relatively older age of the Tutaekuri River water indicates a considerable upstream groundwater reservoir, with active throughflow within its catchment. This is consistent with results from the neighbouring Horizons Region, which has similar geology and MTTs (Morgenstern et al. 2017).

The Tutaekuri-Waimate Stream at its upper site (Moteo Road) displays similar MTTs to the Tutaekuri River, supporting its origin from this river. Further downstream (Goods Bridge and Chesterhope), younger MTTs of 6–7 years indicate an additional contribution of younger water to the older Tutaekuri River water in the Tutaekuri-Waimate Stream, also originating from the Ngaruroro River.

The significantly older surface water in proximity to limestone, sandstone and mudstone areas between the Ruataniwha and the Heretaunga Plains, including the Raukawa and Kaokaoroa Ranges, indicates the presence of upstream catchments with considerable subsurface throughflow. Older water discharging in the south of this formation, in the Papanui catchment, was previously reported by Morgenstern and Gordon (2017). The water in the upper Papanui Stream at Walker Road is relatively young, with a MTT of 4 years, similar to that of the drainage channel and limestone springs further up in the Waipawa River gravels, probably reflecting rapid flow of water through the Quaternary gravels lost from the Waipawa River. The Papanui Stream water becomes significantly older further downstream, due to increasing contribution of discharge from the limestone and mudstone areas in its catchment. At Newman's Ford, the Papanui Stream water has a MTT of 8 years (Morgenstern and Gordon 2017). Samples from further to the north in the Kaikora sub-catchment are significantly older compared to those from the southern Papanui sub-catchment, likely due to the higher fraction of Tertiary limestone and mudstone in the Kaikora sub-catchment. All three surface waters from the Kaikora sub-catchment show a limestone signature. The spring water at Te Aute School, with a MTT of 18 years, contains the oldest of all investigated surface waters in the Papanui catchment, reflecting discharge from a purely limestone formation. Further downstream at College Road, the water has a MTT of 10 years (8 years younger), due to an increasing contribution of discharge from mudstone. Further downstream at the confluence with Papanui Stream, the water in Kaikora Stream is again older, with a MTT of 14 years, likely due to discharges of old water from long flow paths in the lower part of the sub-catchment. The combined flow from the older Kaikora and the younger Papanui Stream results in a MTT of 11 years at Middle Road. The younger age of the water of Papanui Stream at Camp David, with a MTT of 7 years, combined with the significant increase of flow despite an insignificant increase in catchment area, again indicates a hydraulic connection to the Tukituki River, with a significant fraction of the water in Papanui Stream at Camp David likely to originate from the Tukituki River.

Extremely old waters discharge from the northern part of the limestone, sandstone, and mudstone area between the Ruataniwha and the Heretaunga Plains, with MTTs up to 140 years. Discharge of such old water, and apparently low drainage density of this area, suggests that this formation exhibits a high permeability, allowing for a high proportion of rain to infiltrate into the geologic formation. This is in contrast to the other aforementioned geological formations surrounding the Heretaunga Plains that preclude significant groundwater flow pathways. Water is discharged, after years or decades of travel time through the formations, at the margin where they intercept less permeable geologic formations, forcing the water back to the surface. This is similar to the hydrogeological controls on groundwater flow found at boundary of the permeable ignimbrite formations with the less permeable fluvial lake sediments in the Lake Rotorua catchment (Morgenstern et al. 2015b).

The downstream portion of the Karamu Stream, at the floodgates, contains slightly younger water implying addition of young water along its course.

The drainage pattern from the river catchments and the limestone formation obtained from the MTTs (Figure 4.1) is supported by calcium concentration data in the surface waters (Figure 4.2) and silica (not shown). High calcium in the older groundwater discharges (Figure 4.1 and Figure 4.2) suggests that high permeability, allowing for high proportion of rain to infiltrate into the geologic formation resulting in large storage, is primarily related to the limestone formation.

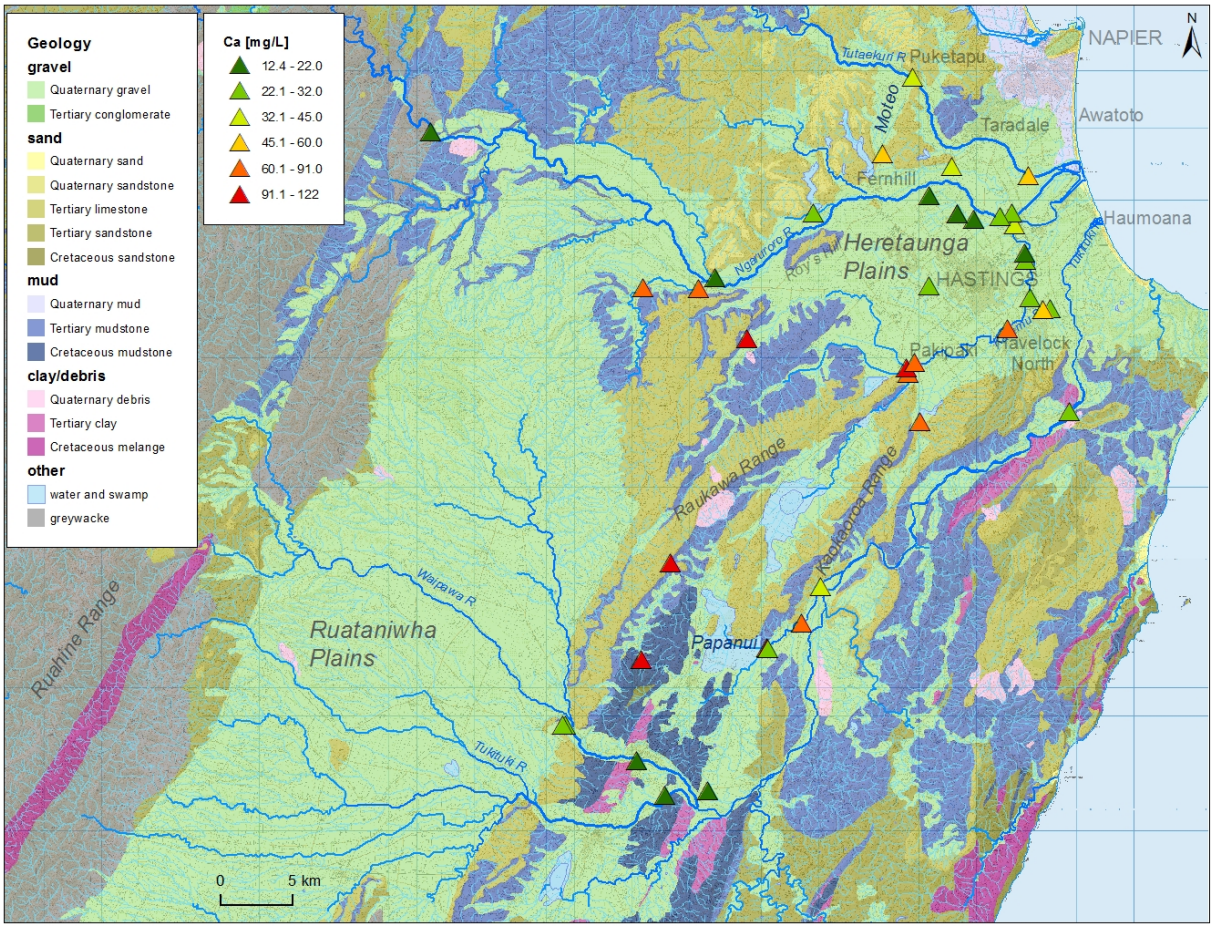

Figure 4.2 Map of calcium (Ca) of surface water.

4.2 GROUNDWATER VOLUMES THAT FEED RIVERS AND STREAMS

The age of the water in stream and river discharges is linked to the age of the water in the groundwater reservoir that feeds the rivers and streams (e.g. Berghuijs and Kirchner, 2017). Water-age tracer data can be used to estimate the groundwater volume (storage) that actively feeds the rivers and streams.

Groundwater storage (S) is related to groundwater flow (Q) and groundwater MTT via the fundamental equation S = Q × MTT (e.g., Maloszewski and Zuber, 1982, Morgenstern et al. 2010). To estimate the storage of groundwater that is actively contributing to the baseflow of the rivers and streams at a certain discharge point, MTT and stream flow rate values at the time of low-flow sampling were used. Storage is listed in the last column of Appendix 2.

Estimates of groundwater storage along the rivers and some streams are shown in Figure 4.3. The Tukituki and Ngaruroro river catchments have similar baseflow groundwater storage, in the order of 600-750 M m^3. The Tutaekuri River catchment has 1000–1500 M m^3, which is the largest baseflow groundwater storage. The Tutaekuri-Waimate Stream is also characterised by a relatively large baseflow groundwater storage, in the order of 230–400 M m^3, with part of it overlapping with that of the Ngaruroro River storage because part of the stream water is derived from Ngaruroro River. Various spring-fed streams in the Heretaunga Plains have relatively small baseflow groundwater storages in the range of 1–20 M m^3, which also partially overlap with the river storages as some streams are derived from river water lost to underground flow further upstream. The streams that discharge within the limestone, mudstone, and sandstone area in the centre of Figure 4.2 also contain relatively large baseflow

groundwater storages of 40–230 M m^3. The old age of the water in these streams implies large storage, despite relatively low flows.

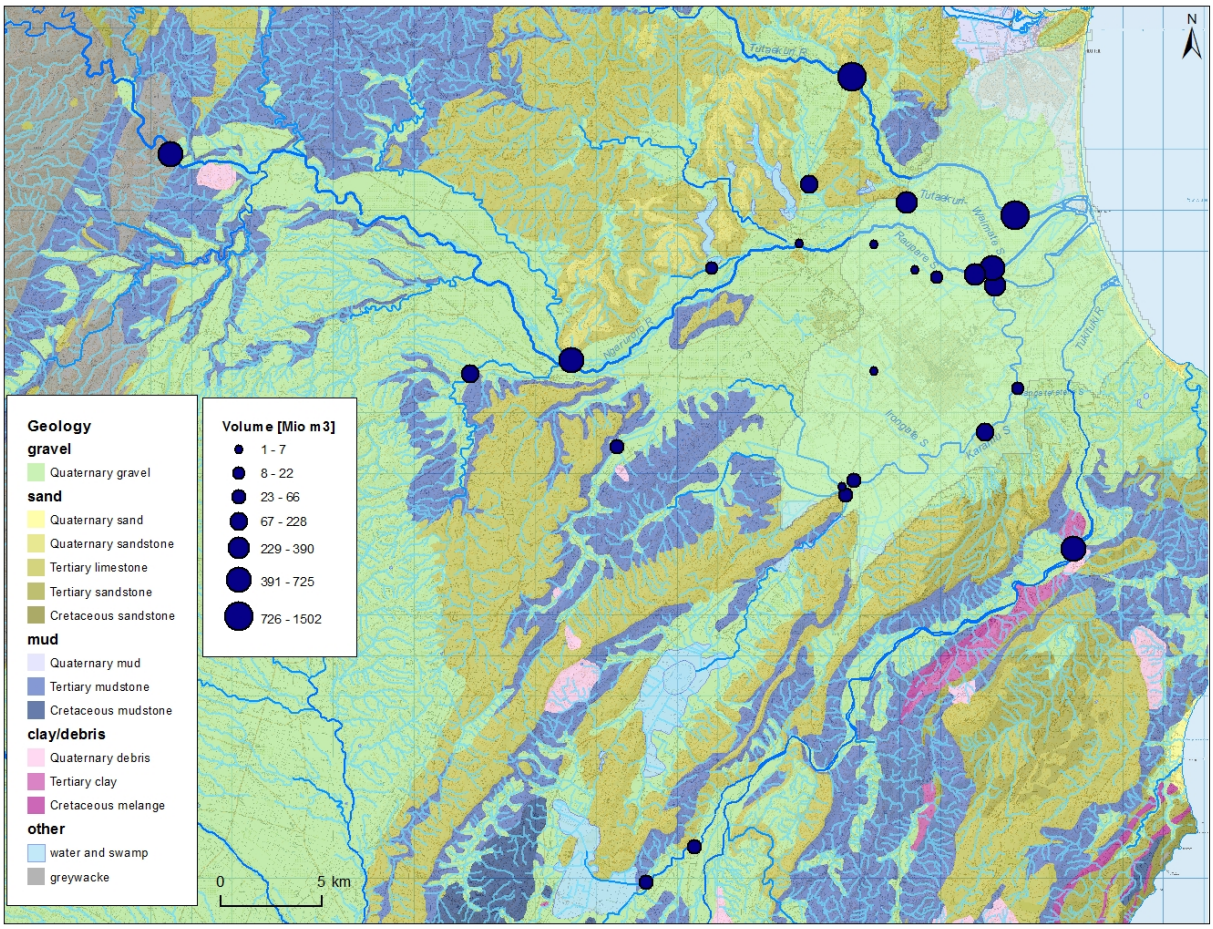

Figure 4.3 Baseflow groundwater storage in catchments upstream from various discharge points in rivers and streams.

4.3 GROUNDWATER AGE

Mean residence times (MRT) in years for the investigated groundwater samples are listed in Appendix 3, along with the fractions of exponential flow volume (E%PM) within the total flow volume of the EPM. The spatial distribution of groundwater MRTs are shown in Figure 4.4. Labelled wells are the drinking water wells that have the most robust age data. Well depths are listed in Appendix 3 and shown in Figure 2.7.

Groundwater in most of the wells within the Holocene unconfined gravel fans of the Ngaruroro and Tukituki rivers is relatively young, with MRT of between 0–10 years (green circles). Along its flowpath from the area of the main water loss from the Ngaruroro River near Omahu at the boundary of confinement, the groundwater within the confined aquifer becomes progressively older. The drinking water wells southwest of Napier contain water with MRT of between 20–40 years. Further toward the coast, groundwater becomes significantly older (MRTs of 40–80 years), with groundwater near the coast being even older, indicating sluggish flow in this part of the aquifer.

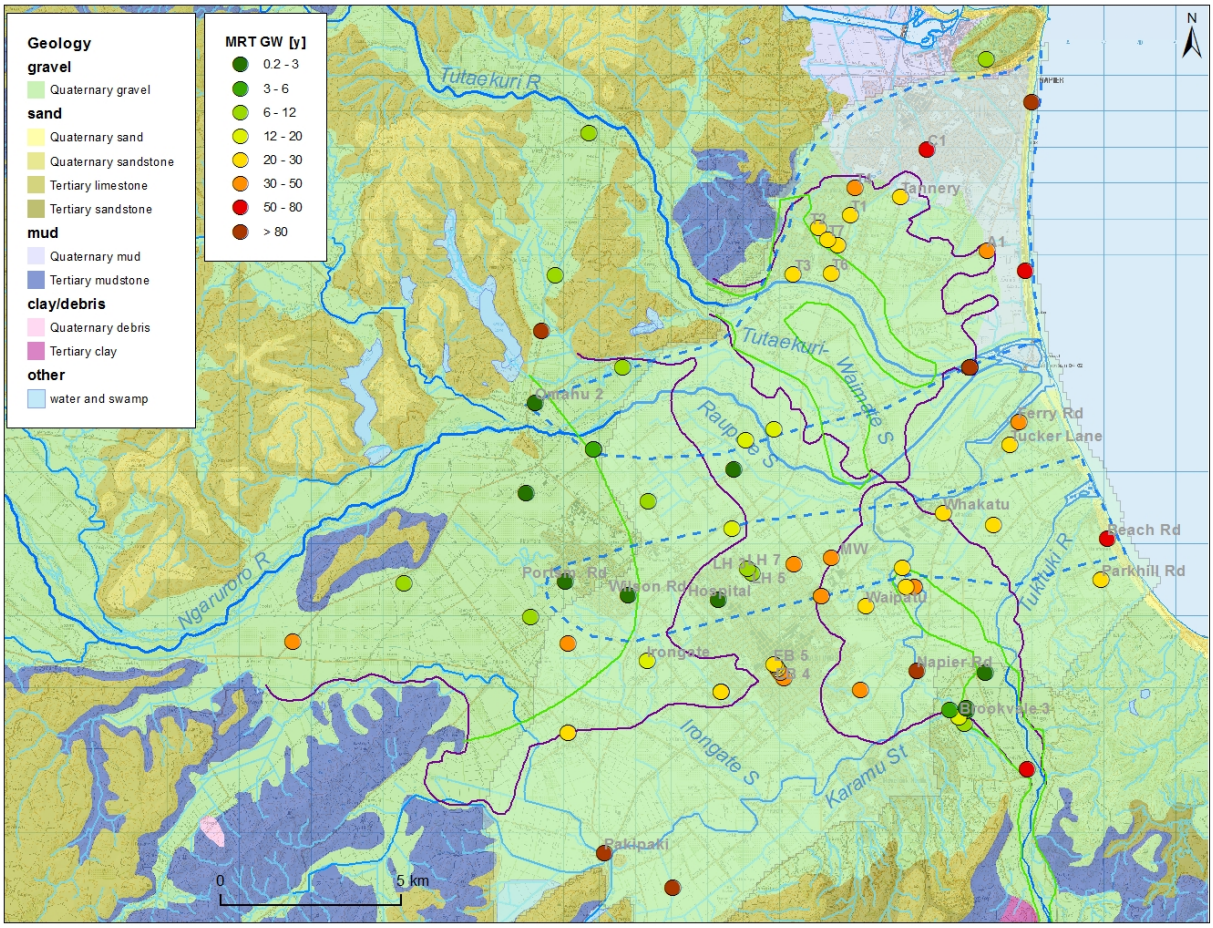

Figure 4.4 Map of groundwater MRT in years. Green and purple lines indicate surface and subsurface extension of the Holocene river gravel fans, respectively. Confined aquifer is indicated in light green. The two areas indicated by blue dotted lines are the areas of clear Ngaruroro River-recharge signature (Figure 4.18).

More vigorous groundwater flow in the confined aquifer toward the coast is indicated further south in the centre of the Plains by a tongue of very young groundwater (MRT <5 years) which reaches up to the Hospital, and the groundwater near the coast at Tucker Lane and Ferry Road, which is relatively young (MRT 27–34 years).

At the southern margin of the confined aquifer, older water (MRT 73 years) near the coast at Beach Road again indicates more sluggish flow. However, the nearby Parkhill Road bore contains significantly younger water, with MRT 21 years, despite that the well has its screen set c. 10 m deeper than the Beach Road bore. This indicates inhomogeneous groundwater flow conditions near the coast, potentially through aquifer heterogeneity, or impact by active faults (Figure 2.1).

Further inland along the southern margin of the confined aquifer, very old water (MRT 88–150 years) at Pakipaki and Napier Road indicates low hydraulic conductivity in this part of the confined aquifer. In the unconfined area of the Tukituki River gravel fan, very young groundwater (MRT <10 years) occurs only around Brookvale (BV), indicating that this groundwater is related to the Holocene gravel fan of the Tukituki River.

Figure 4.5 shows a general positive relationship between water age and well depth. Shallow wells usually contain younger water, but old water can also be found in shallow wells, indicating confined or upwelling groundwater conditions. Oxic, young water occurring at depths of >100 m indicates very high hydraulic conductivity and fast vertical groundwater flow rates in parts of the aquifer.

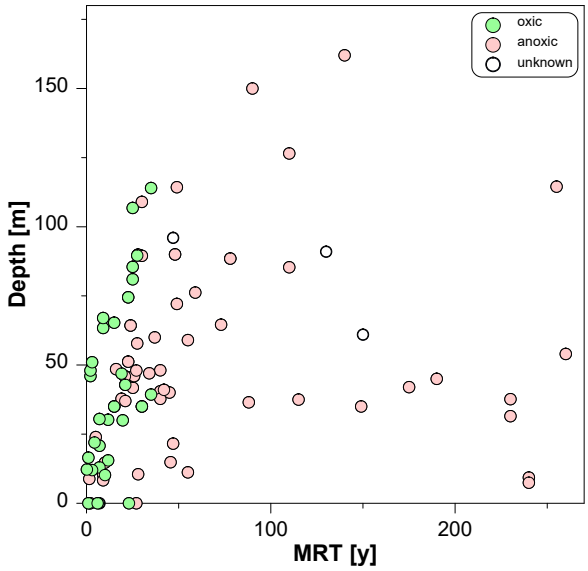

Figure 4.5 Well depth versus MRT. Green and red symbols distinguish between oxic and anoxic groundwater. For samples with open symbols the redox status is not known.

4.4 GROUNDWATER RECHARGE CLIMATE

Some of the investigated groundwaters have MRTs >100 years (Figure 4.5). The waters with a MRT >100 years have tritium concentrations close to the detection limit and could potentially be thousands of years old. In the neighbouring Horizons region, for example, recharge of a large number of groundwaters could be traced back thousands of years, including to the period of colder climate at the last glacial maximum (Morgenstern et al. 2017).

To investigate if any of the water samples from within the Heretaunga Plains also originates from such isolated groundwater systems still containing paleowater, recharge temperatures derived from nitrogen and argon concentration (Section 3.4) are compared to MRT (Figure 4.6a). There is no apparent trend of the older samples having Ar and N_2 concentrations that are indicative of colder recharge conditions relative to those of recent decades, with a mean annual air temperature of c. 14°C. Also, the comparison of $\delta^{18}O$ versus MRT (Figure 4.6b) indicates that the older groundwater samples originate from a climatic period similar to those of recent decades; the older groundwaters do not show more negative $\delta^{18}O$ values (section 3.2).

While the older groundwaters could still potentially be a few thousands of years old, it is unlikely that any of these are so old such that they have originated from a significantly colder climatic period.

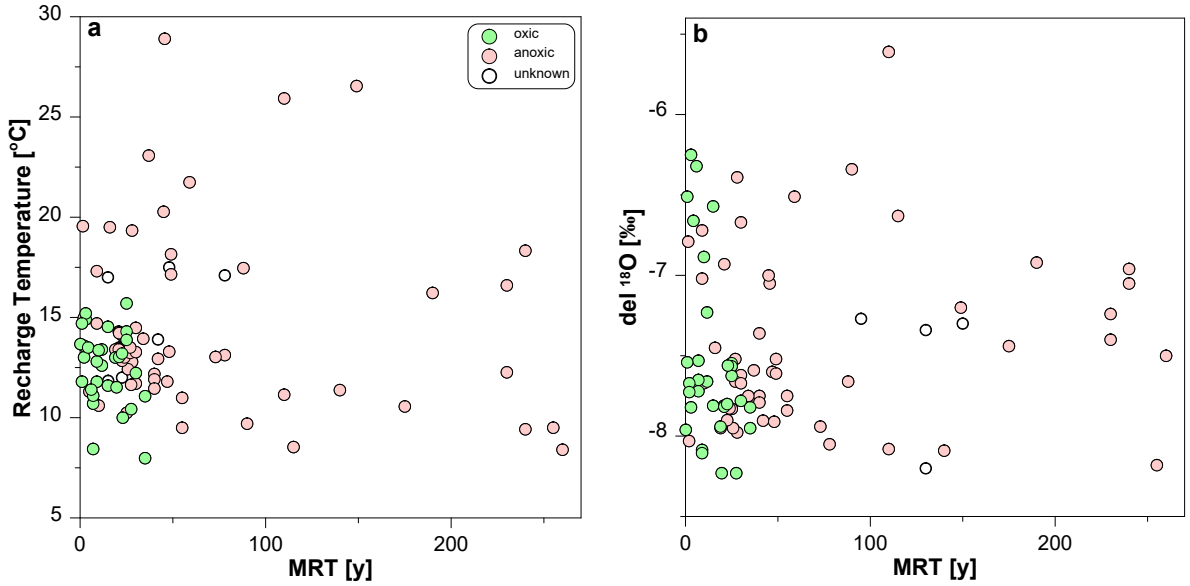

Figure 4.6 Recharge temperature and $\delta^{18}O$ versus MRT. Green and red symbols distinguish between oxic and anoxic groundwater. For samples with open symbols the redox status is not known.

4.5 REDOX CONDITIONS

The available dissolved oxygen (DO) sample data indicates a decreasing DO concentration with groundwater age (Figure 4.7a). All samples, including those from very young groundwater, are to some degree depleted in oxygen (fully oxygenated water c. 10.5 mg/L DO), and with increasing age the groundwater becomes increasingly depleted in oxygen. This indicates the ubiquitous presence of organic matter (OM) in the Heretaunga Plains aquifers, which acts as an electron donor and facilitates microbial reactions that utilise oxygen. Complete depletion of oxygen also has occurred in some very young groundwater samples, suggesting high OM concentrations may occur locally.

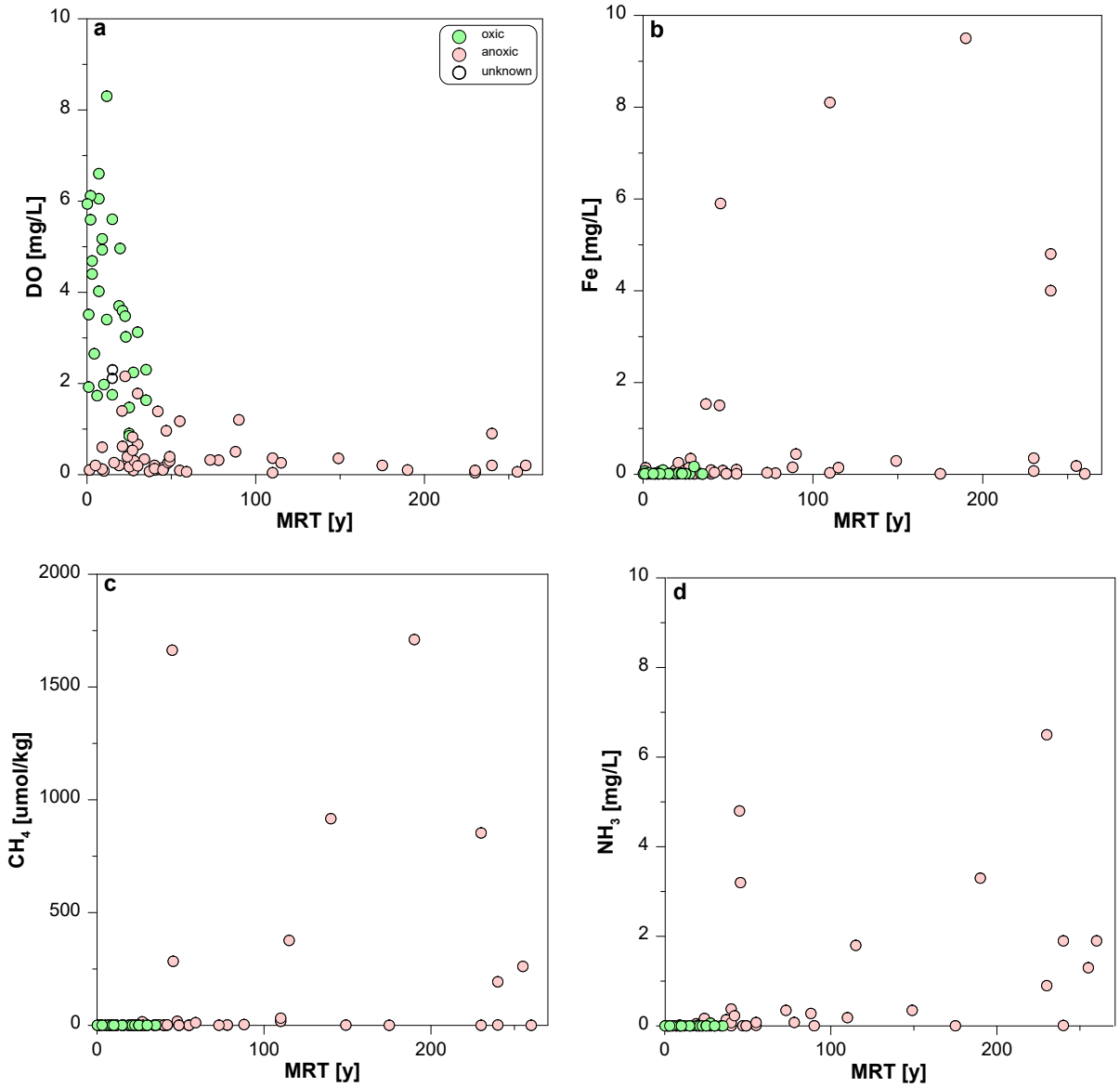

Figure 4.7 Dissolved oxygen (DO), iron (Fe), methane (CH_4), and ammonia (NH_3) concentrations versus MRT. Green and red symbols distinguish between oxic and anoxic groundwater, with anoxic usually defined by DO <1 mg/L and the presence of dissolved Fe or Mn. For samples with open symbols the redox status is not known.

Iron, ammonia, and methane in groundwater are indicators of highly anoxic conditions (Morgenstern and Daughney 2012). Elevated concentrations of iron, ammonia, and methane in the older groundwaters (Figure 4.7b–Figure 4.7d) indicates that those groundwaters have evolved over time towards highly anoxic conditions, up to the stage of methane fermentation. However, this process appears to not only depend on reaction time, but probably also on OM concentrations in the aquifer. After an initial time of several decades required to reach highly anoxic conditions, there is then no further trend of increasing concentrations with time for the old groundwater (Figure 4.7b–Figure 4.7d).

Figure 4.8 shows the spatial distribution of DO in groundwater. Oxic groundwater with DO >2 mg/L (green symbols) occurs only in the upper parts of the Holocene river fans, and along the tongue of very young groundwater towards the coast (Section 4.3). Increasingly anoxic conditions toward the coast highlights the ubiquitous presence of OM. Close to the coast and at the southern part of the Heretaunga Plains, all groundwaters have evolved to an anoxic state (DO <1 mg/L).

South of Napier, in the area of sluggish groundwater flow (as indicated by a large age gradient, Figure 4.4), the groundwater has evolved to the stage of methane fermentation (Figure 4.9). Similar conditions occur in the Holocene gravel fan of the Tukituki River, and at the western margin of the Heretaunga Plains.

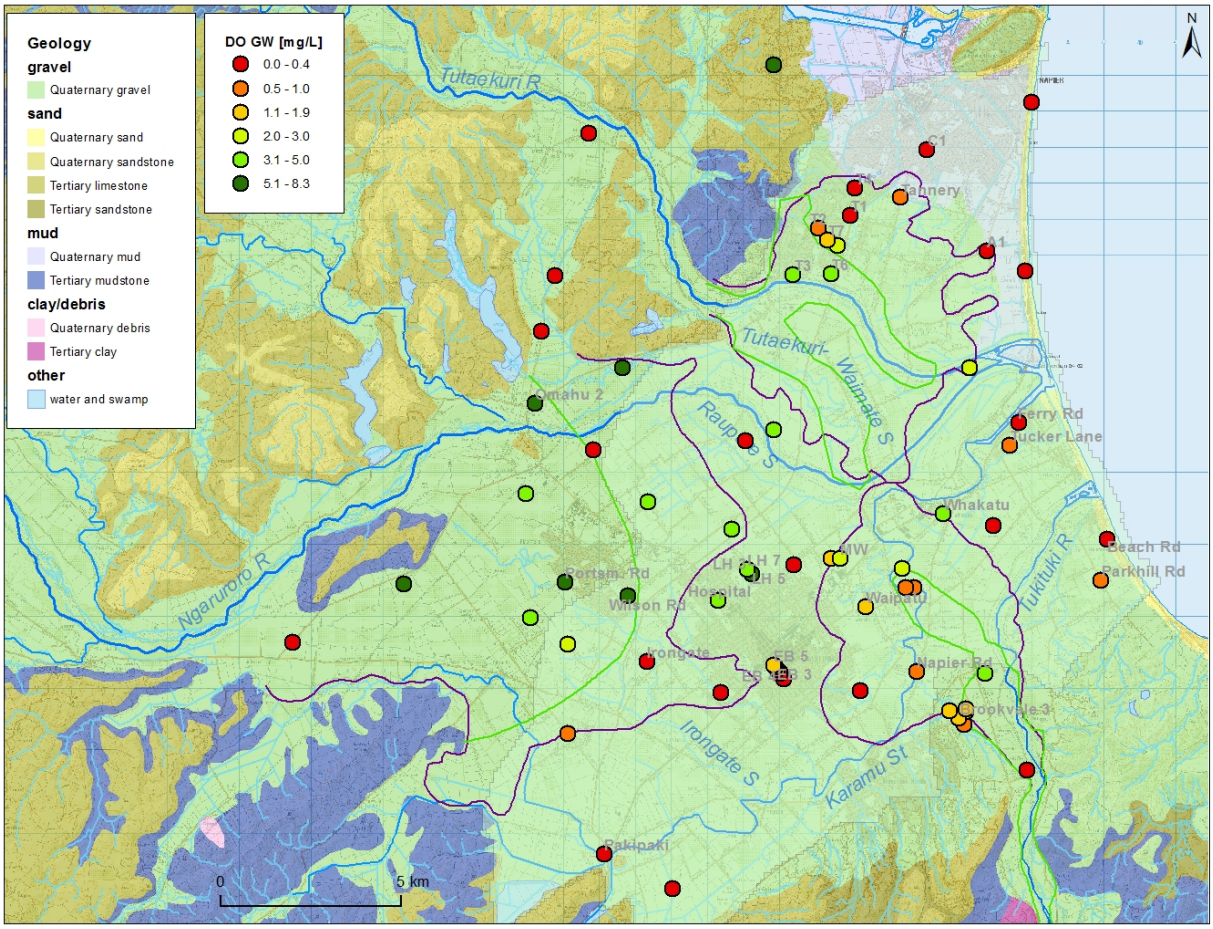

Figure 4.8 Map of dissolved oxygen (DO) in groundwater. Green and purple lines indicate surface and subsurface extension of the Holocene river gravel fans, respectively. Labelled wells are the drinking water wells.

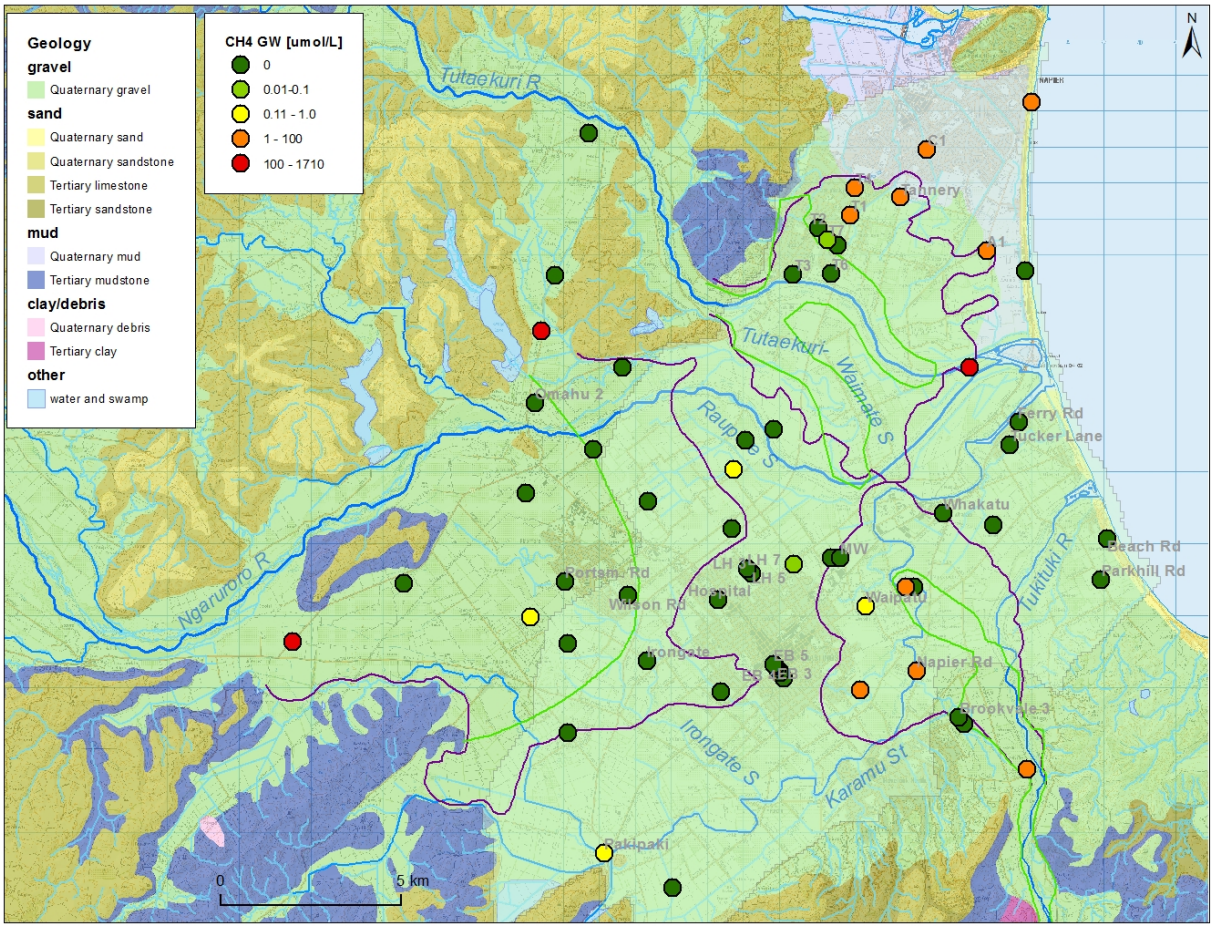

Figure 4.9 Map of methane (CH_4) in groundwater. Green and purple lines indicate surface and subsurface extension of the Holocene river gravel fans, respectively.

4.6 Hydrochemical Evolution — Anthropogenic versus Geologic Impact and Baseline Groundwater Quality

In the following figures, groundwater hydrochemistry parameters are shown versus MRT in order to identify drivers of hydrochemistry, the impacts of land use versus natural processes on groundwater quality. Note that all MRTs >100 years result from data close to the tritium detection limit and may be significantly older (potentially thousands of years). The numbers only indicate the minimum MRT.

During the process of natural groundwater evolution, aquifer matrix minerals are progressively dissolved over time, and increasing ion concentrations with groundwater age indicate a geological source due to leaching from the aquifer material. In contrast, high concentrations (in particular those of nutrients) in young groundwater indicate anthropogenic sources from land-use activities. The main anthropogenic impacts on groundwater quality in New Zealand started with the onset of the industrial agriculture in the 1950s, as deduced from the data set of the National Groundwater Monitoring Programme (NGMP) of New Zealand (Morgenstern and Daughney 2012). Comparison of ion concentrations of recently recharged groundwater, and groundwater that was recharged before 1950 allowed the identification of the pre-industrial baseline groundwater quality and the impacts of land-use activities on groundwater quality.

The NGMP data set enabled the identification of agricultural contaminants (mostly nutrients) from high-intensity land-use, listed in Table 4.1. Comparison of the Heretaunga Plains data to the NGMP data allows identification of anthropogenic versus geological sources, and

determination of the impact from high-intensity land use, for most of the hydrochemistry parameters.

Table 4.1 Agricultural indicators for high-intensity land-use (Morgenstern and Daughney 2012), showing concentration range prior to high-intensity land use, threshold concentrations that indicate high intensity agricultural land-use, and observed maximum concentrations. Threshold concentrations in brackets can be ambiguous.

Agricultural indicator	Concentration range prior to high-intensity land-use (mg/L)	Threshold concentration (mg/L)	Observed maximum concentration (mg/L)
NO_3-N	0–2.5	2.5	34
SO_4	0–12	12	94
Cl	0–60	(60)	100
Br	0–0.2	(0.2)	1.3
Ca	0–50	(50)	110
Mg	0–15	(15)	54
Cr	0–0.0015	0.0015	0.006

Of the agricultural indicators listed in Table 4.1 on a New Zealand level, only NO_3 and SO_4 are elevated in the Heretaunga Plains groundwater, and only marginally, to indicate impact by high-intensity land use, and this only in a few groundwater samples.

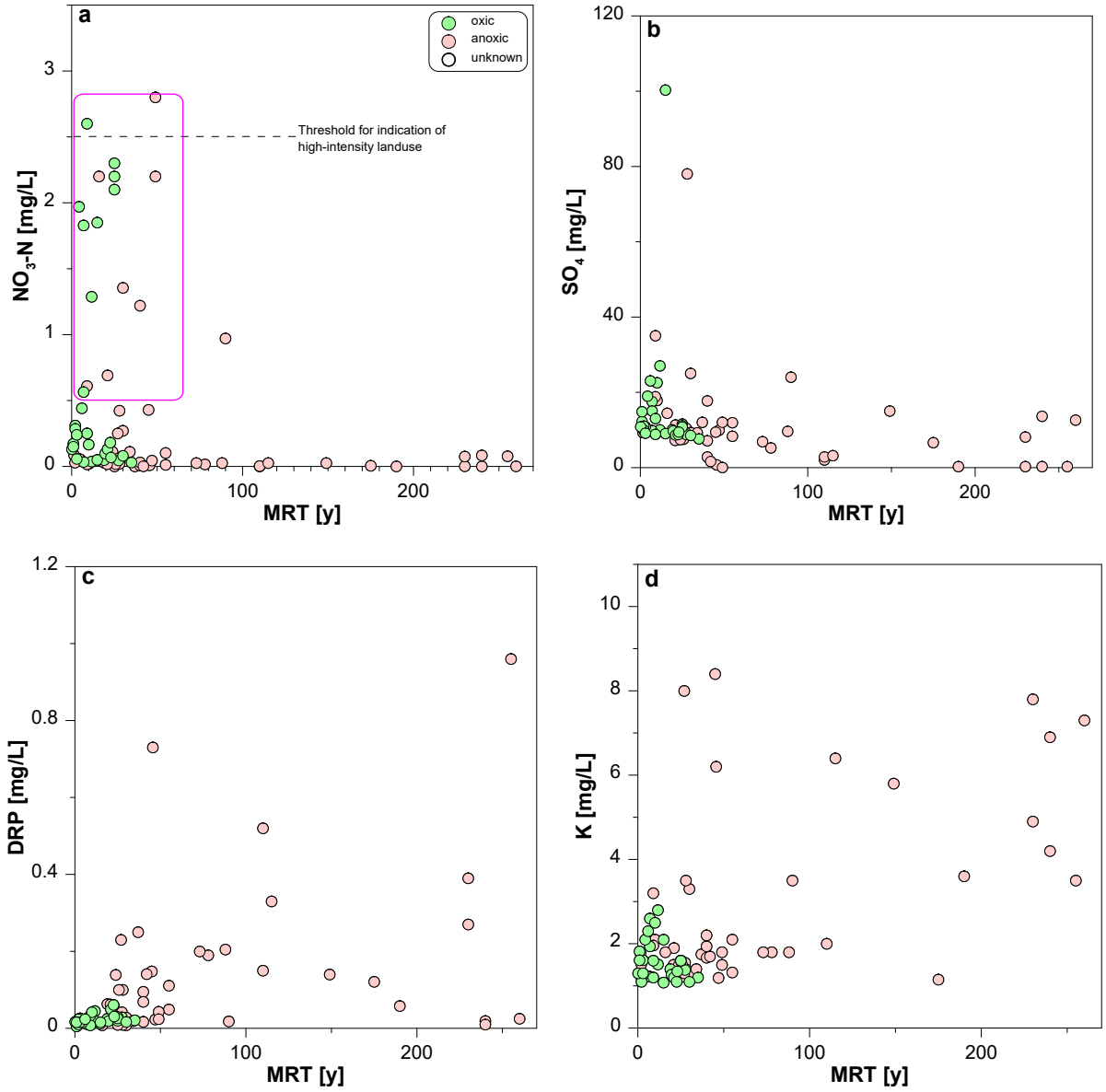

Figure 4.10 Nitrate-nitrogen (NO_3-N), sulphate (SO_4), dissolved reactive phosphorus (DRP), and potassium (K) concentrations versus MRT. Green and red symbols distinguish between oxic and anoxic groundwater respectively. For samples with open symbols the redox status is not known. The purple box indicates elevated NO_3 in waters recharged over the last 60 years, since the start of industrial agriculture.

NO_3-N (Figure 4.10a) is slightly elevated (>0.5 mg/L NO_3-N) in a few groundwaters younger than 60 years, indicating a low-intensity land-use impact may be present. Only two samples display concentrations just above the 2.5 mg/L NO_3-N threshold level, which is indicative of a marginal impact by high-intensity land use (broken line).

SO_4 concentrations of up to 25 mg/L occur in old groundwaters (Figure 4.10b), indicating that such elevated concentrations can be caused by natural processes in this groundwater system, probably due to the effects of limestone dissolution. Three young groundwater samples show higher SO_4 concentrations of up to 100 mg/L. These samples are also elevated in NO_3, indicating that these elevated SO_4 concentrations are likely to be associated with high-intensity land use.

Dissolved reactive phosphorus (DRP) and potassium (Figure 4.10c and Figure 4.10d) show elevated concentrations only in anoxic groundwater greater than a few decades old. This indicates that these elevated concentrations are natural, likely with a geological origin. DRP is

not elevated in any of the very young groundwater samples, indicating that any phosphate from fertilisers has not been transported into the groundwater, but remains stored within the soil.

Figure 4.11 shows hydrochemical parameters that are part of minerals and are usually leached from the aquifer material and therefore may show increasing concentrations with groundwater age. For all of these parameters, namely silica, magnesium, calcium, sodium and bicarbonate, there are no clear trends of increasing concentrations with age of Heretaunga Plains groundwater.

Groundwater data covering the last 100 years allow robust identification of the baseline groundwater quality before land-use intensification, and the impacts of land-use activities on groundwater quality in the Heretaunga Plains. The age and chemistry data include two samples with elevated nitrate-N concentrations of up to 3 mg/L in young groundwater, above the threshold concentration indicating high-intensity land use, recharged since the period of high-intensity land use that commenced c. 60 years ago. Three samples also show elevated SO_4 concentrations of up to 100 mg/L that may also be related to high-intensity land use. None of the remaining hydrochemistry parameters shows elevated concentrations in the most recently recharged groundwater that would be indicative of impact of high-intensity land use on groundwater quality. The reader is referred to Section 4.7.4 for further analyses of agricultural contamination.

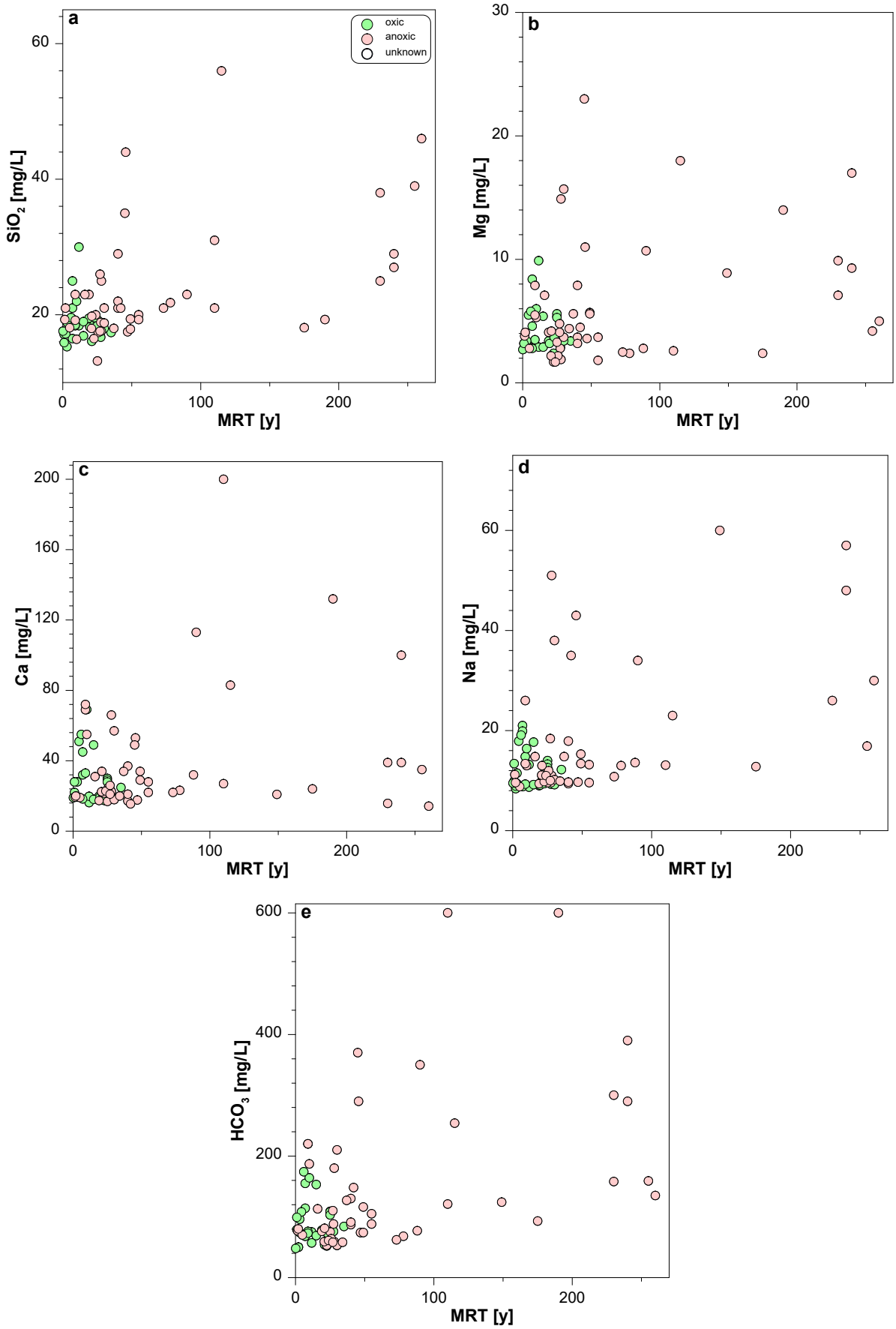

Figure 4.11 Silica (SiO_2), magnesium (Mg), calcium (Ca), sodium (Na), and bicarbonate (HCO_3) concentrations versus MRT. Green and red symbols distinguish between oxic and anoxic groundwater. For samples with open symbols the redox status is not known.

4.7 GROUNDWATER RECHARGE SOURCES — RIVER VERSUS LOCAL RAIN

In this section, various parameters are discussed that can indicate the recharge source of groundwater.

4.7.1 Stable isotopes of the water as a recharge indicator

The signature of the stable water isotopes can provide information on the recharge source of the groundwater if the rivers, usually from higher altitude catchments, have an isotope signature that is distinct from that of local low-altitude rain (Section 3.2). In the northern and central Heretaunga Plains, a significant number of groundwaters have a $\delta^{18}O$ ratio of -8 to -8.3‰. These values are equivalent to the average of the Ngaruroro River (-8 ‰), the river with consistently the most negative stable isotope composition over time (Section 3.2). This indicates that only Ngaruroro River can be the source of recharge, with bias of the recharge towards winter recharge; only the water in the Ngaruroro River during winter has $\delta^{18}O$ ratios of less than -8.0 ‰, up to -8.7 ‰ (Figure 3.6). This can be considered a robust indication of mainly recharge from the Ngaruroro River in these parts of the aquifer.

The $\delta^{18}O$ results of the test bore at Tollemache Orchard, southeast of the Eastbourne (EB) well field, allows for a more detailed understanding of the groundwater recharge and flow conditions in this part of the aquifer (Figure 4.12). At a shallow depth (<100 m), the $\delta^{18}O$ ratio was found to be c. -7.6 ‰. Below 100 m depth, the $\delta^{18}O$ ratio transitioned to <-8.1 ‰, which is consistent with recharge from the Ngaruroro River. The different $\delta^{18}O$ ratio for the shallower water is likely to indicate an influence from local rain. A $\delta^{18}O$ value of -7.6 ‰ may represent the recharge signal of local rain recharge in this area. Most of the shallow groundwaters in this area, from a range of depths, covering a range of ages, and having rain recharge signature indicated by other indicators discussed below (Figure 4.19), have a $\delta^{18}O$ ratio of -7.6 ‰ (Figure 4.13).

For a better understanding of groundwater processes via its stable isotope composition, more data directly from the endmembers, rain or river recharge, are necessary. For that reason, monthly stable isotope samples of rain are currently being collected at Bridge Pa, starting October 2017. Scarce existing rain data from the nearby hills to the north and to the south of the Heretaunga Plains (Baisden et al. 2016) suggests high $\delta^{18}O$ seasonal variability in rain, between -2 ‰ and -13 ‰. It is therefore necessary to identify the isotopic signature of the fraction of the rain water that infiltrates into the groundwater system, for example by sampling from lysimeters, together with the stable isotope signature in rain.

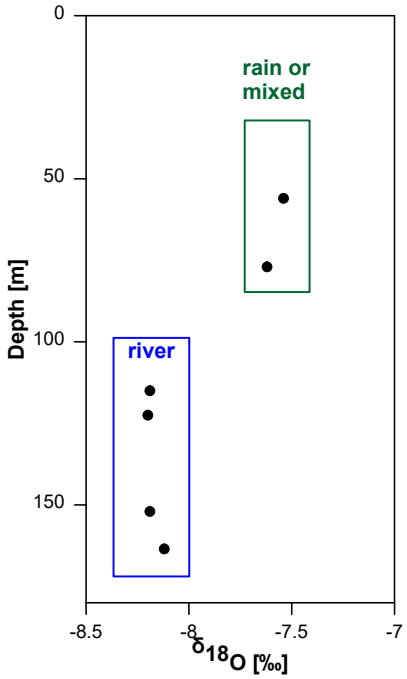

Figure 4.12 $\delta^{18}O$ versus well-depth at Tollemache Orchard test bore.

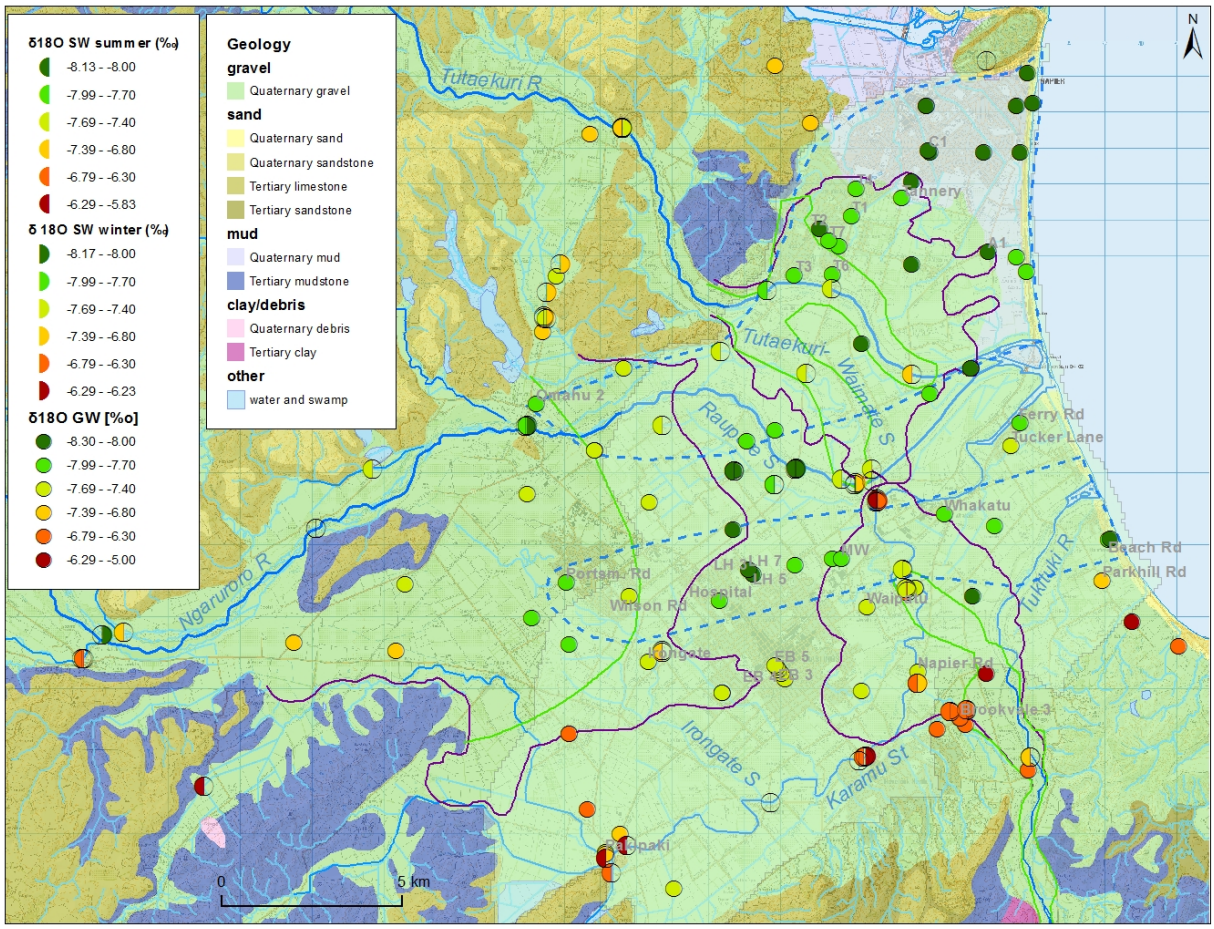

Figure 4.13 Map of $\delta^{18}O$ in groundwater (full circles), and surface water (half circles, left typical summer and right winter signature).The light green in the area of Quaternary gravels indicates the area of confined aquifer.

After a draft version of this report was completed, stable isotope analysis results from a winter survey (23 August 2017) of surface waters became available. These results support the previous finding that the signature of river recharged groundwater matches that of the

Ngaruroro River with bias towards winter signature. Figure 4.13 shows the results of the specific summer- and winter surveys, allowing for further identification of groundwater flow dynamics:

- North of the Heretaunga Plains (north-west of Napier), groundwaters have less negative $\delta^{18}O$ ratios compared to those in the confined aquifer around Napier. As these groundwaters in the hills could not have been recharged from the rivers, these $\delta^{18}O$ ratios may be considered the signature of coastal rain in this area.
- In the Moteo Valley during the winter sampling, all $\delta^{18}O$ ratios are consistently similar to the summer $\delta^{18}O$ ratio of the Tutaekuri River. This may indicate a lag time of the water through the Moteo groundwater system of c. 6 months.
- Ground- and surface water along the Tutaekuri-Waimate Stream have $\delta^{18}O$ ratios between those of Tutaekuri and Ngaruroro, indicating a mixture between these two sources – also indicated by stream water age Section 4.1).
- The groundwaters in the north of the Heretaunga Plains around Napier and Taradale show $\delta^{18}O$ ratios that are completely distinct from those of the Tutaekuri River during any season. The Tutaekuri River is therefore unlikely to contribute significantly to the recharge of this groundwater system. The observed $\delta^{18}O$ ratios resemble only the signature of the Ngaruroro River. So it is likely that the Ngaruroro River is the main recharge source of the groundwater in this part of the aquifer. The same applies to the band of very young groundwater, indicated by the southern blue dotted line. The two areas are the areas of clear Ngaruroro River-recharge signature
- On the southern margin of the Heretaunga Plains, groundwater and surface waters show significantly less negative $\delta^{18}O$ ratios. Some of these waters also display elevated calcium (Figure 4.17), indicating recharge in the limestone area, and therefore representing the $\delta^{18}O$ ratio of the rain recharge from the limestone area. The Tukituki River has similar less negative $\delta^{18}O$ ratios and is therefore not distinguishable from local rain recharge of the limestone area.

4.7.2 Recharge temperatures and excess air

Recharge temperatures and excess air, derived from argon and nitrogen (Section 3.4), are shown in Figure 4.14. Two boxes show the areas where the data are expected to plot for rain-recharged and river-recharged groundwater (Morgenstern et al. 2009). Elevated or high excess air indicates recharge by local rainfall, because water recharged through an unsaturated zone picks up excess air during infiltration. The recharge temperatures for rain recharged groundwaters are expected to be around mean annual air temperature (c. 13.8 °C), the temperature of gas equilibrium at the water table. In contrast, groundwater recharged from rivers/streams is expected to have low excess air because the water does not pass through an unsaturated zone, so there is little potential to pick up excess air. For the river recharged groundwaters, the recharge temperatures are expected to be around mean annual Ngaruroro River water temperature at Fernhill (c. 14.9 °C), the equilibration temperature for river recharged groundwater, and recharge temperatures are expected to show higher variability due to the annual temperature variability in the surface water.

Most of the data in Figure 4.14 plot in or near the areas expected for either river or rain recharge. Data outside the boxes may be influenced by excess nitrogen from denitrification reactions, or from degassing processes in highly anoxic groundwater, and has been excluded from this assessment.

The means of the calculated recharge temperatures for rain and for river recharged groundwater are c. 12.5 °C, below that of mean annual air temperature and mean river temperature. This may indicate preferential recharge during winter months.

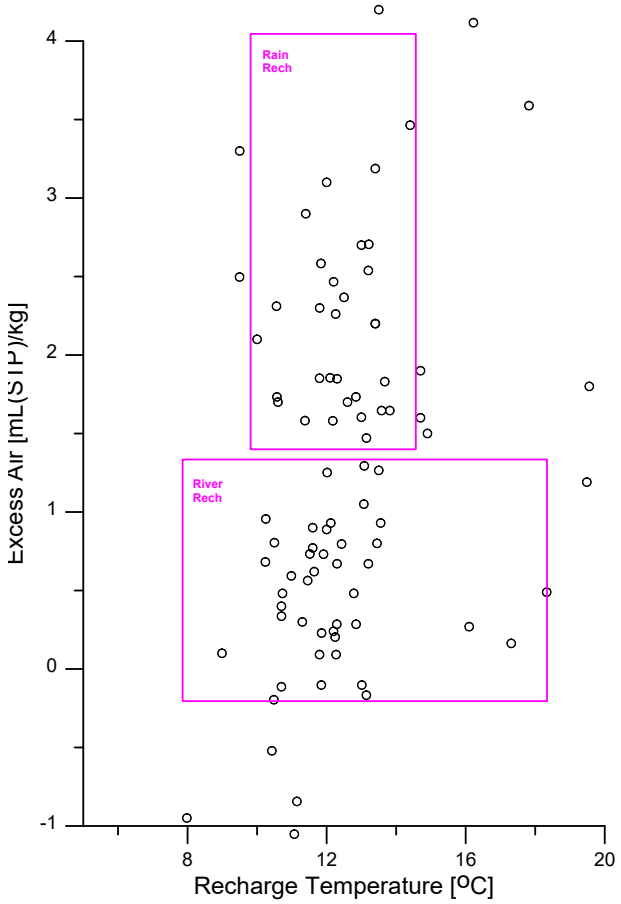

Figure 4.14 Excess air versus recharge temperature. Purple boxes related to expected rain/river recharge properties are specified following Morgenstern et al. (2009).

4.7.3 Anthropogenic contaminants — Chlorofluorocarbons

Chlorofluorocarbons (CFCs) are man-made chemical compounds that were used mainly in refrigeration gear and spray cans. Therefore, CFCs are often found in higher concentrations in groundwater recharged from urban, industrial, and agricultural areas. CFC-11 and CFC-12 contamination has been observed in New Zealand groundwater systems through such point-source contaminations.

In contrast, rivers from near-pristine catchments usually do not have CFC sources. Therefore, the CFC concentration of river water is usually close to that of the equilibrium concentration between the river water and atmospheric air at the time of recharge.

Figure 4.15 shows CFC-11 and CFC-12 concentrations across the Heretaunga Plains. Concentrations above those of naturally occurring equilibrium concentrations for water in contact with air are shown in light green to red colours. Although few in number, these elevated CFC concentrations indicate recharge via local rain for these groundwaters.

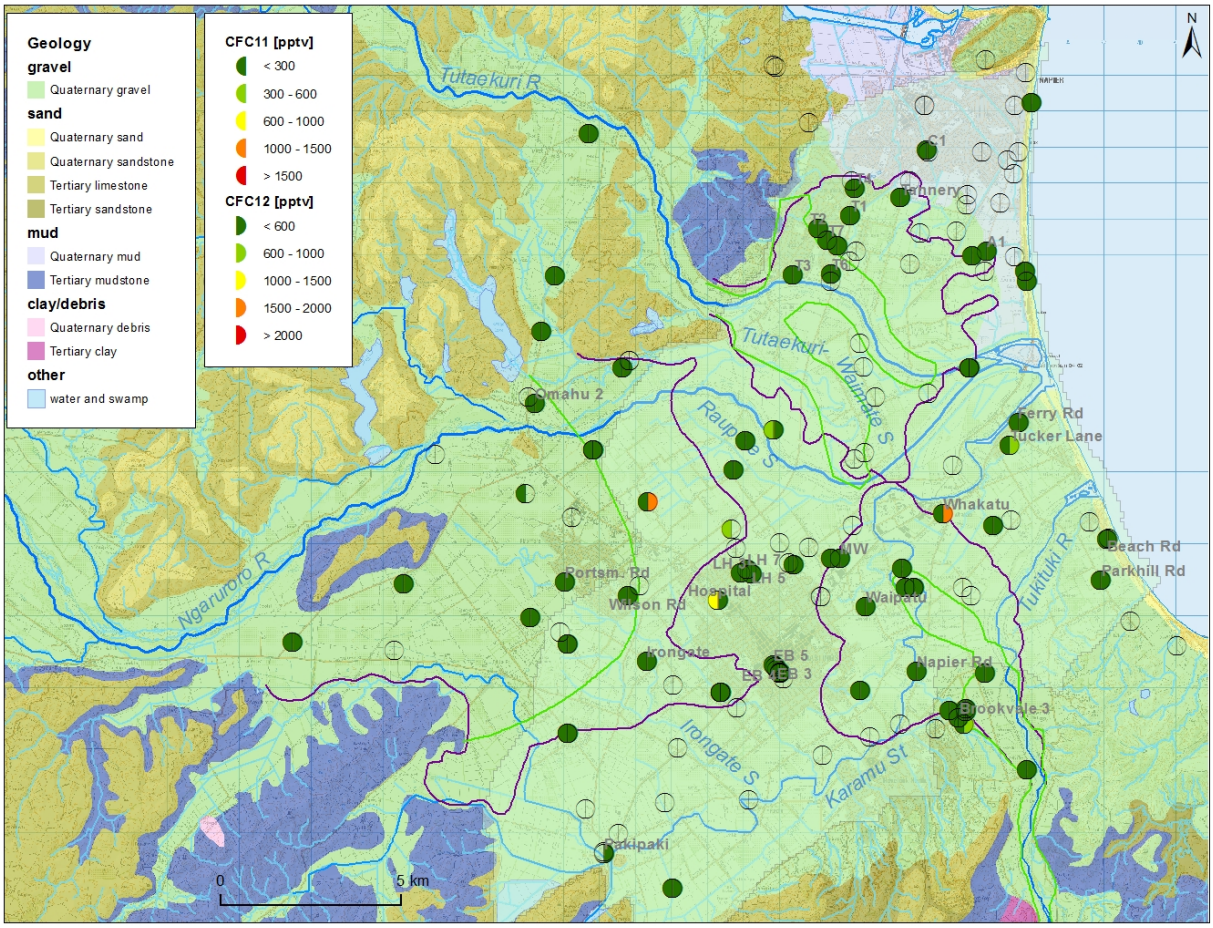

Figure 4.15 Spatial distribution of CFC-11 and CFC-12. Significantly elevated concentrations due to point sources are indicated by yellow and red colours. Green and purple lines indicate surface and subsurface extension of the Holocene river gravel fans, respectively.

4.7.4 Agricultural contaminants

Two agricultural groundwater contaminants, nitrate and sulphate, were found to indicate land-use impact by agriculture in the Heretaunga Plains (Section 4.6, Figure 4.10). As such, increased concentrations of nitrate and sulphate in groundwater can therefore act as an indicator for recharge via local rain. River water, typically from higher-elevation catchments that remain largely unaffected by land-use intensification, does not display such elevated concentrations.

Figure 4.16 shows the nitrate concentration across the Heretaunga Plains, with greatest concentrations in the southern part of the Heretaunga Plains groundwater system. These elevated nitrate concentrations of up to 3 mg/L NO_3-N (Section 4.6) are indicative of some contribution to recharge from local rain. Only two wells show NO_3-N concentrations slightly above 2.5 mg/L, the threshold for indication of high-intensity land use.

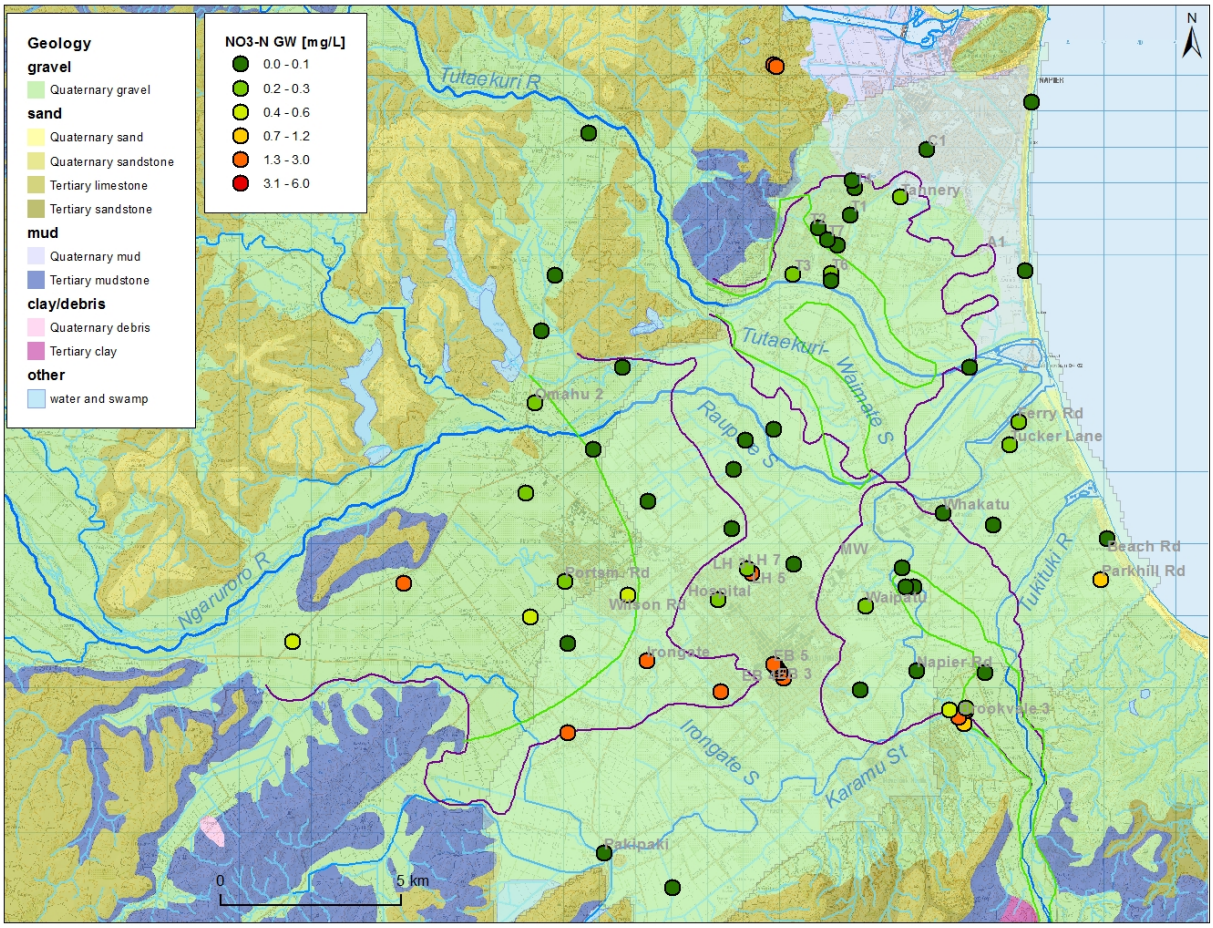

Figure 4.16 Spatial distribution of nitrate-N. Elevated concentrations due to agricultural sources are indicated by orange and red colours. Green and purple lines indicate surface and subsurface extension of the Holocene river gravel fans, respectively.

4.7.5 Local geology signature

Local geologic features, for example the limestone hills around the Heretaunga Plains, can produce a contrasting hydrochemical composition in locally recharged groundwater, compared to the river water from catchments with a different geology. The contact of water with limestone causes high calcium concentrations in groundwater. Figure 4.17 shows the calcium concentration across the Heretaunga Plains.

Groundwaters north of the Heretaunga Plains from limestone formations are characterised by high Ca concentrations. Also the groundwaters in the southern part of the Heretaunga Plains show elevated Ca concentrations, indicating recharge within the local limestone hills.

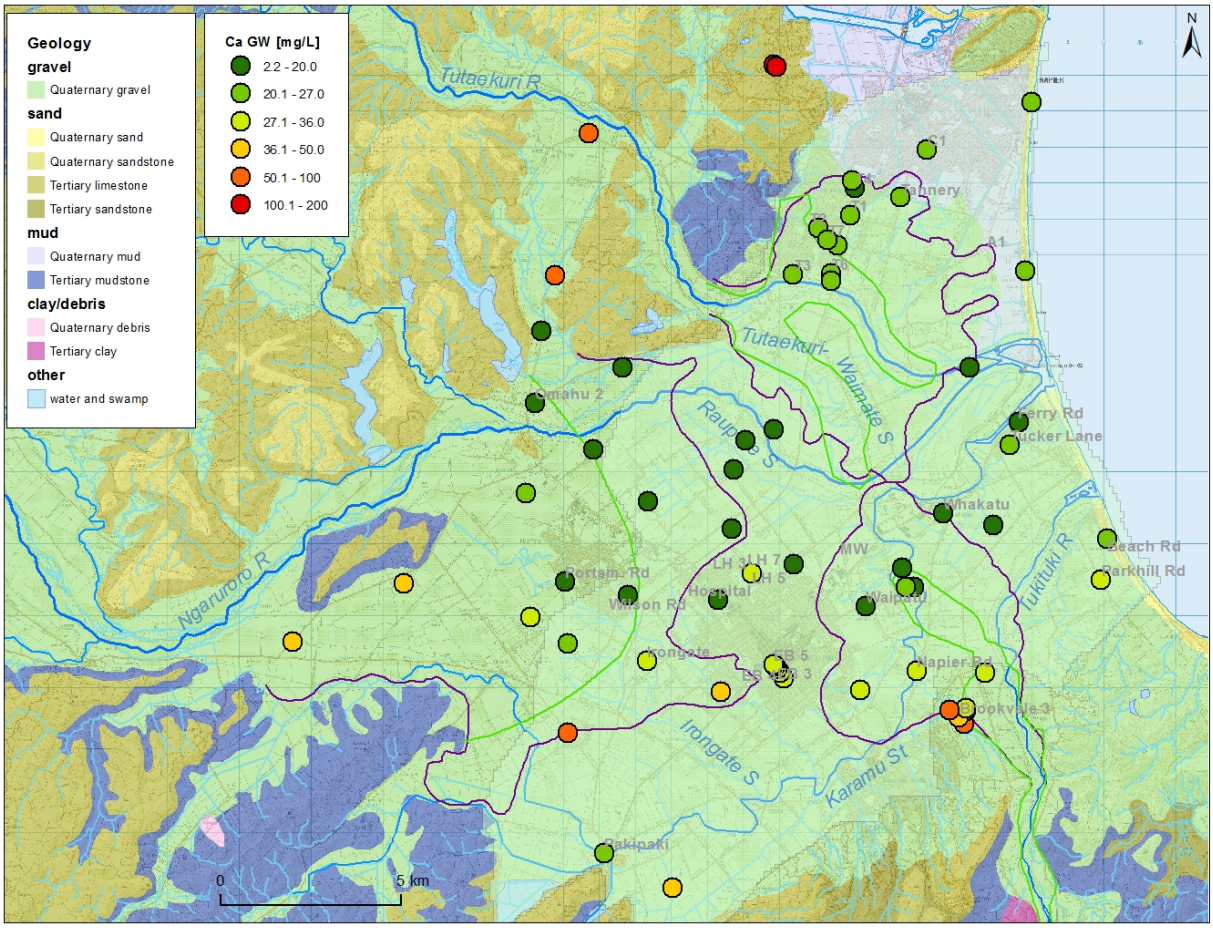

Figure 4.17 Spatial distribution of calcium (Ca). Elevated concentrations indicate impact by local limestone features. Green and purple lines indicate surface and subsurface extension of the Holocene river gravel fans, respectively.

4.7.6 Radon as a recharge source indicator

Low radon concentrations in groundwater can indicate recharge of water from a river if the water is very young, of the order of days to weeks, because it takes weeks until radon in water reaches an equilibrium concentration with the rock matrix. The radon concentrations in the investigated groundwaters in the Heretaunga Plains are relatively low (Section 3.3). However, it is unlikely that fresh low-radon-containing river water is the cause of the low radon concentrations, because the lowest radon concentrations are observed in the oldest waters. Further, the lowest radon concentrations occur in groundwater that is highly anoxic, to the stage of methane fermentation (Figure 4.18, red ellipse). This indicates that these low radon concentrations are likely to be caused by adsorption of radon onto organic matter (Morgenstern et al. 2012) which appears to be ubiquitously present in the aquifers (section 4.5). The radon concentrations in groundwater are therefore considered to not be indicative of a recharge source from low-radon river water.

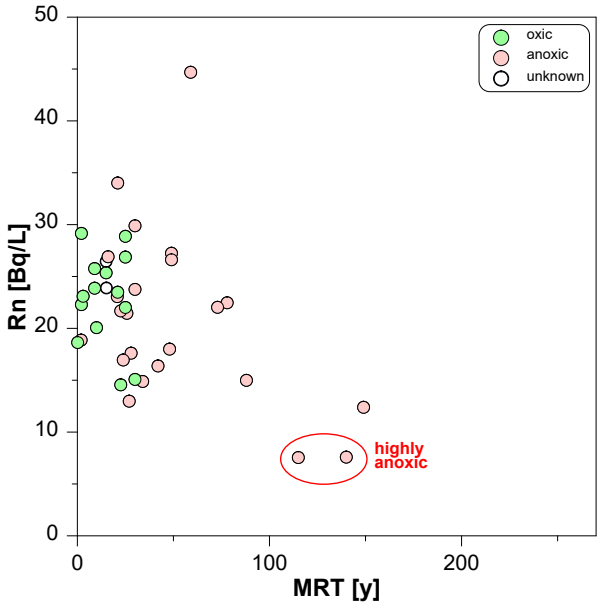

Figure 4.18 Radon concentration vs. MRT. Green and red symbols distinguish between oxic and anoxic groundwater. For samples with open symbols the redox status is not known.

4.7.7 Summary — recharge sources

Distinct differences in the signatures of groundwater hydrochemistry, isotopic composition, and gas concentrations collectively allow us to distinguish between recharge from local rain and river water (Sections 3.1-3.4). The use of HCA, stable isotopes, and excess air has previously enabled identification of different climatic and geologic signatures, and related recharge sources, in groundwater of the Wairarapa, Ruataniwha Plains, Horizons Region, and Marlborough (Morgenstern et al. 2009, 2012, 2017).

Recharge source indicators in the Heretaunga Plains show very characteristic groundwater signatures that can be used to characterise their recharge source. Using a combination of parameters that have different drivers, including climate (high altitude vs local), water table gas exchange processes, industrial contaminants, agricultural contaminants, and local geology, the tracer signature allowed us to gain an informed conceptualisation of areas of locally rain-recharged groundwater, and river-recharged groundwater.

Figure 4.19 shows a summary of all the rain/river recharge source indicators presented throughout this study. These include characteristic signatures of $\delta^{18}O$ ratios (Section 4.7.1), excess air via Ar and N_2 concentrations (Section 4.7.2), CFCs (Section 4.7.3), nitrate and sulphate (Section 4.7.4), and calcium (Section 4.7.5). HCA and radon indicators were not considered to exhibit unique drivers that allow distinguishing between the various recharge sources.

Each site in Figure 4.19 is represented by a circle with five sections, with each section representing one indicator: $\delta^{18}O$, excess air and recharge temperature, CFCs, nitrate and sulphate, and calcium. Where the different tracers indicate recharge source, the relevant sections are filled with colours: blue for river recharge and green for a contribution to recharge from local rain. Blank (grey) sections mean that no data was available or the respective indicators were inconclusive in distinguishing between recharge sources.

The recharge source indicators available to date show a distinct pattern of recharge source within the Heretaunga Plains aquifers (Figure 4.19). Two areas show a strong indication of recharge from the Ngaruroro River, consistent within the areas and also consistent between

the different indicators (identified by dashed blue lines). The aquifer water around and southwest of Napier shows the strongest signature of recharge from the Ngaruroro River. The Tutaekuri River does not appear to be connected to this aquifer, indicated by the stable isotope signature of the ground- and surface waters (Section 4.7.1), but also by chloride (not shown). The second area with a strong indication of river recharge is a band in the centre of the Plains (Figure 4.19). This band of river-recharged groundwater is found in the same location as the band of young groundwaters (Figure 4.4). It is likely that this band represents a buried paleo channel of a previous course of the Ngaruroro River that is still hydraulically connected to its present course, thus enabling fast seaward flow of groundwater lost from the river. A number of public drinking water wells tap into this band of river-recharged fast-flowing groundwater[1].

The wells in the unconfined area of the Ngaruroro River gravel fan (green line in Figure 4.19) show a clear indication of local rain recharge. This is, however, likely to be the result of these wells all being relatively shallow. The $\delta^{18}O$ results of the test bore at Tollemache Orchard clearly showed a layer with some rainfall recharge in groundwater to a depth of about 100 m in this area, underlain by river-recharged groundwater (Figure 4.12). So, the likely scenario is that the water lost from the Ngaruroro River flows at a depth of greater than about 100 m toward the coast, but is overlain by a thick layer with the presence of locally recharged rain water.

There appears to be a band of groundwater with rainfall recharge present, that occurs between the two river-recharged areas. This may represent the drainage of the rain-recharged unconfined area of the Ngaruroro River gravel fan. This rain-recharged groundwater may also drain via the confined aquifer, as indicated by the presence of rainfall recharge in the two confined drinking water wells at Ferry Rd. and Tucker Lane. However, data in this area is still scarce. In addition, no stable isotope data of rain in this area is available yet.

Currently, rain samples are being collected in this area (Bride Pa) over the course of a year to improve our understanding of the stable isotope composition of the local rain-recharged groundwater, to enable better identification of rain recharge contribution.

[1] Note that the presence of highly transmissive aquifer material in this region is also supported by concurrent groundwater modelling of the Heretaunga Plains (Rakowski and Knowling, in prep; Knowling et al., in prep), which suggests that high hydraulic conductivity values (c. >500 m/d) are likely required in this region to achieve satisfactory matches to field observation (e.g., groundwater levels, river gain/loss rates).

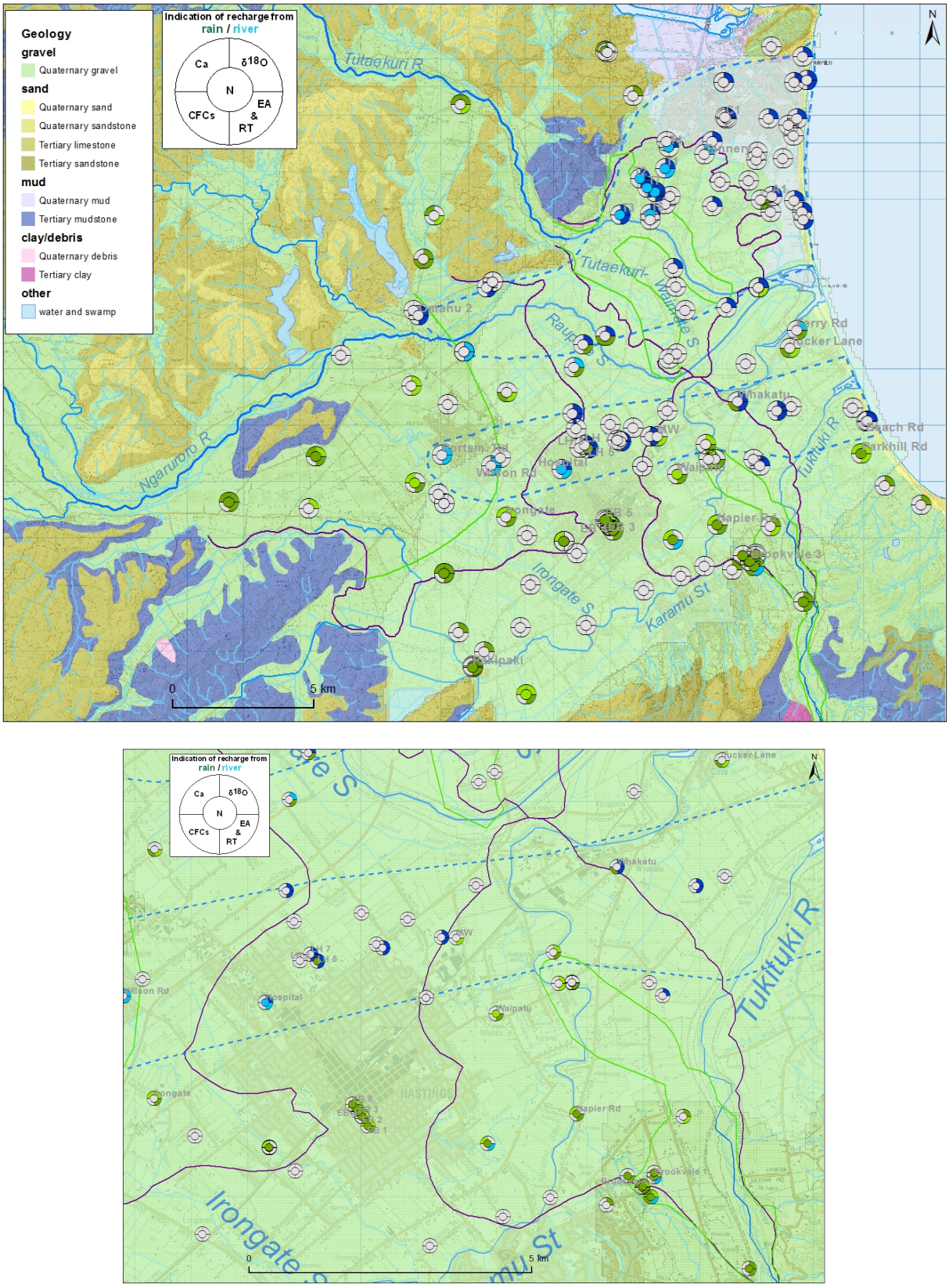

Figure 4.19 Maps of indicators for groundwater recharge source. Green represents local rain, and blue represents river/stream recharge. Darker colours indicate stronger evidence. The light green in the area of Quaternary gravels indicates the area of confined aquifer. Green and purple lines indicate surface and subsurface extension of the Holocene river gravel fans, respectively. Lower figure shows zoom-in of central part of the plains.

The groundwater in the southern half of the Heretaunga Plains aquifer shows indications of recharge from local rain, including that of the drinking water wells that draw water from the

confined aquifer. The distinctly less negative stable isotope composition and high calcium concentration in some of these groundwaters indicate that this groundwater receives some recharge from the adjacent hills (limestone, mudstone, sandstone areas) south of the Heretaunga Plains, and that the groundwater from these areas discharges into the southern part of the Heretaunga Plains aquifers.

4.8 GROUNDWATER AND SURFACE WATER INTERACTION

Elevated radon concentrations in surface water indicate fresh groundwater discharge into the surface water body (Section 3.3). Surface water radon samples have been collected and measured for 20 sites within the Heretaunga Plains area (Figure 4.20). Radon concentrations above 0.5 Bq/L indicate groundwater discharge into the river or stream at or slightly upstream of the sampling site. Concentrations above 3 Bq/L indicate groundwater influx of the order of >10%. Concentrations of radon below 0.3 Bq/L, which is close to background concentration, indicate insignificant groundwater discharge at or near the sampling site.

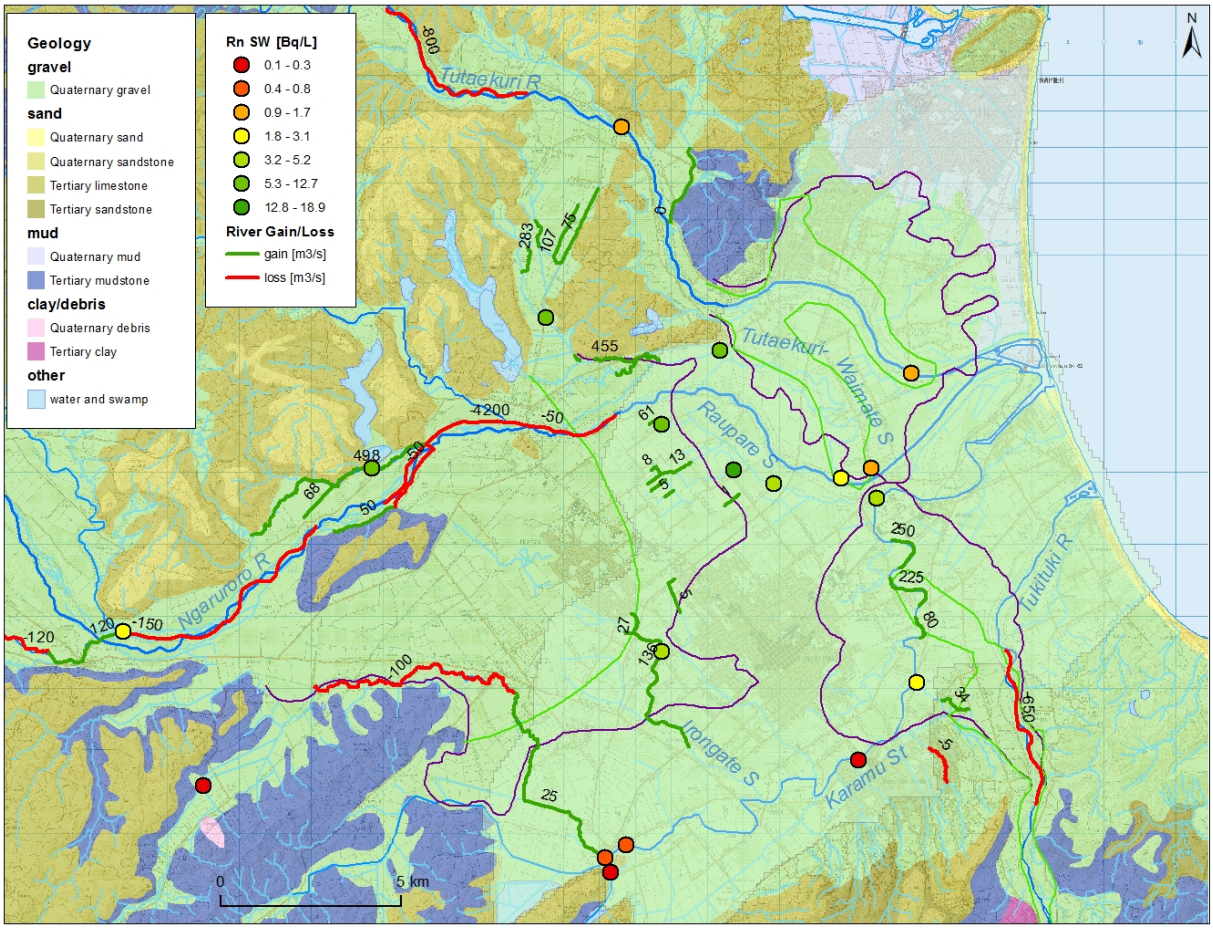

Figure 4.20 Map of radon concentrations in surface waters, including gaining and losing stretches of the rivers. Radon samples were collected at low-flow conditions.

Radon sampling of surface water sites is relatively sparse in the Heretaunga Plains. However, even the small data set shows a discharge pattern that is mostly consistent with observed gain-loss patterns in rivers and streams (red and green river and stream stretches, Figure 4.20):

- Low radon concentrations in the lower reaches of the Tutaekuri River indicate that there is little or no interaction between ground and surface water.

- High radon concentrations south of the Tutaekuri River (Moteo Valley) indicate high groundwater discharge into the streams, probably water lost from the upstream reaches of the Tutaekuri River.
- High radon concentrations in the gaining reaches of the Ngaruroro River (U/S Maraekakahoe) and its tributary (Waitio Stream at Ohiti Road) confirm groundwater discharge into the river and stream.
- High radon concentrations in the drainage area south of the Ngaruroro River (Raupare and tributaries) indicate discharge from the groundwater system, potentially resurfacing water lost from the Ngaruroro River further upstream.
- High radon concentration in the lower reaches of Karamu Stream (Floodgates) and one of its tributaries (Mangateretere Stream at Napier Rd.) indicate discharge from the groundwater system.

Despite being small, the data set demonstrates the utility of the radon method for identifying groundwater discharges into surface water bodies in the Heretaunga Plains. These groundwater discharges contain sufficient radon to allow for easy detection of groundwater discharge into the rivers and streams. Higher resolution radon surveys along rivers and streams (a sample every c. 200 m) would provide a detailed picture of groundwater and surface water interaction in a very cost-effective way while showing areas of groundwater discharge and potentially also indicating losing stretches of the rivers and streams (Figure 4.11 in Morgenstern et al. 2017).

4.9 SUMMARY OF INFERRED GROUNDWATER FLOW SOURCES AND DYNAMICS IN THE HERETAUNGA PLAINS AQUIFER

Figure 4.21 provides a schematic summary of the conceptual flow model of the Heretaunga Plains aquifer system that builds on previous conceptualisations using the age, chemistry and stable-isotope data and their interpretations that are presented in this works. Groundwater flow velocities in the confined aquifer were estimated from horizontal distance and increase in groundwater age.

The water discharging from the Moteo Valley south of the area where the Tutaekuri River loses part of its flow to the groundwater system, and the Tutaekuri River water have similar age, indicating high groundwater velocities of > 5 km/year through this system. Hydrochemistry and isotopic signature indicate limited, or non-existent, connection of the Moteo Valley aquifer to the Heretaunga Plains aquifer. The characteristic hydrochemistry and isotopic signature of the Tutaekuri River (Figure 4.13 and Figure 4.17), containing significant sandstone and limestone formations in its catchment, does not appear in the northern part of the Heretaunga Plains aquifer. This is in some conflict with previous geological and hydrogeological understanding of the Moteo valley, where piezometric surveys indicated connection of the Moteo valley and Heretaunga Aquifer (e.g. Dravid and Brown, 1997). However, the water budget also indicates limited connection between the Moteo valley and Heretaunga Aquifer (Rakowski and Knowling, 2018).

This lack of connection of the Tutaekuri River system to the main aquifer, as indicated by red crosses in Figure 4.21, applies to both, the discharges from the Moteo Valley, and potentially lost water from the river within the Tutaekuri River gravel fan. This apparent disconnection between the Tutaekuri River and the main aquifer is consistent with water balance measurements (Figure 4.20), which suggest that there is no water loss from the Tutaekuri

River into its gravel fan, and the surface water loss from the Tutaekuri River further up is approximately equal to the surface water gain downstream at the end of the Moteo Valley.

The groundwater in the Ngaruroro River gravel fan region, primarily containing water lost from the river, is also very young, indicating groundwater flow velocities of c. 5 km/year towards the north-east, and c. 2.8 km/year towards south-east along the presumed paleo river channel toward the coast (lower area indicated by blue dotted lines). The flow velocity reduces considerably near the coast, by two orders of magnitude, likely related to deposition of finer material.

The north-east flow direction apparent furthest to the north toward Napier slows from the initial large flow velocity of c. 5 km/year to about 0.4 km/year through to about halfway to the coast. Then the flow successively slows to 0.3 and 0.06 km/year. The flow at the southern end of this area characterised by river recharge slows down in a similar way, from c. 0.5 to 0.3 to 0.2 km/year. Similarly, in the southern band of river recharged groundwaters flow velocities slow from c. 2.8 to c. 0.15 km/year near the coast. Data near the coast are too scarce to derive information about continuation of flow off-shore.

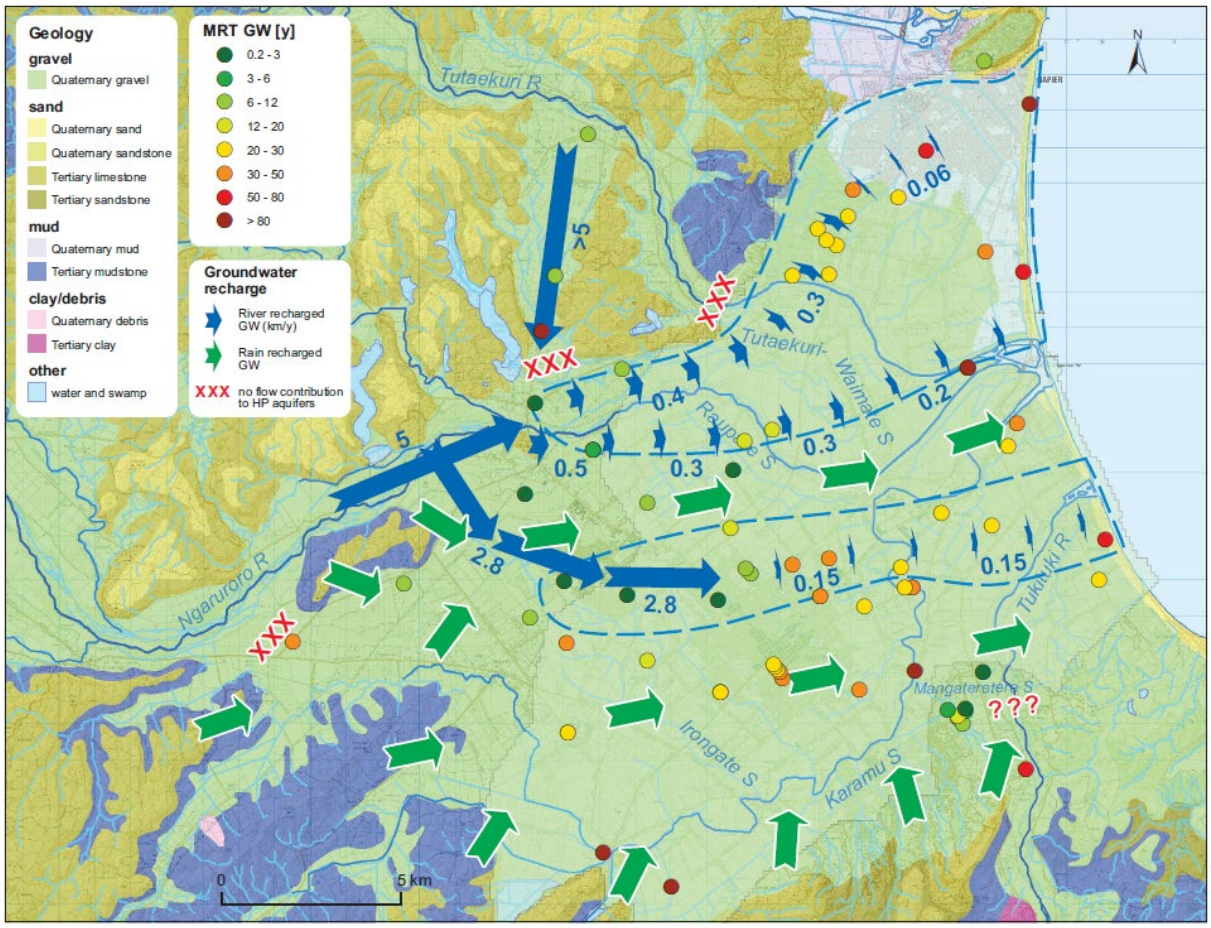

Figure 4.21 Water dynamics in the Heretaunga Plains hydrologic system inferred from groundwater ages (circles). Blue arrows indicate river recharged groundwater flows, with the length of the arrows proportional to the groundwater flow velocity (numbers in km/year). Green arrows indicate rain recharged groundwater flow direction in general, without information on flow velocity. Red crosses indicate no connection of potentially lost surface water to the main aquifer. Red question marks indicate unknown contribution of the river to the main aquifer due to lack of data. The two areas indicated by blue dotted lines are the areas of clear Ngaruroro River-recharge signature (Figure 4.18). The light green in the area of Quaternary gravels indicates the area of confined aquifer.

Water lost from the Ngaruroro River surface flow in the west of Figure 4.20 appears to have no subsurface connection toward the east into the main aquifer (red crosses in the east). A

shallow groundwater well in this area contains anoxic old water, indicating that there is no active subsurface flow.

Water lost in the Tukituki River gravel fan could not be identified in groundwater wells in the area. The wells, including those in Havelock North, display a different chemistry and isotopic signature (Figure 4.13, Figure 4.16 and Figure 4.17). Also other recharge source indicators do not indicate recharge from the river in these wells (Figure 4.19). The discharge area of the water lost from the Tukituki River in the east of Figure 4.20 remains unclear due to lack of data. However, it may re-surface via the springs along Karamu Stream. Their hydrochemistry is similar, and the surface water gain through these springs is about equal to the water loss from the Tukituki River upstream (Figure 4.20).

Green arrows in Figure 4.21 indicate the areas where the tracer signature indicates the presence of recharge from rain, locally and from the adjacent hills. This includes about half of the area that is considered to be confined. Crossing blue and green arrows in the centre indicates river-recharged groundwater flow at depth, overlain by shallower flow draining the local rain recharged groundwater system.

5.0 CONCLUSIONS

This study demonstrates the effectiveness of groundwater age, stable isotope and hydrochemistry data in determining and quantifying water transit times and related time lags between change in land use and its impact on water quality; groundwater recharge mechanisms; available baseflow groundwater storage; interactions between surface- and ground-waters; and groundwater flow pathways.

Through the recent study by Hawke's Bay Regional Council, and through the systematic monitoring of the Hastings District Council and Napier City Council drinking water wells and the GNS' National Groundwater Monitoring Programme and National Tracer survey, and in combination with previous local studies, age tracer data are presently available from approximately 160 sites. This allowed for identification of regional and local pattern in tracer input signatures, which in-turn provided a basis for expanding upon the insights from previous studies, resulting in a large-scale perspective on the dynamics of the Heretaunga Plains groundwater resources.

For most of the groundwater-well sites with age tracer data, it was possible to obtain groundwater ages, allowing the identification of areas of recharge (defined by young water) and flow direction (gradient of groundwater age).

Tritium-derived mean ages show consistent patterns in the main rivers with MTTs of usually less than 2 years in the Tukituki, Waipawa, and Ngaruroro rivers, and somewhat older water with a MTT around 10 years discharging via the Tutaekuri River. Surface water discharging in proximity to limestone, sandstone and mudstone formations between the Ruataniwha and the Heretaunga Plains contain significantly older water, with a MTT of up to 140 years, including the Karamu tributaries, which collectively drain this area.

Groundwater in most of the wells within the Holocene unconfined gravel fans of the Ngaruroro and Tukituki rivers are relatively young, with MRT of between 0–10 years. Along its flow path from the area of the main water loss from the Ngaruroro River at the boundary of confinement, the groundwater within the confined aquifer becomes progressively older. Relatively high groundwater flow velocities in the confined aquifer toward the coast is indicated also in the centre of the Plains by a tongue of very young groundwater (MRT <5 years). At the southern margin of the confined aquifer, older water (MRT 73 years) near the coast at Beach Road also indicates more sluggish flow in this region close to the coast.

Indicators of recharge temperature collectively suggest that all investigated groundwaters were recharged under current climatic conditions. All groundwater samples are to some degree depleted in oxygen, indicating the ubiquitous presence of organic matter in the Heretaunga Plains aquifers.

A number of key hydrochemical data, together with age data, indicate that the impact on groundwater quality by high-intensity land use is minor in the Heretaunga Plains groundwater system. Only a few groundwater samples display nitrate and sulphate concentrations slightly above the threshold concentration indicative of high-intensity land use.

Distinct differences in the signatures of groundwater hydrochemistry, isotopic composition, and gas concentrations collectively allowed us to distinguish between recharge from local rain and river water. Using a combination of parameters that have different drivers, including climate, water table gas exchange processes, industrial and agricultural contaminants, and local geology, the tracer signature allowed us to gain an informed conceptualisation of aquifer parts

with the presence of locally rain-recharged groundwater, and exclusively river-recharged groundwater.

The extensive data set employed in this study has provided a basis for many new insights into groundwater processes and dynamics in the Heretaunga Plains. By systematic application of the multi-tracer methods, the full potential of these tools can be realised in regard to understanding the groundwater dynamics, which is not possible with other techniques.

6.0 RECOMMENDATIONS

To further the understanding of the groundwater processes and the dynamics of the young and actively recharging groundwater resources in the Heretaunga Plains, including their interaction with surface water, we make the following recommendations:

- *Refine River MRTs and groundwater storage in the river catchments*. Currently, there is a relatively high uncertainty around the MRTs of the young river waters due to tritium input uncertainty. Currently, the tritium input in the area is measured in rain collected at the Bridge Pa climate station. After these data are available, the tritium input uncertainty will be reduced, ultimately leading to more accurate MRTs. The MRT uncertainty of the young river waters could also be reduced by performing a second tritium survey at these river sites, during the time when tritium data is collected at Bridge Pa. This additional data will not only lead to better MRTs, but also improve significantly the accuracy of groundwater storage estimates.
- Obtain more tracer data in shallow bores in the rain recharge area to establish recharge rates. From the gradient of groundwater age with depth, recharge rate can directly be established.
- Measure age tracers in non-production observation bores near the coast to investigate if the aquifer flow continues off-shore.
- *Perform a high-resolution stable isotope survey*, including better spatial coverage of the different potential recharge sources, and seasonal variability. This would provide better understanding of the stable isotope composition of the water from the various recharge sources, including seasonal variability and thus be useful to identify recharge sources more robustly, including mixing of water from the various sources.
- *Conduct a detailed radon sampling of the main rivers (200-400 m linear resolution) and waterways* to provide a more spatially detailed understanding of groundwater gains and losses.
- Perform a high-resolution survey of springs to identify the connection of these springs to water lost from the rivers, especially in the Tukituki area where more certainty is required to link the springs along Karamu to the Tukituki River.
- Measure recharge indicators in additional wells in the area between the two river recharged areas, to confirm the presence of a band of rain-recharged groundwater flow toward the coast.
- Obtain more age data in the southern part of the confined aquifer to establish horizontal flow rates also in this area.
- Repeat sampling of the HBRC wells surveyed between 2014 and 2016 to provide time series' of age tracer data. This would allow for identification of young water fractions using binary mixing models.
- Using the improved geologic model, assign well screens to specific aquifers and discuss the tracer results in relation to specific aquifers to enable better 3D understanding of MRT distribution. This will allow identification of horizontal flow rates in these specific aquifers, and potentially also recharge rates.
- Search in historic data bases to identify well details for sites with historic tracer data that are *not already included in the current analysis*. This could increase the number of sites significantly. As a considerable amount of the older tritium data dates back to 1957 and 1964, this may allow identification of changes in the aquifer over the last 60 years.

- Integrate insights gained from this study with concurrent groundwater modelling work being undertaken as part of the greater TANK project. The mean-age estimates presented here are already being used to inform model aquifer properties such as effective porosity and hydraulic conductivity, and, together with other field observations, to construct a series of model parameter realisations that collectively represent the uncertainty associated with model parameters and therefore predictions of management interest made by those models (Knowling et al., in prep). It is suggested that future work also uses the suite of groundwater models developed as a means of testing whether the river-versus-rain recharge patterns identified in this study can be reproduced while maintaining satisfactory matches to other data types, e.g., using model particle-tracking methods.

7.0 ACKNOWLEDGEMENTS

We wish to thank Biljana Lukovic for help with the ArcGIS maps, Catherine Cooper and Eileen McSaveney for help with the manuscript, and Ellen Fransen for formatting this report. Craig Thew (HDC) and Santha Agas (NCC) and their teams are thanked for help with sampling and providing the funds for the tracer analyses for the drinking water wells.

8.0 REFERENCES

Baisden WT, Keller ED, Van Hale R, Frew RD, Wassenaar LI. 2016. Precipitation isoscapes for New Zealand: enhanced temporal detail using precipitation-weighted daily climatology. Isotopes in environmental and health studies, doi: 10.1080/10256016.10252016.11153472.

Bard E, Hamelin B, Arnold M, Montaggioni L, Cabioch G, Faure G, Rougerie F. 1996. Deglacial sea-level record from Tahiti corals and the timing of global meltwater discharge. Nature 382: 241–244.

Beanland S, Melhuish A, Nicol A, Ravens J. 1998. Structure and deformational history of the inner forearc region, Hikurangi subduction margin, New Zealand. *New Zealand Journal of Geology and Geophysics* 41: 325–342.

Berghuijs, W. R., Kirchner J. W. 2017. The relationship between contrasting ages of groundwater and streamflow, Geophys. Res. Lett., 44, doi:10.1002/2017GL074962.

Beyer M, Morgenstern U, Jackson B. 2014. Review of dating techniques for young groundwater (<100 years) in New Zealand. *Journal of Hydrology, New Zealand*. 53(2):93–111.

Black TM. 1992. Chronology of the Middle Pleistocene Kidnappers Group, New Zealand and correlation to global oxygen isotope stratigraphy. Earth and Planetary Science Letters 109: 573–584.

Brown LJ, Dravid PN, Hudson N, Taylor CB. 1999. Sustainable groundwater resources, Heretaunga Plains, Hawke's Bay, New Zealand. Hydrogeology Journal, 7(5), 440–453.

Busenberg E, Plummer LN. 1992. Use of chlorofluorocarbons (CCl3F and CCl2F2) as hydrologic tracers and age dating tools: the alluvium and terrace system of Central Oklahoma. *Water Resources Research*. 28(9):2257–2283. doi:10.1029/92wr01263.

Busenberg E, Plummer LN. 1997. Use of sulfur hexafluoride as a dating tool and as a tracer of igneous and volcanic fluids in ground water [abstract]. In: GSA 1997 Annual Meeting: Abstracts with programs. Boulder (CO): Geological Society of America. A-78. (Abstracts with programs / Geological Society of America; 29(6)).

Cartwright I, Morgenstern U. 2012. Constraining groundwater recharge and the rate of geochemical processes using environmental isotopes and major ion geochemistry: Ovens Catchment, southeast Australia. *Journal of Hydrology*. 475:137–149.

Cecil D, Green J. 2000. Radon-222. In: Cook PG, Herczeg AL, editors. Environmental tracers in subsurface hydrology. Massachusetts: Kluwer Academic Publishers. p. 175–194.

Chapelle FH. 1993. Ground-water microbiology and geochemistry. Wiley and Sons, New York

Close M, Matthews M, Burbery L, Abraham P, Scott D. 2014. Use of radon to characterise surface water recharge to groundwater. *Journal of Hydrology*. 53(2):113.

Daughney CJ, Reeves RR. 2005. Definition of hydrochemical facies in the New Zealand National Groundwater Monitoring Programme. *Journal of Hydrology*, New Zealand. 44(2):105–130.

Daughney CJ. 2007. Spreadsheet for automatic processing of water quality data: 2007 update. Lower Hutt (NZ): GNS Science. 15 p. (GNS Science Report; 2007/17).

Daughney CJ. 2010. Spreadsheet for automatic processing of water quality data: 2010 update, calculation of percentiles and tests for seasonality. Lower Hutt (NZ): GNS Science. 16 p. (GNS Science report; 2010/42).

Dravid, PN, Brown, L.J. 1997 Heretaunga Plains Groundwater study. Hawke’s Bay Regional Council and Institute of Geological & Nuclear Sciences report.

Garcia-Vindas, J, Monnin M. 2005. Radon concentration measurements in the presence of water and its consequences for Earth sciences studies. *Radiation Measurements*, 39(3), 319–322.

Gibb JG. 1986. A New Zealand regional Holocene eustatic sea-level curve and its application to determination of vertical tectonic movements. *Royal Society of New Zealand Bulletin* 24: 377–395.

Güler C, Thyne GD, McCray JE, Turner A.K. 2002. Evaluation of graphical and multivariate statistical methods for classification of water chemistry data. *Hydrogeology* J. 10: 455–474.

Heaton THE, Vogel JC. 1981. "Excess air" in groundwater. *Journal of Hydrology*. 50(C): 201–216.

Hull AG. 1990. Tectonics of the 1931 Hawke's Bay earthquake. *New Zealand Journal of Geology and Geophysics* 33: 309–320.

Ingram RGS, Hiscock KM, Dennis PF. 2007. Noble gas excess air applied to distinguish groundwater recharge conditions. Environmental Science and Technology. 4(6):1949–1955.

Kies A, Hofmann H, Tosheva Z, Hoffmann L, Pfister L. 2005. Using 222 Rn for hydrograph separation in a micro basin (Luxembourg). *Annals of Geophysics*. 48(1):101–107.

Langridge RM, Ries, WF. 2015 Active fault mapping and fault avoidance zones for Hastings District and environs. GNS Science consultancy report 2015/112. 50 p. + 1 DVD

Lisiecki LE, Raymo ME. 2005. A Pliocene-Pleistocene stack of 57 globally distributed benthic □18O records. Paleoceanography 20: PA1003, 17 pp.

Maiss M, Brenninkmeijer CAM. 1998. Atmospheric SF6: trends, sources and prospects. Environmental Science and Technology. 32(20):3077–3086.

Małoszewski P, Zuber A. 1982. Determining the turnover time of groundwater systems with the aid of environmental tracers. *Journal of Hydrology*. 57(3-4):207–231.

Martindale H, Morgenstern U, Singh R, Stewart B. 2016. Mapping groundwater-surface water interaction using radon-222 in gravel-bed rivers: a comparative study with differential flow gauging. *Journal of Hydrology*, 55(2), 121.

Martindale H. 2015. The use of radon and complimentary hydrochemistry tracers for the identification of groundwater–river water interaction in New Zealand. [Unpublished MSc Thesis]. Palmerston North (NZ): Massey University.

McMahon, P. B., & Chapelle, F. H. (2008). Redox Processes and Water Quality of Selected Principal Aquifer Systems. *Ground Water, 46*(2), 259-271.

Ministry for the Environment. 2007. Groundwater quality in New Zealand: State and trends 1995-2006. Wellington (NZ): Ministry for the Environment. Publication No.: ME 831.

Morgenstern U, Brown LJ, Begg JG, Daughney, CJ, Davidson P. 2009. Linkwater catchment groundwater residence time, flow pattern, and hydrochemistry trends. Lower Hutt (NZ): GNS Science. 47 p. (GNS Science report; 2009/08).

Morgenstern U, Daughney CJ, Leonard GS, Gordon D, Donath FM, Reeves RR. 2015. Using groundwater age to understand sources and dynamics of nutrient contamination through the catchment into Lake Rotorua, New Zealand. *Hydrology and Earth System Sciences*. 19(2):803–822.

Morgenstern U, Daughney CJ. 2012. Groundwater age for identification of baseline groundwater quality and impacts of land-use intensification: The National Groundwater Monitoring Programme of New Zealand. *Journal of Hydrology*. 456/457:79–93.

Morgenstern U, Gordon D. 2017. Water and nutrient flow pathways in the Papanui Catchment: Source, mean residence time, and connection between ground- and surface- water. GNS Science Report 2017/08, 27 p. doi: 10.21420/G2KG6G.

Morgenstern U, Stewart MK, Stenger R. 2010. Dating of streamwater using tritium in a post nuclear bomb pulse world: Continuous variation of mean transit time with streamflow. *Hydrology and Earth System Sciences*. 14:2289-2301. http://dx.doi.org/10.5194/hess-14-2289-2010.

Morgenstern U, Taylor CB. 2009. Ultra low-level tritium measurement using electrolytic enrichment and LSC. Isotopes in Environmental and Health Studies. 45(2):96–117.

Morgenstern U, van der Raaij R, Martindale H, Toews M, Stewart M, Matthews A, Trompetter V, Townsend D. 2017. Groundwater dynamics, source, and hydrochemical processes as inferred from Horizon's Regional Age Tracer Data. Lower Hutt (NZ): GNS Science. 63 p (GNS Science Report; 2017/15). doi: 10.21420/G2J596.

Morgenstern U, van der Raaij RW, Baalousha H. 2012. Groundwater flow pattern in the Ruataniwha Plains as derived from the isotope and chemistry signature of the water. Lower Hutt (NZ): GNS Science. 44 p. (GNS Science Report; 2012/23).

Nazaroff WW. 1992. Radon transport from soil to air. *Reviews of Geophysics*. 30(2):137–160.

NIWA National Climate Database. 2015. Wellington (NZ): NIWA. [accessed 2017 Apr 26]. http://cliflo.niwa.co.nz/

Plummer LN, Busenberg E. 1999. Chlorofluorocarbons. In: Cook P, Herczeg A, editors. Environmental tracers in subsurface hydrology. Boston (MA): Kluwer Academic Publishers. p. 441–478.

Rakowski P, Knowling MJ. in prep. Heretaunga aquifer system groundwater model, development report. Napier (NZ): Hawke's Bay Regional Council. Technical Report

R Core Team, 2016. R: A language and environment for statistical computing. R Foundation for Statistical Computing, Vienna, Austria. https://www.R-project. org/

Rochford, J. 1876. Plan of the Napier County Districts, Hawke's Bay, New Zealand. Edward Syndon, Napier.

Rosen MR. 2001. Hydrochemistry of New Zealand's aquifers. In: Rosen MR, White PA, editors. Groundwaters of New Zealand. Wellington (NZ): New Zealand Hydrological Society. p. 77–110.

Siddall M, Rohling EJ, Almogi-Labin A, Hemleben Ch, Meischner D, Schmelzer I, Smeed DA. 2003. Sea-level fluctuations during the last glacial cycle. *Nature* 423: 853–858.

Stellato L, Terrasi F, Marzaioli F, Belli M, Sansone U, Celico F. 2013. Is 222Rn a suitable tracer of stream–groundwater interactions? A case study in central Italy. Applied Geochemistry. [accessed 2017 Apr 26]; 32:108–117. http://dx.doi.org/10.1016/j.apgeochem.2012.08.022.

Stewart MK, Morgenstern U. 2001. Age and source of groundwater from isotope tracers. In: Rosen MR, White PA, editors. Groundwaters of New Zealand. Wellington (NZ): New Zealand Hydrological Society. p. 161–183.

Stewart MK, McDonnell JJ. 1991. Modeling baseflow soil water residence times from denterium concentrations. Water Resources Research 27(10): 2681–2693

Stewart MK, Taylor CB. 1981. Environmental isotopes in New Zealand hydrology. 1. Introduction: The role of oxygen-18, deuterium, and tritium in hydrology. *New Zealand Journal of Science*. 24(3/4):295–311.

Trompetter V, Martindale H, van der Raaij RW, Morgenstern U. 2016 Building a stable isotope map of NZ groundwaters from existing data. Part 2. 1 p. IN: NZ Hydrological Society Annual Conference: from data to knowledge, 1 to 4 December 2015, Hamilton [abstracts]. Wellington: New Zealand Hydrological Society

van der Raaij RW. 2003. Age dating of New Zealand groundwaters using sulphur hexafluoride. [MSc thesis]. Wellington (NZ): Victoria University of Wellington. 122 p.

Waldron R., Kozyniak K. (Draft 2017) "Hawke's Bay hydrological data 2008-2014 - State of the Environment technical report". Hawke's Bay Regional Council.

Ward JH. 1963 Hierarchical grouping to optimize an objective function. J Am Stat Assoc 69:236–244

Wilding T.K. (draft 2017) "Heretaunga Springs: Gains and losses of stream flow to groundwater on the Heretaunga Plains". HBRC Report No. 135645, Hawke's Bay Regional Co

APPENDICES

This page is intentionally left blank.

APPENDIX 1 METHODOLOGY OF GROUNDWATER AGE DATING

A1.1 TRITIUM, CFC AND SF_6 METHODS

Tritium is produced naturally in the atmosphere by cosmic rays, but large amounts were also released into the atmosphere in the early 1960s during nuclear bomb tests, giving rain and surface water high tritium concentration at this time (Figure A1.1). Surface water becomes separated from the atmospheric tritium source when it infiltrates into the ground, and the tritium concentration in the groundwater then decreases over time due to radioactive decay. The tritium concentration in the groundwater is therefore a function of the time the water has been underground. In addition, detection of superimposed bomb tritium can identify water recharged between 1960 and 1975. Groundwater dating using tritium is described in more detail in Morgenstern and Daughney (2012).

As a result of the superimposed atmospheric tritium "bomb" peak in the 1960s, ambiguous ages can occur with single tritium determinations before 2014 in the groundwater age range 15–40 years (i.e., the tritium concentration can indicate any of several possible groundwater ages). This ambiguity can be overcome by using a second tritium determination after about 2–3 years, or combined age interpretation of tritium data and data from an independent dating method, for example CFCs or SF_6. CFC and SF_6 concentrations in the atmosphere have risen steadily over that time and therefore can resolve tritium ambiguity if they are not altered in the aquifer.

Chlorofluorocarbons (CFCs) are entirely man-made contaminants. They were mainly used for refrigeration and pressurising aerosol cans, and their concentrations in the atmosphere have gradually increased (Figure A1.1). CFCs are relatively long-lived and slightly soluble in water and therefore enter the groundwater systems with groundwater recharge. Their concentrations in groundwater record the atmospheric concentrations when the water was recharged, allowing determination of the recharge date of the water. CFCs have been phased out of industrial use because of their destructive effects on the ozone layer. Thus rates of increase of atmospheric CFC concentrations slowed greatly in the 1990s and concentrations are now decreasing, meaning that CFCs are not as effective for dating water recharged after 1990.

Sulphur hexafluoride (SF_6) is primarily anthropogenic in origin, but can also occur in some volcanic and igneous fluids. Significant production of SF_6 began in the 1960s for use in high-voltage electrical switches, leading to increasing atmospheric concentrations Figure A1.1). The residence time of SF_6 in the atmosphere is extremely long (800–3200 years). It holds considerable promise as a dating tool for post-1990s groundwater because, unlike CFCs, atmospheric concentrations of SF_6 are expected to continue increasing for some time (Busenberg and Plummer, 1997).

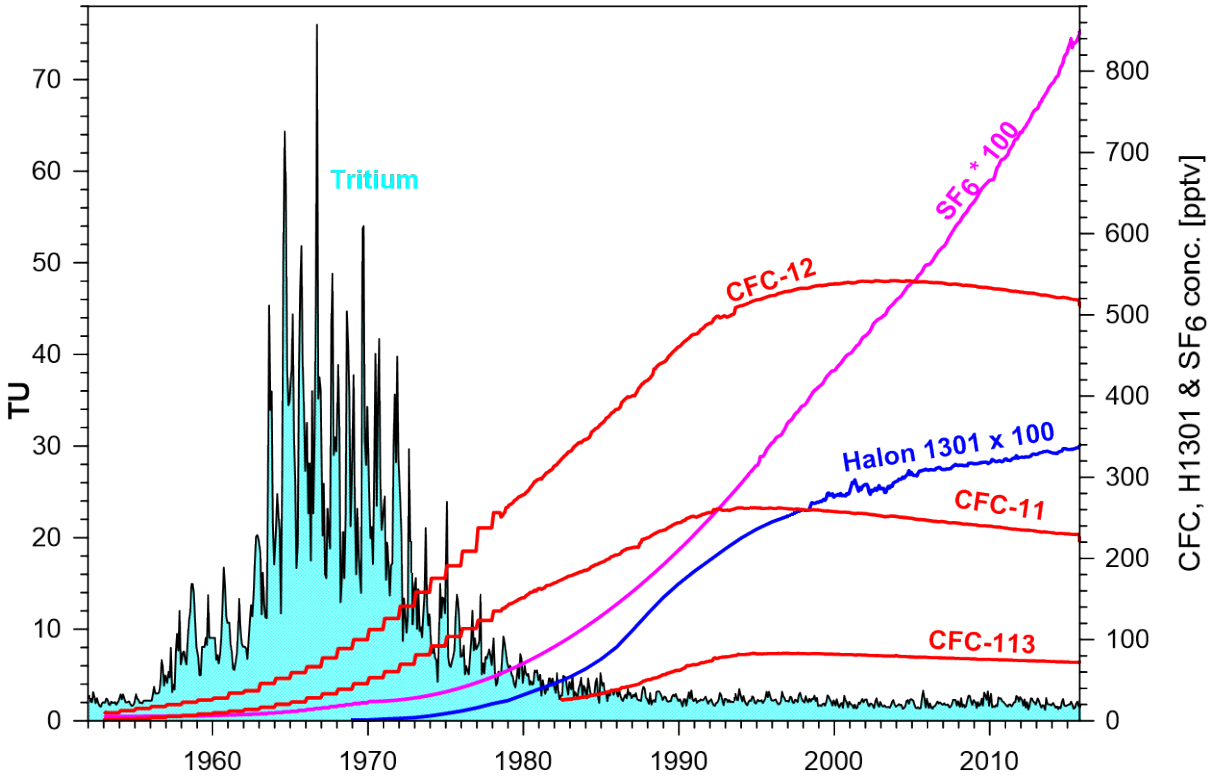

Figure A1.1 Tritium, CFC and SF_6 input for New Zealand rain. Tritium concentrations are in rain at Kaitoke, 40 km north of Wellington (yearly averages), and CFC and SF_6 concentrations are for southern hemispheric air. TR=1 represents a $^3H/^1H$ ratio of 10-18, and 1 pptv is one part per trillion by volume of CFC or SF_6 in air, or 10^{-12}. Pre-1978 CFC data are reconstructed using methods of Plummer and Busenberg (1999), and scaled to the southern hemisphere by a factor of 0.83 (CFC-11) and factor 0.9 (CFC-12). Post-1978 CFC data are from Tasmania. Pre-1970 SF_6 data are reconstructed (USGS Reston), 1970-1995 data are from Maiss and Brenninkmeijer (1998), and post-1995 data was measured in Tasmania.

Tritium is a conservative tracer in groundwater. It is not affected by chemical or microbial processes, or by reactions between the groundwater, soil sediment and aquifer material. Tritium is a component of the water molecule, and age information is therefore not distorted by any processes occurring underground. For CFCs, a number of factors can modify the concentrations in the aquifer (Plummer and Busenburg, 1999), including microbial degradation of CFCs in anaerobic environments (CFC-11 is more susceptible then CFC-12), and CFC contamination from local anthropogenic sources (CFC-12 is more susceptible to this). CFC-11 has been found in New Zealand to be less susceptible to local contamination and age estimates agree better with tritium data. Note that CFC and SF_6 ages do not take into account travel time through unsaturated zones.

The tritium method is very sensitive to the flow model (distribution of residence times in the sample) due to the large pulse-shaped tritium input during 1965–1975. With a series of tritium measurements, and/or additional CFC and SF_6 measurements, age ambiguity can usually be resolved. In that case, both the mean groundwater age and the age distribution can be obtained.

A1.2 GROUNDWATER MIXING MODELS

Groundwater comprises a mixture of water of different ages due to mixing processes underground. Therefore, the groundwater doesn't have a discrete age but, rather, an age distribution or spectrum. Various mixing models with different age distributions describe different hydrogeological situations (Maloszewski and Zuber 1982). The piston-flow model describes systems with little mixing (such as confined aquifers and river recharge), while the exponential model describes fully mixed systems (more like unconfined aquifers and local rain recharge). Real groundwater systems, which are partially mixed, lie between these two extremes. They can be described by a combination of the exponential and piston-flow models representing the recharge, flow and discharge parts of a groundwater system respectively. The output tracer concentration can be calculated by solving the convolution integral, and the mean residence time (MRT) can be obtained from the tracer output that gives the best match to the measured data. If the second parameter in the age distribution function, the fraction of mixed flow, cannot be estimated from hydrogeological information, then two independent tracers (tritium and CFC/SF_6) or two tritium measurements over time are necessary.

Schematic groundwater flow situations are shown in Figure A1.2. The unconfined aquifer situation is described by the exponential model (EM). Flow lines of different length containing water of different age converge in the well or the stream, and the abstracted water has a wide range of ages with an exponential age distribution. The confined aquifer situation is described by the piston flow model (PM) with a narrow range of ages. The partly confined aquifer situation is described by the Exponential Piston flow model (EPM). The free parameter is the fraction of exponential flow within the total flow volume (represented by E%PM, where the fraction is given in %), or the ratio η of the total flow volume to the volume of the exponential part. The water has a wide range of ages, but because part of the flow is piston flow, the age distribution has a minimum age (no water can be younger than the time necessary to pass through the piston flow part). The piston flow part can be represented by a partly confined flow with no vertical input of young water from the surface, or it can be represented by a significant unsaturated zone with vertical piston flow toward the water table and mixing of different ages below the water table.

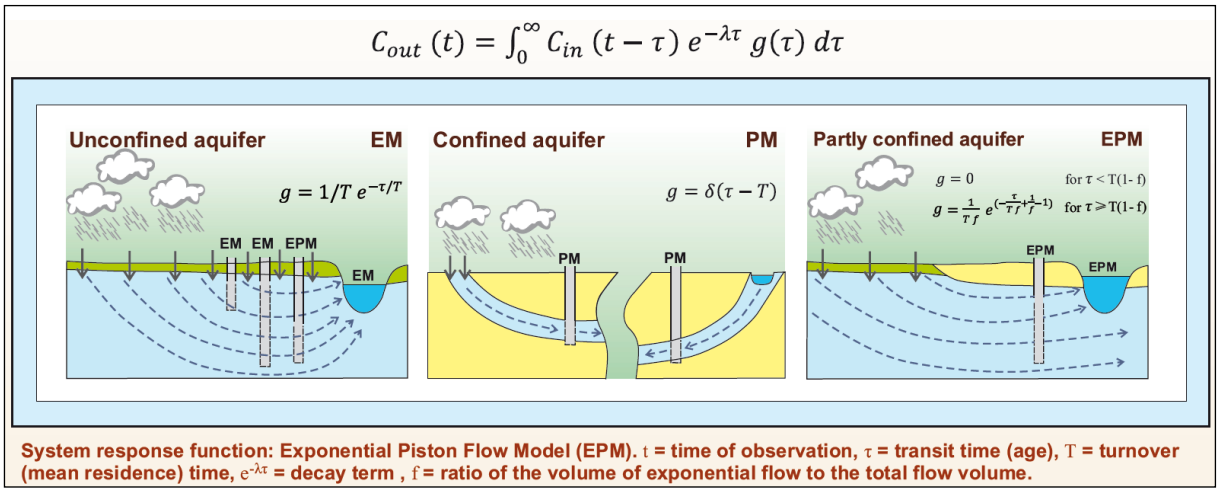

Figure A1.2 Schematic groundwater flow scenarios and corresponding age distribution functions (see Maloszewski and Zuber (1982) for theoretical background)

As an example, the age distribution for the EPM for different fractions of mixed flow is shown in Figure A1.3 for water with a MRT of 50 years. Water with a high fraction of exponential flow of 90% has a wide range of ages, starting at 5 years and still significant contributions of old water with ages over 150 years. Despite the MRT of 50 years, the major part of the water is younger than 50 years. The water can therefore partly be contaminated before the MRT of 50 years has elapsed. About 2% of the water can already be contaminated after 5 years. With each further year, these young fractions accumulate, and increasingly contaminated water arrives at the spring or well. The total fraction of water within a certain age range can be obtained by integrating the age distribution over the specified age range. This is equal to the area below that part of the curve, with the total area below the whole curve being the 100% water fraction. The fraction of water that is younger than a specified age is called the young water fraction (yf). The young water fraction younger than 55 years is about 80% in the example in Figure A3 (hatched area).

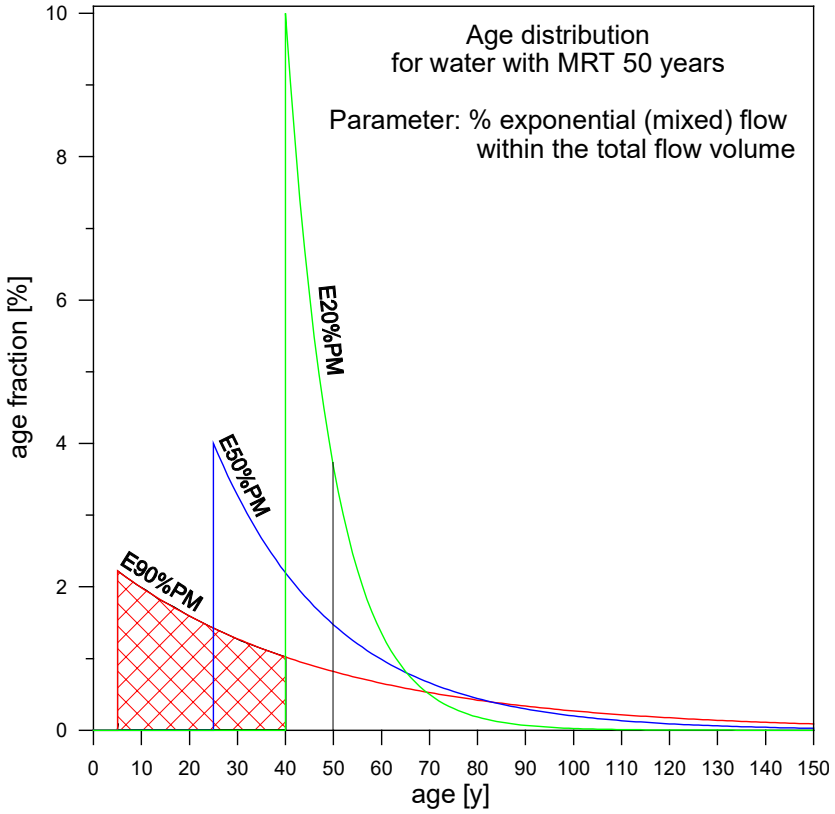

Figure A1.3 Age distribution for the EPM.

In a flow situation with less exponential flow, the age distribution of the water has a narrower spread. At 50% exponential flow, the minimum age is 25 years, and the water does not contain significant fractions older than 150 years. At only 20% exponential flow, the age distribution is relatively peaked around the MRT. The minimum age is 40 years, and there is an insignificant amount of water older than 100 years. This water would just start to show a contaminant introduced 40 years ago, but this contaminant would arrive in a relatively sharp front, with a 10% contribution in the first year of arrival after 40 years' time.

APPENDIX 2 TRACER DATA SURFACE WATER

Surface water site ID, coordinates, HCA clusters, flow, volume, and mean residence time (MRT). Volume is the low baseflow groundwater volume that feeds the rivers/streams. MRTs were calculated with an estimated 70% fraction of the exponential flow volume within the total volume of the exponential flow model. For full tracer data set refer to the supplementary Excel file (Summary Age Data).

Table A2.1 Tracer Data Surface water

Site ID	NZTM E	NZTM N	HCA Cluster	MTT [years]	Flow [L/s]	Volume [M m^3]
Tukituki River at River Rd.	1936960	5602124		2		
Tukituki River at Takapau SH50	1886511	5573925		2		
Tukitiki River at Tamumu Bridge	1914632	5570127		2		
Tukituki River at Parsons Rd.	1897627	5571026		2		
Tukituki River at Tapairu Rd.	1908326	5569525	1	2		
Tukituki River at Red Bridge	1936570	5596260	1	5	4138	653
Waipawa River at SH50	1894615	5581832		0.5		
Waipawa River at RDS/SH2	1906374	5571933	1	0.5		
Papanui Stream at Walker Road	1911310	5569834	1	4	57	
Kaikora Stream at NIWA Gauge Station	1906682	5578966	2	8		
Te Aute School Spring at Kaikora Triburary	1908730	5585731	2	18		
Kaikora Drain U/S Papanui Stream	1915456	5579780	2	14	83	37
Papanui Stream at Newmans Ford	1915530	5579735	1	8		
Papanui Stream at Middle Road	1917832	5581536	2	11	126	42
Papanui Stream at Camp David	1919167	5584050	1	7	524	
Karamu Stream at Havelock Road	1932190	5602020	2	23	219	159
Karamu Stream at Floodgates	1932710	5609270	1	13	808	319
Poukawa Stream at Stock Road	1925313	5598912	2	140	15	66
Paritua Stream at Water Wheel	1914020	5601310	2	37	35	41
Karewarewa Stream at Pakipaki	1925160	5599310	2	12	12	4.5
Te Waikaha Stream at Mutiny Road	1926137	5595551	2	120		
Awanui Stream at Flume	1925735	5599654	2	48	41	62
Spring 22 at Karamu Stream SH2	1933499	5606783		27		
Spring 14 at Karamu Stream Golf Course	1933401	5607331		23		
Mangateretere Stream at Napier Rd.	1933819	5604172	1	10	38	12
Spring 13 at Mangateretere Stream Brookvale Road	1935190	5603427		1		
Spring 12 at Crombie Drain Mangateretere Tributary	1934715	5603375		6		

Site ID	NZTM E	NZTM N	HCA Cluster	MTT [years]	Flow [L/s]	Volume [M m^3]
Irongate Stream at Clarkes Weir	1926737	5605025	1	3	36	3.4
Raupare Drain at Ormond Road	1929836	5609665	1	2	356	22
Raupare Drain at Twyford	1926730	5611316	1	1	50	0.8
Raupare Road Spring	1928734	5610040		2	14	0.9
Ngaruroro River at Ohiti	1917125	5608459		1		
Ngaruroro River at Pakowhai	1932539	5609766		1		
Ngarururo River at Fernhill	1923003	5611329		0	2081	6.6
Ngaruroro River at Whanwhana	1891976	5615740	1	4	5388	595
Ngaruroro River U/S Maraekakahoe	1911787	5605586	1	4	5743	725
Ngaruroro River at Chesterhope Bridge	1932547	5610113	1	6	3728	647
Maraekakaho Stream at Maraekakahoe	1910677	5604844		25	c. 100	
Maraekakaho Stream at Taits Road	1906785	5604891		46	157	228
Waitio Stream at Ohiti Road	1918690	5610114	1	1	524	17
Repokaiterotoroa Stream at Moteo Road	1923529	5614267	2	12	622	226
Tutaekuri Waimate Stream at Goods Bridge	1928340	5613360	1	6	1649	312
Tutaekuri Waimate Stream at Chesterhope	1931723	5609827	1	7	1902	390
Tutaekuri River at Puketapu HBRC Site	1925620	5619570	1	10	3285	1037
Tutaekuri River at Brookfields Bridge	1933670	5612730	2	12	3965	1502
22 Guys rd Napier spring water	1935736	5621425		7		
Drainge channel spring	1901365	5574410		2		
Limestone spring	1901204	5574375		2		

APPENDIX 3 WELL AND TRACER DATA GROUNDWATER

Well ID, coordinates, well and screen depth, mean residence time (MRT), fraction of the exponential flow volume within the total volume of the exponential flow model (E%PM), and Hierarchical cluster analysis (HCA) clusters. For full tracer data set refer to electronic data file. The tracer age data for the groundwater wells are provided in the supplementary Excel file (Summary Age Data), together with the coordinates of the sampling sites, well and lithology data, and hydrochemistry as provided by the various institutions.

Table A3.1 Well and Tracer Data groundwater

Site ID	Secondary Site ID	Easting (NZTM)	Northing (NZTM)		Screened Interval (m)	HCA Cluster	MRT	EPM
222		1936827	5615561		57.3–59.13	1	55	20
413		1936994	5620244		76.5–82.6	1	110	50
611		1931427	5607593			1	35	25
705		1930388	5607410		39.02–40.54	1	40	21
844		1925640	5612874		11.45–12.97	1	7	BMM
1191		1919583	5606896		18.86–21.86	3	7	50
1459		1932239	5603942		44–53	1	37	21
1674		1928677	5608418		32–38	1	19.6	BMM
1799		1935927	5608503		28.61–32.61	1	25.1	BMM
1940		1936871	5601730			2	59	67
2502		1929836	5611166		45.4–46.9	1	19	BMM
2580		1935702	5604421		9–12	1	3	67
3336		1928379	5603871		47–47.5	1	40	21
3525		1927032	5598451			2	230	
3697		1928379	5603871		64.31–65.31	1	30	60
4362		1904776	5613228		11.5–15.5	1	11.7	BMM
5006		1913126	5578864		28.8–29.8	1	190	70
5023		1904773	5613220		53–54	2	260	80
5690		1923774	5615445		13.46–14.66	2	10	67
5915		1929066	5610864		34.9–37.8	1	19	BMM
5988		1924136	5610864		106–109	2	30	67
8521		1923104	5605948			1	7	50
10340		1922964	5609399			1	1	80
10496		1935135	5603000			2	9	80
15002		1935268	5612897			1	27.5	BMM
15003		1935268	5612897		54.5–55.5	1	27.5	BMM
15006		1926346	5609157			1	11.7	BMM
15011		1924123	5605229			1		BMM
15012		1928379	5603871		113.5–114	4	255	80

Site ID	Secondary Site ID	Easting (NZTM)	Northing (NZTM)		Screened Interval (m)	HCA Cluster	MRT	EPM
15022		1935268	5612897		29.5–30.5	1	40	21
15465		1924136	5602754		12–14.85	4	45.6	BMM
15795		1923397	5613906		37.15–37.65	5	47	60
15884		1924708	5619381		9.39–10.39	2	9	80
16066		188444	5674549		11.76–13.76			
16067		188448	5681071		17.44–19.44			
16068		1884950	5683815		9.94–11.94			
16070		1885536	5686086		14.94–16.94			
16074		1884553	5676775		11.76–13.74			
16078		1916485	5605277		37.15–40.05	5	45	
16202		1933732	5606791			1	55	56
16203		1933736	5606797		19.44–21.56	1	47	30
16207		1885716	5688169		10.95–19.95			BMM
16208		1911247	5569726		36.81–38.68	1	175	70
16209		1911246	5569722		5.29–7.43	4	240	80
16211		1912255	5572240		6.67–8.82	1	1.5	80
16212		1913289	5574865		8.36–10.5	4	28	70
16256		1912999	5578868		7.17–9.3	4	240	80
16360		1924830	5610618		64.31–65.31	1	15	BMM
16361		1924830	5610619		22.94–23.94	1	5	33
16383		1934970	5603163			2	90	98
16300-J-1		1924843	5610616		126.5	4	110	50
16300-J-2		1924843	5610616		126.5	4		
22 Irongate		1926996	5604744		43.55–46.35	2		
A1	5913	1935751	5616114		74–76 & 78–84	1	48	BMM
A2	293	1935356	5616001		112–118			50
Beach Rd	1187	1939099	5608127		22–28	1	73	56
Brookvale 1	1329	1935190	5603357		11.4–17.4 & 19–22	3	4.3	56
Brookvale 3	4151	1934991	5603183		15.5–20 & 22–26.5	3	15-41	20/70
C1 Coverdale	4671	1934092	5618948		72–80.5	1	78	BMM
Clive (Ferry Rd)	1658	1936636	5611356		41–47	1	34.1	BMM
Eastbourne 1	469	1930117	5604260			3	49	BMM
Eastbourne 2	15588	1930015	5604429			3		BMM

Site ID	Secondary Site ID	Easting (NZTM)	Northing (NZTM)		Screened Interval (m)	HCA Cluster	MRT	EPM
Eastbourne 3	766	1929966	5604510			3	25	
Eastbourne 4	1171	1929906	5604586			3		
Eastbourne 5	1302	1929848	5604644			3	25	BMM
Hammond Road	16360	1924830	5610619		64.31–65.31	1	5	80
Hospital	4497	1928313	5606442		45–51	1	3	20
Lyndhurst	130	1929225	5607179		52–60	3	9	
Lyndhurst 5	15022	1935268	5612897		54.5–55.5	1	27.5	BMM
Lyndhurst 7	16167	1929116	5607293			2		32
Napier Road	439	1933818	5604468		30.5–36.5	1	88	60
Omahu	10334	1923223	5611906		6.1–12.2	1	0.2	90
Pakipaki	1905	1925137	5599411		21.9–28.96	2	149	50
Parkhill	5830	1938931	5606995		32.5–36.5	1	20.8	BMM
Portsmouth Road	3253	1924038	5606956		37–48	1	2.1	50
T1	472	1931956	5617103			3	28	BMM
T2	480	1931082	5616763			1	26	40
T3	872	1930367	5615466			1	21	BMM
T4	1389	1932076	5617848			1	42	59
T5	1998	1931609	5616281			1	23	BMM
T6	4144	1931424	5615484			1	23	BMM
T7	4595	1931332	5616436			1	21	BMM
TAN	2390	1933358	5617624		55.5–59.5	1	23.9	BMM
Tucker Lane	542	1936394	5610730		41.45–47.55	1	27	BMM
Waipatiki	3516	1942708	5642681		23.7–28 & 31.3–34.3	2	115	50
Waipatu	15415	1932393	5606249		30–35	1	29.9	BMM
Whakatu	473	1934546	5608832		30–35	1	29.9	BMM
Whirinaki	5033	1933183	5632651		7.2–10.2	2	10	17
Wilson Rd	897	1925798	5606558		38.5–46	1	2.1	40